ABSTRACT

COCKSON, PAUL A. Exploration of the Mineral Fertility Needs of *Brassica carinata* and Other Brassica sp. (Under the direction of Brian Earl Whipker).

The quantification and categorization of mineral fertility stress within *Brassica carinata* and Brassica oleracea 'Red Bor' are explored. The impacts of different macronutrient and micronutrient fertility treatments on leaf tissue accumulation, biomass production, fatty acid composition and concentrations, and visual nutrient deficiency symptomology is elucidated.

Different levels of macronutrients and micronutrients are required at different optimal concentrations over the life stages of *B. carinata*. The optimal fertility level can be extrapolated as the fertility concentration after which increasing the fertility does not result in a greater or lesser accumulation of leaf tissue. For each of the micronutrients tested, each of the tables, equations, and graphs (2.3.1, 2.3.2, 2.3.4, 2.3.5, 2.3.6, 2.3.7). These data compare tissue values to known *B. carinata* and *B. napus* tissue values from published literature as well as providing trends in leaf tissue mineral accumulation and biomass production based on life stage. The cells within these tables indicate the plateau value for leaf tissue accumulation when the statistical letters indicate no change above a certain fertility treatment.

Finally, little to no discernable impact or trend was observed regarding micronutrient rate and the fatty acid composition of the lipid profile of the *B. carinata* seeds. This trend may indicate that the fatty acid composition and concentrations within *B. carinata* may be regulated by other abiotic factors or genetic regulation rather than mineral nutrient fertility.

Different levels of macronutrients are required at different optimal concentrations at different life stages for *B. carinata*. Optimal fertility by life stage can be

extrapolated from these data by identifying the point after which increasing the fertility does not result in a greater biomass or leaf tissue concentrations. For each of the macronutrients tested, the optimal fertility concentrations varied and can be summarized in the tables, equations, and graphs (3.3.1, 3.3.2, 3.3.3, 3.3.4, 3.3.5, 3.3.6). These data indicated that maximum leaf tissue accumulation was not obtained for S (bolting, flowering, and pod set stages only), Mg (rosette, flowering, and pod set stages only), and Ca (flowering stage only). These results may indicate that the above elements are required at higher concentrations at the specified life stages. Alternatively, the lack of a plateau could also indicate that these resources were being stored and utilized within the plant and concentrated in leaf tissue. More research is needed to elucidate if these results are a concentration and reallocation effect or if higher fertility needs are required. If the above elements are needed in higher concentrations, then fertility levels or additional fertilization may need to be provided at these critical points in *B. carinata* development to optimize mineral resources.

Additionally, the biomass production often resulted in an unclear optimization model when trying to maximize biomass under differing fertility treatments. This may indicate that other factors play into plant biomass production such as genetics, and other abiotic factors.

This work seeks to form a foundation for maximal mineral nutrient levels in leaf tissue based on differing fertility. Thus, this forms the foundation for which levels to target in a new and emerging crop. Moving forward, an uptake and partitioning study is needed to elucidate how nutrients are utilized and translocated. These data will form as the reference points for such a study to ensure optimal fertility is provided. Additionally, these works categorize and visualize differing nutrient deficiencies on *B. carinata* and B. oleracea 'Red Bor' to help aid in diagnosis and progression of nutrient stress within Brassica sp.

Exploration of the Mineral Fertility Needs of *Brassica carinata* and Other *Brassica sp.*

by
Paul A. Cockson

A thesis submitted to the Graduate Faculty of
North Carolina State University
in partial fulfillment of the
requirements for the degree of
Master of Science

Horticultural Science

Raleigh, North Carolina
2020

APPROVED BY:

_____	_____
Dr. Brian Whipker Committee Chair	Dr. Robert Patterson

_____
Dr. Angela Post

DEDICATION

To my mother Carla Cockson for seeing the unique and wonderful individual I am and for pouring her life, effort, and advocacy into my education. The boy with "the spinning brain" would never have come this far without your love and support.

To my father Scot Cockson for teaching me to love reading and learning. Your support of my natural curiosity gave me the courage and confidence to ask the hard questions and follow the answers.

To my brothers for the years of support and love. For always being there to listen and support when I need to verbally process.

To my major professor Dr. Brian Whipker, grazie mille.

To all those who came along side in my journey to support, mentor, guide, advise, and assist. I am the person I am today because of the millions of everyday deeds and your small acts of love and kindness.

BIOGRAPHY

Paul Cockson graduated cum laude from NC State University with a B.S. in Plant and Soil Sciences from the Department of Crop and Soil Sciences with an Agroecology concentration. Paul started his graduate work in the Department of Horticulture Science in Spring of 2019. In January 2021, he will begin his doctoral work at the University of Kentucky.

ACKNOWLEDGMENTS

This material is based on work that is supported by the National Institute of Food and Agriculture, USDA, under award number 2016-1123. Any opinions, findings, conclusions, or recommendations expressed in this publication are those of the author(s) and do not necessarily reflect the view of the U.S. Department of Agriculture.

TABLE OF CONTENTS

LIST OF FIGURES

LIST OF TABLES

CHAPTER 1. Introduction

1.1. INTRODUCTION

Human's relationship with agriculture developed during the Paleolithic and Neolithic periods (Tauger, 2013). The human, land relationship has gone through many iterations including the Industrial Revolution and mechanization, and the Green Revolution. Throughout these changes, developments and complexities have arisen. The modern agricultural relationship is predicated on challenges of decreasing agricultural land, urban sprawl, decreases in available water resources, salinization of agricultural fields, increased demands on fossil fuels due to mechanization, and a growing global populace (Siegel, 2015). These challenges and demands will result in a future of agriculture which strives to produce more food, fuel, and fiber on less land, with fewer resources, and for more people than ever before. To meet these challenges, producers, and consumers of agricultural products will have to be creative and diversify their inputs and outputs in a production system to achieve optimal yields.

One of the major challenges facing the future of food, fuel, and fiber production is the prospects of global climate change. Increases in temperatures, changes in rainfall patterns, and shifting ecological environments will all present unique and challenging pressures to food production (Adams et al., 1998). While the exact causes and impacts of global climate change are still being explored and defined, it is quite clear that climate change will be a challenge for the future.

One major factor contributing to global climate change is carbon dioxide (CO_2) emissions from the combustion of fossil fuels. These limited resources will increasingly become more challenging to locate, extract, and refine in an economically feasible fashion for petroleum companies. With the increase in population and the increasing demand for fossil fuel-derived services, this limited petroleum resource will experience increased pressures of consumption.

One such heavy consumer of fossil fuels is the aviation industry. In addition to their heavy consumption of fossil fuels, their impact is compounded given their emissions take place at higher altitudes. These high-altitude emissions can result in greater impacts on global climate change given the CO_2 is expelled directly into the atmosphere (Bulzan, 2010; Govardhan et al., 2017). Additionally, these CO_2 emissions can have higher residency time given they are far removed from the terrestrial plant resources which are largely responsible for much of our CO_2 sequestration. By finding a renewable combustible carbon source with low carbon emissions, the impacts of air travel on global climate change can be reduced through a decrease in CO_2 emissions, and through renewable sources such as biofuels.

One such renewable combustible carbon source would be an aviation biofuel produced from an oilseed crop called *Brassica carinata* and commonly known as Ethiopian mustard or in its truncated nomenclature carinata. This plant's seeds are high in oil content and contain high concentrations of long chain fatty acids (LCFA) and

very long chain fatty acids (VLCFA) (Seepaul et al., 2016). Aviation fuels produced from VLCFA biofuels can undergo a simple refinement process and result in a "drop-in" fuel that is optimized for aviation engines (U.S. Federal Aviation Administration, 2014).

The feasibility of carinata-derived biofuels has already been tested. A flight completed in 2012 used a 100% blend of carinata aviation fuel. The flight was shown to reduce aerosol emissions by 50%, a reduction in particle emissions up to 25%, and a reduction in black carbon emissions up to 49% (Govardhan et al., 2017; Satheesh, 2017; U.S. Federal Aviation Administration, 2014). In this test flight, it was also shown that during the steady-state of the turbine, the use of carinata biofuels resulted in a 1.5% improvement of specific fuel consumption (Satheesh, 2017). The amazing potential of carinata aviation fuel as not only a sustainable but also lower carbon emission fuel source can have huge impacts on the energy stability and sustainability of the future.

Due to the milder winter climatic conditions in the Southeastern US, carinata is targeted to be grown from Florida up to North Carolina and potentially further north (Agrisoma, 2017). *Brassica carinata* has the added benefit of being grown in the cool season of production and can be grown as a winter cover crop. Cover crops help reduce soil erosion and many brassica species produce compounds that can suppress soil nematodes (Oka, 2010). Additionally, carinata possess the ability to recover or scavenge nutrients from the soil profile resulting in higher fertilizer use efficiency (Chen et al., 2007). Given its benefits to producers and soil health, carinata represents a unique

opportunity for Southeastern US producers to grow a sustainable fuel source over the winter.

One major challenge to using biofuel as a substitute for traditional petroleum products is that of quality control. In petroleum sources, often quality and homogeneity are obtained through different methods of refinement using heat and density. This refinement process ensures that a constant quality and grade of petroleum-derived fuel is obtained. However, when utilizing a biological system for the production of biofuel, complications with oil quality and quantity can confound fuel integrity and supply.

By utilizing a biological organism for biofuel, the quality and quantity of the end-product are subject to many internal and external variables. Carinata oil is dependent upon seed size, percentage of oil within the seed, the quantity, and types of fatty acids within the oil, and finally, the acreage successfully grew. Each of these variables can impact the quantity and quality of the biofuel, and consequently, any research which homogenizes the biofuel will help stabilize alternative fuel markets.

Additionally, the quantity and quality of the biofuel produced from a natural system are subjected to internal biological processes. Carinata undergoes two distinct growth patterns in its lifecycle. During its initial phase, the plant exists as a rosette. The plant will continue in this stage through the cool season until warm conditions trigger the plant to initiate its reproductive phase. During this stage, the plant will

begin rapid cell division and produce a flower spikelet which will grow vertically and become highly branched. Upon full development of the inflorescence, the plant will set flowers on the terminus and axillary shoots. Given successful fertilization, the plants will set siliques and the resultant seeds will develop. After full seed maturity has been achieved, the plant will begin to defoliate, and the siliques will desiccate. These distinct biological factors predicate that certain sources and sinks will be present at different growth stages and in different intensities. Thus, the internal source and sinks as well as the growth stage will also have an impact on the final quantity and quality of biofuel produced.

The above factors impact the quantity and quality of oil, protein, and fatty acids produced by carinata and thus, must be addressed to ensure a consistent and reliable biofuel is maintained.

Rapeseed (*Brassica napus*) and other brassicas such as B. oleracea, B. nigra, *B. carinata*, and *B. rapa* are predicted to have a common ancestor and have been crossbred and interbred to produce our current species (OECD, 2012; Rakow, 2004). It is believed that there are certain crosses and genetic linkages that have been made or may be made among the major oilseed brassica species (Chen et al., 2011). The center of origin is believed to have been in and around Europe, although other centers of origin have been proposed such as the African plateau and the Baltic Region (Rakow, 2004). Regardless of origin, brassica species have risen to become a globally important crop and are

projected to become increasingly more important crops as the world's food, fiber, and fuel needs continue to expand.

While oilseed crops have been grown in the US for many decades, especially in northern latitudes, *Brassica carinata* is a relatively new crop for both the north and southeast. Consequently, little research exists on *Brassica carinata*. However, given its proposed genetic past and breeding, it would be reasonable to draw some general conclusions and inferences from other brassica species, which have more extensive research.

In biological systems, external factors, both abiotic and biotic, can impact yield (Angadi et al., 2000; Ahmadi and Bahrani, 2009; Appelqvist, 1968; Noquet et al., 2004). These abiotic factors will either reduce or increase the supply of raw materials (nutrients, photosynthates, metabolites, etc.) available for oil production and by extension, biofuel production. Additionally, these biological systems have complex chemistries and physiologies which will produce more or less of certain molecules such as fatty acids based on their environment, resource availability, and growth stages.

Thus, if a carinata crop experiences stress during growth, yield, and oil quality can be impacted. For example, VLCFA represents a huge sink of energy and resources given the high energy investments required to produce a fatty acid chain where each carbon to carbon bond represents an energy investment of 80 kcal/mol and every carbon to carbon double bond is 145 kcal/mol. These energy investments must be

perpetuated into chains >19 carbon to carbon bonds to produce one VLCFA. If a carinata plant experiences drought stress or a lack of essential nutrients, the plant's ability to produce a high amount of oils and a high content of VLCFA may be impacted. This negative or positive impact on oil quantity and quality is yet unknown in *Brassica carinata* but has been explored in other brassica species.

1.2. MINERAL NUTRIENT IMPACTS ON BRASSICA GROWTH AND FATTY ACIDS

Aside from water, temperature, and fertilization (Ahmadi and Bahrani, 2009; Angadi et al., 2000; Polowick and Sawhney, 1988; Tayo and Morgan, 1978) macro- and micro- nutrients are the most yield-limiting factor to oilseed brassicas (Berry and Spink, 2006). To ensure that the highest quantity and quality of the oil is produced, the impacts of different stresses on plant growth and oil production must be explored. One such impact on plant growth and oil quantity and quality is plant nutrients. If essential macro or microelements are limited, this can impact the yield and production of quality oil in brassica species (Miller et al., 2003; Govahi and Saffari, 2006; Gao et al., 2010; Durenne et al., 2018; Nuttall et al., 1987; Fismes et al., 2000; Ma et al., 2015).

Yousaf et al. (2016) explored the impacts of the top three macro elements on the productivity and quality of *Brassica napus* L. This work looked specifically at the most limiting element of the three macro elements (nitrogen (N), phosphorus (P), or potassium (K)) in yield, oil production, and protein amounts. Their findings showed

that N was the most limiting element followed by P and K nutrients, and that yield increased by 61-72% under an NPK fertility regime when compared to just a PK treatment. Protein and oil constituents and other fatty acids were not influenced significantly by the application of P and K fertilizer even though oil and protein yields were affected in applied N, P, and K fertilizers. An increase in N fertilizer resulted in a reduction of oil contents and an increase in protein content. This inverse relationship between protein and oils has been studied in other works (Brennan et al., 2000; Krauze and Bowszys, 2000). These studies show that the three essential macronutrients have an impact on the growth, oil production, and protein content in oilseed brassicas.

University of Florida researchers have identified a strong correlation between *Brassica napus* and *Brassica carinata* and photosynthetic activity and concentration based on nitrogen fertility concentrations. This work used differing N concentrations and studied the impacts on both brassicas showing that when N is limited, biomass accumulation, total dry matter, and leaf area are reduced when compared to the highest N treatments (Seepaul et al., 2016). Another work by Seepaul et al. (2019) studied the dry matter accumulation of *Brassica carinata* under different nitrogen fertilizer regimes. This work showed that the life stage of *Brassica carinata* impacted N uptake as well, with the greatest uptake occurring in the bolting and flower stages of the plant's lifecycle.

Govahi and Saffari (2006) investigated K and sulfur (S) fertilization on yield, seed quality, and yield components of *Brassica napus* L. By varying both concentrations of K

and S, the group was able to determine that an increase in S resulted in an increase in biomass production, primary and secondary branching, and average seed/pod number. Their results also indicated that increasing S concentrations from 0 to 40 and 40 to 80 kg/ha resulted in an increase in seed oil content of 3.89% and 6.0% respectively. However, at the highest concentrations of 80 and 120 kg/ha of S applied, there was no significant increase in seed oil content. Increasing K concentrations had no impact on seed oil content. The highest protein yield was seen at the highest S concentration of 120 kg/ha.

Sulfur is needed at much higher levels in brassicas than in other traditional row crops. Varényiová et al. (2017) explored the impacts of varying S nutrition in the yield, oiliness, oil production, seed nutrient content, and plant nutrient content in *Brassica napus* L. By varying the rates of S applied (0, 15, 40, 65 kg/ha), the impacts of S on plant growth and yield were elucidated. Their results showed no significant impacts on oil content among all treatments were observed. This is interesting given that Ahmad et al. (2007), saw a significant increase in oil content at a dose of 20 kg/ha. More research is needed to further describe the complex relations of sulfur nutrition on plant physiology and yield metrics.

Two works by Nuttall et al. (1987) and Ma et al. (2015) looked at the impacts of N, S, and boron (B) on the yield and quality of oilseed brassicas. Nuttall et al. (1987) showed that S fertilizer increased the glucosinolate concentration of rape meal and

increased oil concentrations. Nitrogen fertility increased the content of protein while N plus B treatments resulted in a decrease of protein and an increase in oil percentage. Sulfur helped remedy poor seed set and B helped to improve pod development and decreased the number of sterile florets. Ma et al. (2015) showed that a foliar application of B resulted in a 10 percent increase in yield when applied at the early flowering stage. They also showed that there was a strong correlation (r^2=0.99) between N rates and yield. Sulfur applications resulted in an increase of canola yields of 3-31% varying by location. Additionally, work completed by Ali et al., (2003) showed direct impacts on irrigation and nitrogen fertility to oil yield in canola plants.

Mei et al. (2009) looked at the impacts of micronutrients (B, molybdenum (Mo), and zinc (Zn)) on seed yield in *Brassica napus* L. When B was applied, there was a 46.1 percent increase in seed yield even when compared to the Mo and Zn treatments. This could indicate that B is a limiting factor in seed formation and yield. When all three micronutrients were applied together, the greatest yield was seen at 68.1 percent above the control. There was a significant yet small increase in oil content and oil quality in all treatments. This work indicates that micronutrients are just as vital as macronutrients in impacting seed yield and oil quantity and quality.

The above works show how important both macro and micronutrients are in brassica oilseed crops. They can impact a wide range of yield components such as flower maturation, pod development, seed count, seed development, seed yield, seed

oil content, oil quantity, and quality. The complex and dynamic nature of plant and nutrient interactions and usage needs further study. The above work while mainly focusing on *Brassica napus* could help inform the study of *Brassica carinata* nutrient use and oil quality and quantity.

1.3. RESEARCH OBJECTIVES

The above literature demonstrates a correlation between plant growth and yield and oil quantity and quality in brassicas. Given the deficit of information available for *B. carinata* and its optimal nutrient requirements, and how these nutrients will impact the production of metabolites and lipids, this study will seek to elucidate the optimal fertility concentration for all macro and micronutrients. The optimal fertility concentration will be determined using a modified Hoagland's Solution calibrated to provide differing concentrations (0, 25, 50, 75, 87.5, and 100%) of the full strength Hoagland's solution. Plants will be grown, and data procured at distinct stages of lifecycle development (rosette, bolting, flowering, pod set, and mature pod). Data will consist of leaf tissue mineral analysis and plant dry weights. This data will determine optimal leaf tissue concentrations based on fertility concentrations for each growth stage.

Additionally, for the micronutrient data set, data will be taken on the resultant siliques and seeds from each fertility treatment and subjected to NIR analysis to determine the impacts differing nutrient concentrations may have on the lipidome. For

the macronutrients, an additional life stage sampling will occur during the pod fill stage.

1.4. ACKNOWLEGEMENTS

This material is based on work that is supported by the National Institute of Food and Agriculture, USDA, under award number 2016-1123. Any opinions, findings, conclusions, or recommendations expressed in this publication are those of the author(s) and do not necessarily reflect the view of the U.S. Department of Agriculture.

LITERATURE CITED

Adams, R.M., Hurd, B.H., Lenhart, S., and Leary, N., 1998. Effects of global climate change on agriculture: an interpretative review. Climate Research, 11(1), pp.19-30.

Agrisoma. 2017. Carinata Management Handbook, Southeastern US 2017-18. Agrisoma USA, Tifton, GA.

Ahmad, G., Jan, A., Arif, M., Jan, M.T. and Khattak, R.A., 2007. Influence of nitrogen and sulfur fertilization on quality of canola (*Brassica napus* L.) under rainfed conditions. Journal of Zhejiang University Science B, 8(10), pp.731-737.

Ahmadi, M., and Bahrani, M.J., 2009. Yield and yield components of rapeseed as influenced by water stress at different growth stages and nitrogen levels. American-Eurasian Journal of Agricultural and Environmental Sciences, 5(6), pp.755-761.

Ali, A., Munir, M.K., Malik, M.A., and Saleem, M.F., 2003. Effect of different irrigation and nitrogen levels on the seed and oil yield of canola (*Brassica napus* L.). Pakistan Journal of Agricultural Sciences, 40, pp.137-139.

Angadi, S.V., Cutforth, H.W., Miller, P.R., McConkey, B.G., Entz, M.H., Brandt, S.A. and Volkmar, K.M., 2000. Response of three Brassica species to high temperature stress during reproductive growth. Canadian Journal of Plant Science, 80(4), pp.693-701.

Appelqvist, L.Å., 1968. Lipids in Cruciferae: III. Fatty Acid Composition of Diploid and Tetraploid Seeds of Brassica campestris and Sinapis alba Grown under Two Climatic Extremes. Physiologia Plantarum, 21(3), pp.615-625.

Berry, P.M., and Spink, J.H., 2006. A physiological analysis of oilseed rape yields: past and future. The Journal of agricultural science, 144, p.381.

Brennan, R.F., Mason, M.G. and Walton, G.H., 2000. Effect of nitrogen fertilizer on the concentrations of oil and protein in canola (*Brassica napus*) seed. Journal of Plant Nutrition, 23(3), pp.339-348.

Bulzan, D. 2010. High Altitude Emissions. NASA Green Aviation Summit, NASA, 2010. www.hq.nasa.gov/office/aero/pdf/10_bulzan_hae_green_aviation_summit.pdf.

Chen, G., Clark, A., Kremen, A., Lawley, Y., Price, A., Stocking, L. and Weil, R., 2010. Brassicas and mustards. Managing cover crops profitably, pp.81-89. SARE, 2010.

Chen, S., Nelson, M.N., Chèvre, A.M., Jenczewski, E., Li, Z., Mason, A.S., Meng, J., Plummer, J.A., Pradhan, A., Siddique, K.H. and Snowdon, R.J., 2011. Trigenomic bridges for Brassica improvement. Critical reviews in plant sciences, 30(6), pp.524-547.

Diepenbrock, W., 2000. Yield analysis of winter oilseed rape (*Brassica napus* L.): a review. Field Crops Research, 67(1), pp.35-49.

Durenne, B., Druart, P., Blondel, A. and Fauconnier, M.L., 2018. How cadmium affects the fitness and the glucosinolate content of oilseed rape plantlets. Environmental and experimental botany, 155, pp.185-194.

Fismes, J., Vong, P.C., Guckert, A. and Frossard, E., 2000. Influence of sulfur on apparent N-use efficiency, yield, and quality of oilseed rape (*Brassica napus* L.) grown on a calcareous soil. European Journal of Agronomy, 12(2), pp.127-141.

Gao, J., Thelen, K.D., Min, D.H., Smith, S., Hao, X. and Gehl, R., 2010. Effects of manure and fertilizer applications on canola oil content and fatty acid composition. Agronomy Journal, 102(2), pp.790-797.

Govahi, M. and Saffari, M., 2006. Effect of potassium and sulphur fertilizers on yield, yield components and seed quality of spring canola (*Brassica napus* L.) seed. Journal of Agronomy, 5 (4), pp.577-582.

Govardhan, G., Sreedharan, K.S., Nanjundiah, R., Moorthy, K.K. and Surendran, S.B., 2017. Possible climatic implications of high-altitude black carbon emissions. Atmospheric Chemistry and Physics, 17(15), p.9623.

Hall, T.M. and Prather, M.J., 1993. Simulations of the trend and annual cycle in stratospheric CO2. Journal of Geophysical Research: Atmospheres, 98(D6), pp.10573-10581.

Jez J, editor. Sulfur: A missing link between soils, crops, and nutrition. ASA-CSSA-SSSA; 2008.

Koch, G.W. and Mooney, H.A., 1996. Response of terrestrial ecosystems to elevated CO2: a synthesis and summary (pp. 415-429). Academic Press, San Diego.

Krauze, A. and Bowszys, T., 2000. Effect of nitrogen fertilization on the chemical composition of FIDE cultivars of spring oilseed rape. Rośtłiny Oleiste–Oilseed Crops, 22, pp.285-290.

Ma, B.L., Biswas, D.K., Herath, A.W., Whalen, J.K., Ruan, S.Q., Caldwell, C., Earl, H., Vanasse, A., Scott, P., and Smith, D.L., 2015. Growth, yield, and yield components of canola as affected by nitrogen, sulfur, and boron application. Journal of Plant Nutrition and Soil Science, 178(4), pp.658-670.

Marschner, H., 2011. Marschner's mineral nutrition of higher plants. Academic press.

Mei, Yang, Lei, Shi, Fang-Sen, Xu, Jian-Wei, Lu and Yun-Hua, Wang, 2009. Effects of B, Mo, Zn, and their interactions on seed yield of rapeseed (*Brassica napus* L.). Pedosphere, 19(1), pp.53-59.

Miller, P.R., Angadi, S.V., Androsoff, G.L., McConkey, B.G., McDonald, C.L., Brandt, S.A., Cutforth, H.W., Entz, M.H. and Volkmar, K.M., 2003. Comparing Brassica oilseed crop productivity under contrasting N fertility regimes in the semiarid northern Great Plains. Canadian journal of plant science, 83(3), pp.489-497.

Noquet, C., Avice, J.C., Rossato, L., Beauclair, P., Henry, M.P. and Ourry, A., 2004. Effects of altered source–sink relationships on N allocation and vegetative storage protein accumulation in *Brassica napus* L. Plant Science, 166(4), pp.1007-1018.

Nuttall, W.F., Ukrainetz, H., Stewart, J.W.B. and Spurr, D.T., 1987. The effect of nitrogen, sulphur and boron on yield and quality of rapeseed (*Brassica napus* L. and B. campestris L.). Canadian Journal of Soil Science, 67(3), pp.545-559.

OECD. 2012. Organisation for Economic Co-operation and Development. Consensus document on the biology of the brassica crops (Brassica sp.). Series on Harmonisation of Regulatory oversight of Biotechnology, No 54, OECD, Paris, pp 142.

Oka, Y., 2010. Mechanisms of nematode suppression by organic soil amendments—a review. Applied Soil Ecology, 44(2), pp.101-115.

Polowick, P.L. and Sawhney, V.K., 1988. High temperature induced male and female sterility in canola (*Brassica napus* L.). Annals of Botany, 62(1), pp.83-86.

Rakow, G., 2004. Species origin and economic importance of Brassica. In Brassica (pp. 3-11). Springer, Berlin, Heidelberg.

Rawsthorne, S., 2002. Carbon flux and fatty acid synthesis in plants. Progress in lipid research, 41(2), pp.182-196.

Satheesh, S.K., 2017. High Altitude Emissions of Black Carbon Aerosols: Potential Climate Implications. AGUFM, 2017, pp. U21D-01.

Seepaul, R., George, S., and Wright, D.L., 2016. Comparative response of *B. carinata* and *B. napus* vegetative growth, development, and photosynthesis to nitrogen nutrition. Industrial Crops and Products, 94, pp.872-883.

Seepaul, R., Marois, J., Small, I.M., George, S., and Wright, D.L., 2019. Carinata dry matter accumulation and nutrient uptake responses to nitrogen fertilization. Agronomy Journal, 111(4), pp.2038-2046.

Siegel, F.R., 2015. Population assessments: 2013–2050–2100: Growth, stability, contraction. In Countering 21st Century Social-Environmental Threats to Growing Global Populations (pp. 1-8). Springer, Cham.

Tauger, M.B., 2013. Agriculture in world history. Routledge. Ch. 1.

Tayo, T.O. and Morgan, D.G., 1979. Factors influencing flower and pod development in oil-seed rape (*Brassica napus* L.). The Journal of Agricultural Science, 92(2), pp.363-373.

United States, Federal Aviation Administration, and Pratt & Whitney. 2014. Evaluation of ARA Catalytic Hydrothermolysis (CH) Fuel. Continuous Lower Energy, Emissions and Noise (CLEEN) Program, Federal Aviation Administration.

Varényiová, M., Ducsay, L. and Ryant, P., 2017. Sulphur nutrition and its effect on yield and oil content of oilseed rape (*Brassica napus* L.). Acta Universitatis Agriculturae et Silviculturae Mendelianae Brunensis, 65(2), pp.555-562.

Warwick, S.I., Gugel, R.K., McDonald, T., and Falk, K.C., 2006. Genetic variation of Ethiopian mustard (*Brassica carinata* A. Braun) germplasm in western Canada. Genetic Resources and Crop Evolution, 53(2), pp.297-312.

Yousaf, M., Li, X., Ren, T., Cong, R., Ata-Ul-Karim, S.T., Shah, A.N., Khan, M.J., Zhang, Z., Fahad, S. and Lu, J., 2016. Response of Nitrogen, Phosphorus and Potassium Fertilization on Productivity and Quality of Winter Rapeseed in Central China. International Journal of Agriculture & Biology, 18(6) pp.1137-1142.

CHAPTER 2. The Impacts of Differing Fertility Concentrations of Micronutrients on the Fertilizer Uptake and the Lipidome of *Brassica carinata* During Different Life-Stages.

Paul Cockson [1,*], Patrick Veazie[1], Matthew Davis[1], Gabby Barajas[1], Angela Post[2], Carl Crozier[2], Ramone Leon[2], Robert Patterson[2], and Brian E. Whipker [1]

[1]Department of Horticultural Science, North Carolina State University, Raleigh, NC 27695, USA; bwhipker@ncsu.edu (B.E.W.)

[2]Department of Crop and Soil Science, North Carolina State University, Raleigh, NC 27695, USA;

*Correspondence: pcockson@gmail.com

Abstract: Many abiotic factors impact the yield and growth of *Brassica carinata* (commonly referred to as carinata). Very little is known about carinata and how mineral nutrients impact its growth, and more specifically the sufficiency values for fertility over the plant's growth cycle and life stages. Thus, this study explored the impacts that plant nutrients, specifically micronutrients, can have on the growth and development of carinata over its distinct life stages (rosette, bolting, flowering, and pod set). Additionally, this study sought to explore the impacts these micronutrients have on the fatty acid composition of the seed lipidome. Plants were grown under varying micronutrient concentrations (0.0, 25.0, 50.0, 75.0, 87.5, and 100.0%) of a modified Hoagland's solution. Data was collected on plant height, diameter, leaf tissue mineral nutrient concentrations, and biomass as well as the fatty acid composition, protein content, and lipid concentrations within the seeds. The results demonstrated that micronutrient fertility can have profound impacts on the production of *Brassica carinata* during different life stages. Boron (B) was reported to have the greatest impact on the growth and reproduction of *Brassica carinata*. This is most likely due to the death of the apical meristem which resulted in a lack of siliques or seeds at the lowest rate. Little impact was observed in the fatty acid composition regarding fertility concentrations. The only exception to this trend was in the concentration of eicosenoic acid (20:1) which

reported varying impacts in all fertility treatments except Manganese (Mn). Additionally, optimal rates of micronutrients, maximization of biomass production varied dramatically based on the fertility provided and element. For some elements, linear trends in nutrient accumulation were modeled without reaching a maximum fertility level. While other life-stages and elements produced distinct plateau values regarding leaf tissue mineral uptake. This work demonstrates that *Brassica carinata* has different optimal mineral needs based on life stage and micronutrient.

Keywords: oilseed, *Brassica carinata*, fatty acids, lipidome, fertility, life-cycle, micronutrients, symptomology, foliar, aviation biofuel

2.1. INTRODUCTION

Over the past few decades, concerns of global climate change have resulted in increased attention and policy directed toward CO_2 emissions. These concerns have resulted in many policies for countries and nations seeking to mitigate carbon emissions through different means. One such mitigation policy is the diversification of the sources of fuel used for transportation, utilities, and industry. By diversifying the sources of fuel, we create a more robust and secure energy portfolio.

One energy source which has gained attention is that of aviation fuel. Aviation emissions are problematic given they produce CO_2 at high altitudes (Govardhan et al., (1); Satheesh, (2)). This high-altitude emissions releases CO_2 into a system which has a longer residency time due to poor cycling (Craig, (3); Friend et al., (4)). Additionally, plants and algae are terrestrially bound which means high altitude carbon emissions place CO_2 out of reach of the organisms which traditionally sequester carbon. Theoretically then, by sourcing aviation fuels from a renewable biofuel, the impacts on aviation emissions would be lessened or negated.

One such biofuel option is lipid sourced biofuels. These biofuels already have an established precedent in the form of soybean and corn source fuels such as ethanol and biodiesels (U.S. Energy Information Administration, (5); Seepaul et al., (6)). These biofuels played an important part in the energy system during increases in petroleum prices.

Aviation fuel, much like other fuel sources, requires a certain constituency to obtain optimal functionality in a turbine engine (Federal Aviation Administration, (7)). One such source of biofuel which would have the necessary physical and chemical properties after refinement would be the oilseed crop *Brassica carinata*, also known as Ethiopian mustard. This oilseed crop has a unique oil profile (Gesch et al., (8)) which has a higher distribution of mid chain (MCFA), long chain (LCFA), and very long chain fatty acids (VLCFA) which after refinement produce a fuel molecule similar to petroleum-derived aviation fuel (U.S. Energy Information Administration, (5)). The biofuel derived from carinata was tested in a flight in 2012 and reported to have lower particle emissions, black carbon emissions, aerosol emissions, and increased specific fuel consumption as compared to standard petroleum-based fuel (Govardhan et al., (1); Satheesh, (2); Federal Aviation Administration, (7)).

Despite the success already observed in aviation biofuels produced from carinata, some challenges remain for the utilization of a biological source for fuel. For example, abiotic stresses can have deleterious impacts on yield, plant growth, and oil quantity and quality which may disrupt the continuous supply chain of a bio-derived fuel. One such abiotic stress is that of plant nutrients and fertility.

Plants require certain macro and micronutrients to optimize growth, yield, and to complete their lifecycle (Marschner, (9)). These nutrients have direct impacts on yield, especially in Brassicas (Gibson et al., (10); Grant and Bailey, (11)). Additionally, Brassicas have distinct life stages each requiring different nutrients to ensure adequate development and yield.

Brassicas undergo distinct phases of their growth habit after germination (SPARC, Appendix 1; Seepaul et al. (6, 12); Harper and Berkenkamp, (13)). The first stage of growth is that of the rosette stage. During this stage, plants remain vegetative and low to the ground focusing on the production of vegetative biomass and root biomass. The next stage is bolting, during this stage, plants initiate their reproductive phase and will produce a vertical flower spikelet which will become highly branched. The next stage of development is flowering and reproduction. During this phase, resources are translocated into developing flowers and siliques upon fertilization. The next stage is pod fill and set when plants reallocate resources into the developing embryos and seeds. Finally, the plants will defoliate and desiccate. During different life stages, fertility requirements will vary largely due to changes in growth rate, and developing sources and sinks. These differences were explored to elucidate the differences in plant nutrient requirements at different life stages.

In addition to different fertility needs based on life stage, different micronutrient needs exist in Brassicas. For example, during the bolting phase, rapid cell polarization and expansion necessitates a higher use of elements which aid the expansion and stabilization of the cell wall. Boron is primarily found in the cell wall contained within the B-dimeric rhamnogalacturonan II (RG-II) complex (Matoh, (14)). Within this complex, both B and calcium (Ca) help to stabilize the structure, and allow the complex to carry out its function of creating calcium ion bridges between the pectin chains within the cell wall (Chebli and Geitmann, (15); Matoh, (14)). When the RG-II complex was monomeric and the cell walls swelled rather than differentiating polarly (Matoh, (14)). Given the stabilizing nature of the RG-II complex plays within the cell wall and stabilizing the pectin matrix, under Ca or B deficient conditions, cells cannot expand properly or directionally. The bolting phase produces the flower spikelet and undergoes rapid cell development, thus any limitation of B or Ca can directly impact flower formation and, by extension, siliques and seeds.

The impact of B on yield as a foliar application, resulted in a 10% increase in yield when applied at the early flowering stage Ma et al. (16). Another study in 2009 (Mei et al., (17)) looked at the impacts of micronutrients (B, molybdenum (Mo), and zinc (Zn)) on seed yield in *Brassica napus* L. When B was applied, there was a 46.1% increase in seed yield even when compared to the Mo and Zn treatments. This suggests that B is a limiting factor in seed formation and yield. When all three micronutrients were applied together, the greatest yield was observed at 68.1 percent above the control. There was a significant yet small increase in oil content and oil quality in all treatments.

Iron (Fe) is important to plant growth and development and are integral parts to many enzymatic, active and structural sites, and gradients for plant processes. One of the most important functions of Fe is in the redox system through the biosynthesis of heme coenzymes, the chlorophyll molecule, and iron-sulfur proteins (Marschner, (9); Gardner et al., (18)). Another important function of Fe is in the development of chloroplasts. Within the chloroplasts, under Fe-deficient conditions, protein synthesis is greatly reduced (Shetty and Miller, (19)). Additionally, the thylakoid membrane contains ~20 Fe constituents which are involved in Photosystem I and II (PS I & II) (Terry and Abadia, (20); Rutherford, (21)). In addition to the deleterious impact Fe deficiency can have on the production of photosynthates which have a direct impact on lipid metabolism, Fe deficiency can cause lipid peroxidation in some brassicas (Fei et al., (22)). This would have a direct impact on the stability and polymerization of lipid molecules as well as seed viability and storage.

Copper (Cu) is also an essential plant micronutrient. Copper is primarily used within plants in the Photosystem II pathway as a structural component of the enzyme plastocyanin (Sandmann et al., (23)). Additionally, Cu is involved in the lignification process of the cell walls though the exact mechanism remains unclear (Hopmans, (24)).

Zinc also plays an important role in plants. It is present in many plant enzymes, plays a role in mitigating the production of ethanol under aerobic conditions within

meristematic regions, is involved in the carbonic anhydrase pathway, is integral in carbohydrate metabolism as an activator of fructose 1,6-bisphosphatease and aldolase (Coleman, (25); Moore and Patrick, (26); Sandmann and Boger, (27); O'Sullivan, (28)). Additionally, Zn is related to the stability, integrity, and longevity of membranes. In particular, Zn helps to bind with different complexes in order to create polypeptide and cysteine structures which in turn help to guard against harmful oxidative processes with regard to lipids (Cakmak and Marschner, (29, 30)).

Molybdenum is an element which is primarily important to nodulating crops such as legumes which form symbiotic associations with atmospheric nitrogen (N_2) fixing bacterium. Additional roles of Mo are to aid in the assimilation and utilization of N (Agarwala and Hewitt, (31)). A symptom known as "whiptailing" has been observed in brassicas under Mo deficient conditions in which the reproductive leaves appear elongated and distorted (Hewitt, and Bolle-Jones, (32)).

Manganese could arguably have the widest impacts on plant growth and development of any micronutrient given its role within Photosystem II and the superoxide simutase molecule (MnSOD). Within PS II, under Mn deficient conditions, the true level of chlorophyll will only result in a slight decrease. However, when Mn is deficient the O_2 evolution within younger developing leaves can drop by almost half (Eyster et al., (33); Nable et al., (34); Kriedemann et al., (35)).

The impacts of Mn shortages on the metabolic activities of the plant can be severe. Within plants, the thylakoid membrane can be deleteriously impacted due to a shortage of or degradation of glycolipids and polyunsaturated fatty acids (Constantopoulus, (36)). The impacts of Mn can be observed within seeds as well as the seeds and developing embryos (Wilson et al., (37)). Seed proteins and lipids are impacted inversely as Mn concentrations increase with seed oil being higher under increasing Mn concentrations within the plant (Constantopoulus, (36)). Additionally, the types of fatty acids within the seeds can be impacted under different Mn

concentrations. Within seeds, oleic acid content is typically higher under greater Mn conditions with linoleic acid following an inverse relationship to oleic acid (Constantopoulus, (36)).

While micronutrients are needed in much smaller quantities within the plant than macronutrients, they are still necessary elements (Henry et al., 38). When levels of a microelement fall below a critical range, negative impacts are observed on plant growth and development, physiological functions and pathways, metabolites, and seed and embryo development (Taylor et al., (39)). To rectify or avoid these negative impacts, proper fertility must be administered to plants during all stages of development. This work seeks to explore the impacts of micronutrients on the growth and development of a new and emerging biofuel oilseed crop *B. carinata*. The optimal micronutrient fertility ranges were explored by supplying each micronutrient at reducing fertility levels based off a modified Hoagland's solution. The impacts on total plant above ground biomass as well as leaf tissue concentration were cataloged. At each of the distinct life stages of the crop (rosette stage, bolting, and flowering) the above metrics were taken. Finally, the mature seeds were collected and analyzed to see the impacts of the varying nutrients on the plant lipidome.

2.2. MATERIALS AND METHODS

Brassica carinata 'Avanza 641' (Agrisoma, Gatineau, Quebec) seeds were sown on 3 November 2018 into 72-cell plug trays filled with a substrate mix of 80:20 (v:v) Canadian sphagnum peat moss (Conrad Fafard, Agawam, MA) and horticultural grade perlite (Perlite Vermiculite Packaging Industries, Inc., North Bloomfield, OH). The substrate mix was amended with dolomitic lime at 8.875 kg/m^3 (Rockydale Agricultural, Roanoke, VA) and wetting agent (Aquatrols, Cherry Hill, NJ) at 600 g/m^3. The premade substrate mix ensured no micronutrient charge or contaminants were present in the

seeding substrate. Seedlings were then grown at 22.8 ± 2.8°C day/night (D/N) temperatures (73.0 ± 5.0°F) in a glass greenhouse in Raleigh, NC (35.8°N Latitude) under a mist bench set at irrigation intervals (5 sec. every 3 minutes). After the second true leaves emerged, the plants were removed from mist and hand irrigated with a nurse fertility solution (33.4 g KNO_3, 33.4 g Ca $(NO_3)_2 \bullet H_2O$, 6.6 g KH_2PO_4, 13.2 g $MgSO_4 \bullet 7H_2O$ in 20L H_2O per 100L deionized (DI) H_2O).

Plugs were then grown out and hardened until they developed four true leaves after which time, they were transplanted on 13 December 2018 into 15.24-cm diameter (1.76 L) plastic pots filled with acid washed silica-sand (Millersville #2 (0.8 to 1.2 mm diameter) from Southern Products and Silica Co., Hoffman, NC) (Henry et al., (38)). Each pot received one rooted plug. At transplant fertility treatment regimens started.

After transplant, the plants were grown at 15.5/12.8 ± 2.8°C D/N temperatures (59.9/55.0 ± 5.04°F) day/night temperatures. On, 7 February 2019 the day temperature and night temperature were increased to 18.3/15.5 ± 3.1°C D/N temperatures (65/60 ± 5.58°F) respectively to encourage bolting with the bolting harvest occurring at 15 February 2019 and the flowering harvest occurring 1 March 2019. Plants were grown in an automated, recirculating irrigation system made from 10.2-cm diameter PVC pipe (Charlotte Plastics, Charlotte, NC), fit with 12.7-cm diameter openings to hold the pots (Henry et al., (38)). Plants were distributed into rows capable of holding either 8 or 6 pots with 6 rows blocked per group and 4 groups per bench with a total of four benches in the greenhouse. Each row received a different micronutrient fertility treatment with treatments distributed among benches, blocks, and lines using a randomized block design. Fertility micronutrient treatments were sub-divided into different concentrations (0, 25, 50, 75, 87.5, and 100%) of a modified Hoagland's Solution (Hoagland and Arnon, (40); Henry et al., (38); Barnes et al., (41)). Control plants were grown with (macronutrient concentrations in mM) 15 nitrate-nitrogen (NO_3^-), 1.0 phosphate-phosphorus ($H_2PO_4^-$), 6.0 potassium (K^+), 5.0 calcium (Ca^{2+}), 2.0 magnesium

(Mg^{2+}), and 2.0 sulfate-sulfur (SO_4^{2-}) plus (micronutrient concentrations in μM) 72 Fe (Fe^{2+}), 18 Mn (Mn^{2+}), 3 Cu (Cu^{2+}), 3 Zn (Zn^{2+}), 45 B (BO_3^{3-}), and 0.1 Mo (MoO_4^{2-}) (Hoagland and Arnon, (40)). Micronutrients were altered based on the above baselines. Complete listing of nutrients and rates are presented in Table 2.2.1. All nutrient solutions were tested and confirmed for concentrations using the North Carolina Department of Agriculture & Consumer Services (NCDA) testing lab using 50 mLs of the solutions after letting the concentrations sit for 48 hours after mixing (Raleigh, NC). Upon mixing more fertilizer solutions, each new batch was visually inspected for precipitates and the pH and EC were tested to ensure the values were within the desired ranges.

Plants were drip irrigated utilizing their assigned modified micronutrient solutions using a sump-pump (model 1A, Little Giant Pump Co., Oklahoma City, OK) system. Irrigations occurred every hour and ran for one minute between 6:00 and 19:00 hours. Irrigation solution drained from the pot and was captured for reuse with solutions being emptied and replenished weekly (Henry et al., (38)). For more details on the modified Hoagland's solution and the setup, please refer to Barnes et al., (41).

Plants were grown in their respective micronutrient treatments until either visual nutritive deficiency symptoms were observed, or the respective physiological stage was observed in over 50% of the control plants (100% Modified Hoagland's solution). Physiological stages for harvest were set at the rosette, bolting, flowering, and pod-set stages. Stages were determined using the decimal code (1.5-1.9: rosette, 3.0-3.3: bolting, 6.5: full flowering, 8.9-9.5: pod-set) developed by the SPARC working group (Appendix 1).

After the onset of initial visual deficient symptoms of each micronutrient treatment occurred, four symptomatic plants were selected and sampled. If visual symptoms did not develop, plants were harvested when over 50% of control plants reached physiological and morphological changes based on life cycle (SPARC,

Appendix 1). After sampling of the four replicates, the remaining plants (n=12) were grown to document symptomological and nutritive stresses into the remaining physiological stages. Thus, four more replicates were harvested when 50% of the control plants (100% of the concentration of the modified Hoagland's solution) reached bolting stage (SPARC, Appendix 1), and so on and so forth for the other physiological stages listed above.

For the four harvested replicates, most recently matured leaves were sampled to evaluate the critical micronutrient tissue concentrations for each fertility treatment and concentration. Plants were destructively harvested, and the most recently matured leaves were initially rinsed with deionized water, then washed in a solution of 0.5 M HCl for 1 min and again rinsed with DI water (Henry et al., (38)). The remaining shoot tissue was harvested separately, and roots were discarded.

Each harvest followed the above protocol with the exception of the final harvest (8.9 – 9.5: pod set; SPARC, Appendix 1) which had total dry mass taken and pods removed. For this harvest, total dry weight was taken by adding the plant biomass and the pod dry weights together. The remaining harvests had plant biomass data, symptomology, and most recently matured leaf tissue analysis taken for data at their respective physiological and morphological stages.

Upon sampling, the plant tissues were dried at 70 °C for 96 hours, and the dry mass was weighed and recorded. After drying, leaf tissue was ground in a Foss Tecator Cyclotec™ 1093 sample mill (Analytical Instruments, LLC; Golden Valley, MN; $\leq$0.5 mm sieve). The ground tissue was then placed in vials containing ~8 g of tissue and sent for analysis to AgSource Laboratories (Lincoln, NE). A composite sample was taken from the vial (0.250g $\pm$ 0.003g) and digested with nitric acid (12 M) at 60 °C. After the nitric acid digestion, 3 mLs of 30% hydrogen peroxide was added to the sample and further digestion took place at 120 °C. Upon cooling, the sample then was then diluted

to 25 mLs using a 20% hydrochloric acid solution. Analysis took place using an ICP-OES machine (Agilent 5110; Santa Clara, CA) using a 0.5 mL loop.

During the final harvest (24 April 2019), pods were removed from the plants by hand. Siliques were then dried in the greenhouse at 25.8 °C (78.5 °F) for 96 hours. After drying, the siliques were hand threshed to remove the seeds and the resultant seeds and chaff were then passed through a hand sieve (0.42 mm x 0.42 mm sieve) and a sub-sample (~5 g seed) of the total plant seed composite was taken. The sub-sample was then sent to be tested for fatty acid composition and seed metric analysis through Agrisoma Biosciences (Gatineau, QB, Canada).

Upon arrival, seed samples were dried at 40 °C in a hot air drier for 24 hours or until seed samples registered at < 6% moisture content. Samples were then placed in a FOSS XDS rapid content analyzer (Hilleroed, DK). The samples were non-destructively analyzed with sample spectra data being taken every 50 nm between 400 – 2499.5 nm. Every 50^{th} sample contained a sample with a known calibration and was tested against the reading to ensure proper readings. If sample values deviated more than 3 standard deviations from the known calibration level, the machine was re-calibrated.

Data from the analyzer was processed using ISIscan (Program version 4.10.0.15326, Database version 4.6.0.14416). Values for oil content were determined using nuclear magnetic resonance spectroscopy (NMR) using an Oxford MARAN Ultra (Witney, UK) using fresh carinata oil with a known oil value as a calibration baseline. The fatty acid composition was analyzed utilizing gas chromatography (Agilent 6890N; Santa Clara, CA) with the fatty acid methyl esters (FAMEs) protocol laid out by Taylor et al. (38). Values for glucosinolates were determined using values provided by the Canadian Grains Commission which were determined by a synthesis between their own equipment database values and the ISO 9167 method.

Machines and software were updated yearly to ensure optimal accuracy and calibration. Furthermore, validation and verification were completed, and an equation

developed, following analysis, of a subset of highly variable samples is analyzed using the same methods to determine the accuracy of the NIR methodology. These measurements were then used to produce the next generation of equations for the Agrisoma in-house predictive model. The resultant equations and reading were verified and compared to several institutions using their equipment. Values and equations tested and verified were within the acceptable range of variability from each seed batch randomly selected for verification from the different elements and concentrations.

Once tissue values, plant dry weights, and the oil profile information was obtained, data were analyzed using SAS program (version 9.4; SAS inst., Cary, NC). All leaf tissue mineral nutrition values and plant dry weights (tissue + rest of above ground plant biomass) were subjected to GLM using PROC GLM. The GLM procedure calculated the differences in means of the total plant dry weight and element and utilized the concentration as the predictor. Means were adjusted utilizing Tukey's multiple comparison test. The resultant report indicated which samples were statistically different from each other and are reported in the summary tables.

Data were then subjected to first and second order polynomial regression using PROC REG. Regression models treated the element as the y variable, and the concentration of fertility as the x variable. Each element was analyzed separately from the rest to eliminate any competition or enhancement that may have resulted from nutrient antagonisms or synergisms of uptake (see Mudler's Chart Appendix 1; Bariya et al., (42)). Regression models were compared, and the polynomial model which resulted in the greatest statistical significance (α = 0.05, 0.01, 0.001) and the greatest adjusted r^2 values were selected. The lipid data were analyzed utilizing the above methods.

Additionally, if data displayed a non-linear pattern in which a maximum value for leaf tissue or dry weights was obtained, PROC NLIN was utilized to determine the fertility values which resulted in the maximum values within the plateau. The general

equation forms for the models can be located in Appendix 1. The corresponding X_0 values indicated the predicted concentration at which the plant dry weight or leaf tissue nutrients were obtained, and the associated average dry weight or leaf tissue corresponding to that value (Henry, (43)).

Tables were populated with the means from the statistical outputs above. Figures were created using JMP (version 14.2.0; SAS inst., Cary, NC). Data are organized by element with concentrations modeling impacts on both dry weights and leaf tissue element concentrations. The data reports the means of each dataset with the associated r^2 and adjusted r^2 and regression polynomial equations presented.

2.3. RESULTS AND DISCUSSION

2.3.1. Boron (B)

Results varied by life-stages and across B concentrations. The impacts of B deficiency were observed acutely at the 0.00 and 11.25 μmol • L^{-1} B levels. The plants grown under 0.0 μmol • L^{-1} B did not reproduce due to the death of the apical meristem. Visual deficiency symptoms occurred at both B fertility concentrations (0.0 and 11.25 μmol • L^{-1}) across all life stages.

2.3.1.1. B Deficiency Symptomology

The first symptoms of B scarcity in carinata manifested as a general stunting and distortion of newly expanding leaves (Fig. 2.3.1). The upper foliage of the plant folded inward and downward creating a wilted leaf appearance, while new growth was distorted, creating a wrinkled leaf effect. Petioles and midribs of upper foliage, as well as new growth, also developed cracking (Fig. 2.3.2 & 2.3.3).

Under advanced B deficiency conditions, the leaf margins cupped inward (Fig. 2.3.3). As symptoms progressed, B deficiency resulted in death of the growing tip (Fig. 2.3.4) and release of axillary shoots (Fig. 2.3.5). As B continued to be limited, axillary shoots became necrotic, and the plant eventually died.

2.3.1.2. Rosette Stage B Rates

Rosette plants varied in the distribution of their dry weights based on B fertility concentrations. Total plant dry weight increased as B concentrations increased (Table 2.3.1, Graph 2.3.1). The quadratic model accounted for 73.3% of the data when treating dry weight as the dependent variable and B fertility concentration as the predictor (Graph 2.3.1). The lowest concentration (0.00 μmol • L^{-1} B) produced less biomass when compared to the next three highest concentrations (11.25, 22.50, 33.75 μmol • L^{-1}). The two highest concentrations (39.38 and 45.00 μmol • L^{-1} B) produced the greatest biomass when compared to all other values. (Table 2.3.1, Graph 2.3.1).

Leaf tissue B concentration exhibited a plateau at 11.25 μmol • L^{-1} B concentration. The lowest B concentration (0.00 μmol • L^{-1}) contained 81.2% less B than the control at 45.0 μmol • L^{-1} B (Table 2.3.1, Graph 2.3.1). When modeling the impacts of B fertility on leaf tissue accumulation, a quadratic model provided the best interpretation of the variance within the study (Equations 2.3.1).

Limited literature quantifies nutrient and dry weight concentrations of Brassicas sp. at different stages of growth, with two studies reporting a strong increase in final yield with B applications (Matoh, (44); Nuttall et al., (45)). The lack of response in plant leaf tissue accumulation of B above the 11.25 μmol • L^{-1} concentration was most likely due to the utilization of B within the plant. Boron is utilized at a much higher concentration during periods of rapid cell expansion and growth. Boron is primarily found in the cell wall contained within the B-dimeric rhamnogalacturonan II (RG-II) complex (Matoh,

(43)). Within this complex, both B and Ca help to stabilize the structure, and allow the complex to carry out its function of creating calcium ion bridges between the pectin chains within the cell wall (Chebli and Geitmann, (46); Matoh, (44)). When the RG-II complex was monomeric and the cell walls swelled rather than differentiating polarly (Matoh, (43)). It may be, that given the stabilizing nature of the RG-II complex plays within the cell wall and stabilizing the pectin matrix, the cells may cannot expand properly or directionally. This role may explain the early plateau observed in the leaf tissue B concentrations of the rosette stage.

2.3.1.3. Bolting Stage B Rates

Bolting plants within the B treatments manifested visual deficiency symptoms only at the 0.00 μmol • L^{-1} concentration. Plants grown with 0.00 μmol • L^{-1} B resulted in young and expanding leaves with necrosis of the apical meristem (Fig. 2.3.4 & 2.3.5). The necrosis resulted in proliferation of axillary shoots which displayed stunting and severe distortion (Fig. 2.3.1 & 2.3.3).

An increasing trend in total plant dry weights occurred from the 0.00 to 11.25 and 22.5 μmol • L^{-1} B rates. All concentrations greater than the 11.25 μmol • L^{-1} B were statistically similar, and all were greater as compared to 0.00 μmol • L^{-1} B treatment (Table 2.3.1, Graph 2.3.1). Regression analysis demonstrated a quadratic model provided greater explanatory power of the dependent variable when compared to a linear model (Equations 2.3.1).

Leaf tissue B concentration exhibited a quadratic increase as B fertility increased (Table 2.3.1, Graph 2.3.1) with the two lowest concentrations (0.0 and 11.25 μmol • L^{-1} B) being statistically different from each other, the 22.50 and 33.75 μmol • L^{-1} B treatments were statistically similar, and the next two highest concentrations (39.38 and 45.00 μmol • L^{-1} B) as a pair also being statistically similar (Table 2.3.1, Graph 2.3.1). The highest B

leaf tissue concentration occurred at the 39.38 μmol • L^{-1} B (Table 2.3.1, Graph 2.3.1). While the linear and quadratic models were similar, the quadratic model should be utilized given a plateau in leaf tissue B was observed in both the rosette and flowering stages (Graph 2.3.1).

These results indicate during times of rapid cell growth and expansion, B requirements are much higher given B's role in cell development. The greater need for B resources was reported at the lowest B fertility concentration of 0.0, though plants did not exhibit a complete loss of yield, despite a small amount of B being applied to prevent complete yield loss (Yang et al. (47)). Yang's work demonstrates that under-applying B can negatively impact plant biomass production and potentially result in complete yield loss if corrective measures are not taken.

2.3.1.4. Flowering Stage B Rates

Flowering plants mirrored the bolting stage plateau at 11.25 μmol • L^{-1} B for dry weights (Table 2.3.1, Graph 2.3.1) indicating bolting and flowering carinata plants require the same concentrations of B fertility to maximize biomass production. Leaf tissue B concentration modeled an increasing trend as B concentrations increased (Table 2.3.1, Graph 2.3.1). Leaf tissue B concentrations were statistically significant between the lowest concentration and the remaining concentrations. A quadratic model accounted 84.0% of the variation within the dataset when treating leaf tissue B as the dependent variable and B fertility concentration as the predictor (Equations 2.3.1).

As stated earlier, B is important for proper cell wall formation and cellular development and expansion. Thus, the lack of silique and seed formation at the lowest rate (0.00 μmol • L^{-1} B) indicates concentrations above 11.25 μmol • L^{-1} B should be targeted for the rosette and flowering stages increasing to 22.50 μmol • L^{-1} B for the bolting stage to optimize biomass.

2.3.1.5. Lipidome Impacts B Rates

Seed analysis resulted in no discernable difference in the lipidome and seed constituents except for the distribution of glucosinolates and eicosenoic acid (20:1) (Table 2.3.7). The lowest fertility concentration resulted in death of the apical meristem (Fig. 2.4) and consequently no yield (Table 2.3.7). While distribution of glucosinolates within the seeds showed statistical differences, no discernable trend was observed among the fertility concentrations (Table 2.3.7).

Similarly, the lowest value of eicosenoic acid occurred at the highest B fertility concentration (Table 2.3.7). The highest eicosenoic acid levels occurred with 11.25 μmol • L^{-1} B and was statistically different from the highest B fertility concentration but was statistically similar across all other values (Table 2.3.7).

The impact of B fertility with regards to fatty acids resulted in statistically significant variances but displayed no clear trend regarding B fertility (Table 2.3.7). These results mirrored the work done by Nuttall et al. (45) which reported no change in glucosinolate levels in canola seeds at a 0 and 1.4 kg • ha^{-1}. The values of glucosinolates in this study were much lower than values reported in reference values for carinata seeds which average 92.9 μmol • g^{-1} from Nattall et al. (45) and 7.6 and 12.3 μmol • g^{-1} (Mulvaney et al., (48)).

Both canola and carinata are grown for oil, however, their seeds vary in fatty acid distribution. Carinata is grown specifically for its high concentrations of LCFA and VLCFA and, more specifically, high erucic acid levels (Seepaul et al., (6); Mulvaney et al., (48)). Thus, any comparison of fatty acids, oil content or protein content should be interpreted loosely within *B. carinata* data and care should be taken when comparing among other oilseed brassicas such as *Brassica napus*, *B. rapa*, and B. nigra, B. oleracea, and B. juncea (Seepaul et al., (12)).

Therefore, the differences observed in the erucic acid levels should be interpreted within the species or conservatively within the genus. Work by Mulvaney et al., (47) quantified the general lipid values that carinata seed possess in their study. This work serves as a reference value for carinata seed constituents. Regarding erucic acid, the values observed for the B concentrations in this study were much lower than values reported (Mulvaney et al., (48)). The differences in the pool of erucic acid may be the result of synthesis of the molecule itself given erucic acid is synthesized from the pool of oleic acid (Bao et al., (49)). The pool of oleic acid within the seeds was statistically similar regardless of B concentration and thus, the differences would indicate another regulator of production of erucic acid may be at play such as genetic controls (Ecke et al., (50)). Additionally, differences in carinata growth and fatty acid compositions were reported when comparing greenhouse trials to field trials (Mulvaney et al. (48), Seepaul et al., (6)).

2.3.2. Iron (Fe)

Iron treatment values displayed inconsistent results despite visual symptomology being present at the lowest (0.0 μmol • L^{-1} Fe) fertility concentrations at all life stages.

2.3.2.1. Fe Deficiency Symptomology

The first symptom of Fe scarcity in carinata was interveinal chlorosis of the upper foliage (Fig. 2.3.6). During the bolting stage, upper leaves along the flower spikelet displayed interveinal chlorosis. which continued into flowering and pod set (Fig. 2.3.7). Under Fe deficient conditions nutritive stress was present at all carinata life stages.

2.3.2.2. Rosette Stage Fe Rates

Rosette plants varied in the distribution of their dry weights based on Fe fertility concentrations. Total plant dry weight increased as Fe concentrations increased (Table

2.3.2, Graph 2.3.2). The lowest concentration (0.00 μmol • L^{-1}) was statistically smaller than all other concentrations except for the 36.00 μmol • L^{-1} Fe. The quadratic model interpreted the greatest amount (0.67) of the variance in plant dry weights (Equations 2.3.2).

Leaf tissue Fe values were statistically similar for the rosette stage. This may indicate that a potential contamination occurred at the lowest treatment given leaf tissue Fe concentrations increased after this treatment despite the increase being statistically insignificant (Table 2.3.2).

During the rosette stage, differences were observed in total plant dry weights, however, when those values were compared to the leaf tissue values, none of the values varied statistically from each other. Given the solutions were replaced weekly, and the tested values for the solutions were within the target ranges, some other contamination or physiological impact may have been present. Given this was a 0.00 μmol • L^{-1} concentration and the solution utilized provided no Fe, it seems likely that the lack of growth with the 0 μmol • L^{-1} rate resulted in a concentration of Fe within the leaf tissue. This concentration effect is reflected in the higher Fe values at this rate when compared to the lower plant biomass. The dilution effect has been reported extensively in other crops (Bryson et al., (51)). Additionally, brassicas are very effective at scavenging nutrients from the soil profile (Chen et al., (52)). This scavenging of nutrients could have resulted in a higher Fe seed load which were higher in concentration given the dilution effect discussed above.

Additionally, in a study conducted by Wu et al. (53), a half strength Hoagland's solution was utilized to grow 111 different *Brassica napus* ascensions to explore the differences in accumulation of Zn, Fe, and Mn. They reported different individuals accumulated a wide range of leaf tissue concentrations of 60.3 – 350.1 μg • g^{-1} Fe even with half strength Hoagland's solution. The leaf tissue Fe values reported by Wu were much higher than our reported values. Given Wu's experiment utilized a half-strength

Hoagland's solution for 14 days, and certain brassica ascensions accumulated leaf tissue values within our ranges, it may be that *B. carinata* is efficient at scavenging Fe given a week of wrongful fertility was most likely experienced (Chen et al., (52)).

2.3.2.3. Bolting Stage Fe Rates

Bolting plants varied in the distribution of their dry weights and leaf tissue Fe based on Fe fertility concentrations with the only statistically significant interaction being among the 18.0, 63.0, and 72.0 μmol • L^{-1} Fe concentrations when compared to 36.0 μmol • L^{-1} Fe concentration which had the lowest dry weight values (Table 2.3.2, Graph 2.3.2).

Leaf tissue Fe concentrations were similar except for the 63.00 μmol • L^{-1} Fe concentration which contained almost double the leaf tissue Fe concentration when compared to other rates (Table 2.3.2, Graph 2.3.2). Regression models for the plant dry weights and the leaf tissue concentrations each provided little explanatory power and in the case of the plant dry weights and resulted in statistically insignificant modeling (Equations 2.3.2).

The lowest fertility rates in both the bolting and flowering stages contained higher concentrations of Fe than observed at the rosette stage. The higher Fe values could be the result of a dilution effect given the bolting stage plants weighed over 26 times greater than the smaller rosette stage plants (Table 2.3.2).

2.3.2.4. Flowering Stage Fe Rates

Flowering plants produced statistically similar dry weights regardless of Fe concentration. Leaf tissue Fe concentration only displayed statistical differences between the 63.00 μmol • L^{-1} Fe concentration and all other concentrations except the 54.00 μmol • L^{-1} concentration which was statistically similar (Table 2.3.2, Graph 2.3.2). The highest Fe leaf tissue concentrations were observed at the 63.00 μmol • L^{-1}. Except for the 72.00

μmol • L^{-1} concentration, there is an increasing trend of leaf tissue Fe accumulation with increasing fertility. Regression models from these confounding results only accounted for 25.0% (linear) and 30.0% (quadratic) of the variation when treating leaf tissue Fe as the dependent variable and Fe fertility concentration as the predictor (Equations 2.3.2).

2.3.2.5. Lipidome Impacts Fe Rates

Seed analysis resulted in some statistical differences in protein content and the eicosenoic acid content though no discernable trend was detected (Table 2.3.8). Given the visual Fe deficiency symptomology, results indicate rates above the 18.0 μmol • L^{-1} treatment should be utilized to avoid Fe stress.

2.3.3. Copper

2.3.3.1. Cu Deficiency Symptomology

The visual impacts of Cu deficiency were not present even at the lowest fertility concentrations across all life stages. Despite the lack of visual deficiency symptoms, a strong impact occurred in the response of leaf tissue to Cu concentrations across all life stages.

2.3.3.2. Rosette Stage Cu Rates

Rosette plants varied in dry weights based on Cu fertility concentrations, but with no discernable trend as Cu concentrations increased (Table 2.3.3, Graph 2.3.3). The regression models resulted in no statistically significant results for either linear or quadratic models for the relationship between plant dry weight and Cu fertility (Equations 2.3.3).

Despite the lack of a discernable trend within the plant dry weights, the leaf tissue Cu concentration exhibited an increasing trend in Cu with the exception of the 2.25 μmol

• L^{-1} Cu which was slightly lower than the 1.50, 2.63, and 3.00 μmol • L^{-1} concentrations (Table 2.3.3, Graph 2.3.3). The lowest Cu concentration (0.00) differed significantly from all other concentrations and was the lowest recorded value (Table 2.3.3, Graph 2.3.3). The highest Cu leaf tissue value occurred at the highest concentration and was significantly higher than the lowest concentration, the 0.75 μmol • L^{-1} concentration, and the 2.25 μmol • L^{-1} Cu, but was statistically similar to the remaining treatments (1.50 and 2.63 μmol • L^{-1} Cu) (Table 2.3.3, Graph 2.3.3). The quadratic regression model accounted for the most variability when treating leaf tissue Cu as the dependent variable and Cu fertility concentration as the predictor (Table 2.3.3).

These results indicate increasing Cu levels may not result in a consistent increase in plant dry weight at the rosette stage, despite an increase accumulation of leaf tissue Cu levels. Among the Cu treatments, many growth metrics were maximized at lower fertility levels indicating that carinata may require less Cu fertility than other brassica crops (Gibson et al., (10)).

2.3.3.3. Bolting Stage Cu Rates

Bolting plant dry weights modeled best on a parabolic trend with the middle concentrations forming the vertex and the lowest and highest concentrations forming the tails though the quadratic model interpreted only a low proportion of the data accurately (Table 2.3.3, Graph 2.3.3). Given the variability of the dry weights, and the low statistical significance, the models presented should be used with only a small degree of certainty (Equations 2.3.3).

Leaf tissue Cu concentration exhibited an increasing trend in Cu concentration except for the 2.63 μmol • L^{-1} Cu (Table 2.3.3, Graph 2.3.3). Leaf tissue Cu concentration was lowest at 0.0 μmol • L^{-1} Cu and was statistically less than all other concentrations.

The three highest concentrations (2.25, 2.63, and 3.00 μmol • L^{-1} Cu) were all statistically similar (Table 2.3.3, Graph 2.3.3).

The results observed at the bolting stage regarding plant dry weights indicate an optimization of leaf tissue Cu would be obtained when plant leaf tissue is at 7.34 mg · kg^{-1} (Table 2.3.3, Graph 2.3.3). These results indicate that during times of rapid cell growth and expansion, the Cu requirements of the plant vary little from the Cu needs at the rosette stage.

This may be indicative of the role of Cu in plants. Most of the Cu contained within plants is utilized in the chloroplasts as plastocyanin (Marschner, (54)). The main role of this protein is to assists in the electron transport chain in the Photosystem I complex. A study conducted with Pisum sativum plants showed a decrease of 87.5% of plastocyanin resulted in a decrease of photosynthetic electron transport from 100 to 19 (nmol • μmol^{-1} chlorophyll) between leaf Cu fertility concentrations of 6.9 to 2.2 μmol • g^{-1} respectively (Ayala et al., (55)). Additionally, this study reported a decrease in other Cu-related enzymes with a marked decrease in activity of diamineoxidase, ascorbateoxidase, and CuZnSOD. Given most photosynthates are produced in the rosette and bolting stage, the data implies that the Cu containing molecules within brassicas will be most active during these stages (Khan et al., (56); Ayala et al., (57); Marschner, (54)).

After initiation of flowering, the sources and sinks within brassicas are altered significantly (Khan et al., (56)). Thus, the limiting factors within the flowering stage would be more regulated based on other predictors such as photosynthates and Cu fertility.

2.3.3.4. Flowering Stage Cu Rates

Flowering plant models indicated a general increasing trend in dry weights with regard to Cu fertility with the exception of the 0.75 and 1.50 μmol • L^{-1} Cu which

displayed upper and lower outliers of the general trend, respectively (Table 2.3.3). The upper three concentrations (2.25, 2.63, and 3.00 μmol • L^{-1}) were all statistically similar and the highest Cu values were present in the 1.50 μmol • L^{-1} concentration. The lack of a clear trend is reflected in the low adjusted r^2 values within the linear and regression models (0.30 and 0.36 respectively).

Leaf tissue Cu concentration also exhibited a general increasing trend as Cu concentrations increased except for the 2.63 μmol • L^{-1} concentration (Table 2.3.3, Graph 2.3.3). Leaf tissue Cu concentration were statistically significant between the lowest concentration and the remaining concentrations apart from the 0.75 concentration which was statistically similar (Table 2.3.3, Graph 2.3.3). The highest Cu leaf tissue concentration occurred at 2.25 μmol • L^{-1}.

A strong plateau was observed within this dataset indicating optimal uptake for plant leaf tissue Cu may be at 1.50 μmol • L^{-1} Cu (Table 2.3.3, Graph 2.3.3). These results also indicate that Cu may be less regulating in the flowering stage than in the rosette stage.

2.3.3.5. Lipidome Impacts Cu Rates

Seed analysis resulted in inconsistent difference in the lipidome and seed constituents except with regard to the distribution of protein concentration, monosaturated fatty acids, eicosenoic acid, long chain fatty acids, and very long chain fatty acids (Table 2.3.9). Statistical differences occurred in the protein concentration of the 1.50 μmol • L^{-1} Cu concentration when compared to the 2.63 μmol • L^{-1} concentration, which was lower. All other trends within protein concentrations were similar to each other (Table 2.3.9).

While statistical differences were present within the distribution of monosaturated fatty acids, the only statically significant difference occurred between the lowest Cu

concentration 1.50 μmol • L^{-1} Cu with the highest concentration of monosaturated fatty acids being associated with the lowest Cu fertility concentration (Table 2.3.9).

The lowest value of eicosenoic acid occurred at the lowest Cu fertility concentration and was statistically different from the 0.75, 1.50, and 2.25 μmol • L^{-1} concentrations, but were similar to the remaining concentrations (Table 2.3.9). The highest value of eicosenoic acid was observed at the 2.25 μmol • L^{-1} concentration.

The distribution of LCFA displayed no discernable trend regarding Cu fertility concentration (Table 2.3.9). The highest concentration of LCFA was observed in seeds from the 1.50 μmol • L^{-1} Cu treatment and was statistically higher than the 0.0 μmol • L^{-1} Cu and the 2.63 μmol • L^{-1} Cu, which were all lower. The remaining concentrations had similar values to the 1.50 μmol • L^{-1} concentration (Table 2.3.9).

The VLCFA concentration in the seeds of different fertility treatments little to no trend among fertility concentrations (Table 2.3.9). The lowest concentration of VLCFA was found in the 1.50 μmol • L^{-1} Cu treatment and was statistically different from 2.63 and 0.0 μmol • L^{-1} Cu, which were both higher. The remaining Cu concentrations had similar seed values for VLCFA (Table 2.3.9).

The impact of Cu fertility on seed quality resulted in statistically significant variances but displayed no clear trend regarding concentrations (Table 2.3.9). Nuttall et al. (45) reported similar results with no change in glucosinolate levels in canola seeds at 0 and 1.4 kg • ha^{-1} Cu. The values of glucosinolates in Nutall's study were much lower than values observed in carinata seeds, which average 92.9 μmol • g^{-1} when compared to the reference values of 7.6 (Nuttall et al., (45)) and 12.3 μmol • g^{-1} (Mulvaney et al., (48)).

Additionally, the lack of predictive power of Cu fertility concentrations on seed constituents and the lipidome may be explained by the role of Cu within the plant. Cu is responsible for the formation of polypeptides in the PS II factor (Dropa et al., (58)). This limitation of Cu will impact the lipidome by favoring the formation of less unsaturated fatty acids given Cu's function in desaturation of LCFA (Ayla et al., (57); Wahle and

Davies, (59)). This relationship was not observed in the distribution of linoleic (18:2) or α-linolenic (18:3) fatty acid chains in the seeds with regard to Cu fertility and did not occur in the survey of *B. carinata* seed and lipidome constituents (Mulvaney et al., (48)). The lack of changes in the seed constituents and lipidome makeup again point to the possibility of external regulations to carinata regarding mineral nutrition (Ecke et al., (50))

2.3.4. Zinc (Zn)

Limited symptomology occurred with Zn which manifested as a slight decrease in bolting vigor and branching when compared to the controls. After the initiation of the reproductive phase, the sources and sinks changed within the plants and growth slowed given carinata is determinant.

2.3.4.1. Zn Deficiency Symptomology

Deficiency symptoms of Zn were only present with 0.00 μmol • L^{-1} Zn. Zinc deficiency symptoms were observed later in carinata growth compared to other nutrients. Zinc deficient plants appeared large and healthy, and displayed only subtle signs of nutritive stress (Fig. 2.3.8). Symptomology appeared on the mid to upper foliage as a slight paling of the leaf margin and gall-like structures (Fig. 2.3.9). As symptoms advanced, the slight yellowing or paling progressed to a slight purple coloration on the margin of the leaves (Fig. 2.3.9).

2.3.4.2. Rosette Stage Zn Rates

Rosette plants exhibited no discernable pattern or trend among Zn treatments with total plant dry weight varying greatly as Zn concentrations increased (Table 2.3.4, Graph 2.3.4). The highest Zn concentration (3.00 μmol • L^{-1}) had the greatest dry weight and was

statistically significant from the other concentrations except for the 2.25 μmol • L^{-1} concentration which was larger than other treatments (Table 2.3.4, Graph 2.3.4).

Leaf tissue Zn levels increased until the 2.25 μmol • L^{-1} Zn concentration after which point all other concentrations were statistically similar (Table 2.3.4, Graph 2.3.4). Both a linear and quadratic regression model accounted for little variance within the Zn leaf tissue values (Equations 2.3.4, Graph 2.3.4). However, there was a strong quadratic trend regarding increasing Zn concentration and plant biomass production. The plateau in leaf tissue at 2.25 μmol • L^{-1} Zn indicates a greater Zn fertility requirement for *B. carinata* in the rosette stage.

The differences observed in Zn uptake in the rosette stage could be a result of the growth stage and the physiological function of Zn within the plant. The major role of Zn within plant cells and functions aremainly enzymatic activity (Vallee and Auld, (60); Vallee and Falchuk, (61)) and regulation of genetic expression and replication (Coleman, (24)).

There are also indications that when Zn levels are elevated, the phloem could absorb and store Zn within the plant (Kochian, (62)). This storage ability in Zn concentrations may have resulted in an unexpectedly higher value of Zn within the leaf tissue during the rosette stage.

2.3.4.3. Bolting Stage Zn Rates

Bolting plants resulted in no discernable trends among Zn concentrations. The dry weights varied greatly with the lowest dry weight occurring at 0.75 μmol • L^{-1} concentration and being statistically similar to 1.50 and 2.63 μmol • L^{-1} Zn levels. The highest dry weights were observed at 2.25 μmol • L^{-1} Zn and were statistically similar to the 0.00, 1.50, and 3.00 μmol • L^{-1} Zn treatments (Table 2.3.4, Graph 2.3.4).

Leaf tissue Zn levels exhibited an increasing trend until 0.75 μmol • L^{-1} Zn concentration after which leaf tissue values plateaued (Table 2.3.4, Graph 2.3.4).

In the bolting stage, the plant dry weights displayed no discernable trend despite some significant differences (Table 2.3.4, Graph 2.3.4). This is not surprising given the extreme variability in bolting times observed within the Zn treatments. Zinc requirements may be lower in the bolting stage given the plateau occurred at a lower Zn concentration when compared to the rosette stage.

At the bolting stage, the lack of statistical significance within plant above ground biomass was not surprising. At the rosette stage, *B. carinata* has a very compact growth habit (Seepaul et al., (6)). When bolting occurs, a very rapid vertical flower spikelet and branching architecture results. Additionally, brassicas can vary greatly in their bolting vigor and timing (Ajisaka et al., (63)). Thus, the lower plateau observed at the concentrations above 0.75 μmol • L^{-1} Zn may indicate a dilution effect given biomass increased greatly during the bolting stage or simply differences in bolting time among plants. The lack of statistically significant trend regarding dry weights may indicate that factors other than nutritive stress play a larger regulating role in bolting *B. carinata*.

2.3.4.4. Flowering Stage Zn Rates

Flowering plant dry weights plateaued at 1.50 μmol • L^{-1} Zn including all higher concentrations. The lowest dry weight occurred at 0.75 μmol • L^{-1} Zn.

Leaf tissue Zn concentration mirrored the plateau at 0.75 μmol • L^{-1} Zn regarding leaf tissue Zn at the bolting stage (Table 2.3.4, Graph 2.3.4). Leaf tissue Zn concentration was lowest at 0.00 μmol • L^{-1} which was statistically different from all other concentrations (Table 2.3.4, Graph 2.3.4).

While plant dry weights did not display a clear trend, the explanatory power of the Zn fertility was apparent. The plateau observed at the 0.75 μmol • L^{-1} Zn for both the

bolting and flowering stage may be due to the role of Zn in many enzymatic functions within the plant. Work done by Cakmak and Marschner (29) reported when cotton plants were subjected to Zn deprivation conditions, activity of superoxide dismutase (SOD) within the roots decreased and a resultant increase in superoxide oxygen radicals occurred. Additional work by the above authors also reported a decrease in NADPH production of oxides, plasma membrane permeability, and differences in nutrient uptake and partitioning under Zn deficient conditions (Cakmak and Marschner, (29, 64, 65)). Given many of the above impacts are on enzymatic driven processes, the lower concentrations of Zn could indicate that said functions are optimized at 0.75 μmol • L^{-1} Zn.

2.3.4.5. Lipidome Impacts Zn Rates

Seed analysis resulted in limited discernable differences in the lipidome and seed constituents including differences in oil content, polyunsaturated fatty acids, and eicosenoic acid (20:1). While statistical differences were present within the distribution of oil content within the seeds, no discernable trend occurred among the fertility concentrations. The lowest oil content values were observed in the lowest fertility concentration and were statistically different from the oil values of the seeds from the 0.75 and 2.63 μmol • L^{-1} Zn (Table 2.3.10).

The distribution of polyunsaturated fatty acids at 0.00, 1.50, 2.25, and 3.00 μmol • L^{-1} Zn were all statistically similar. The highest polyunsaturated value occurred in the seed produced under 2.63 μmol • L^{-1} Zn and was statistically different from 0.75 μmol • L^{-1} concentration.

The highest Zn fertility treatment resulted in the lowest concentration of eicosenoic acid which differed from the 1.50, 2.25, and 2.63 μmol • L^{-1} concentrations, despite being similar the 0.75 and 0.00 μmol • L^{-1} Zn concentrations. This may point to a

negative relationship of Zn fertility regarding eicosenoic acid content with higher values occurring at the middle (1.50, 2.25, and 2.63 μmol • L^{-1}) fertility concentrations and lower values being observed at the lowest concentrations (Table 2.3.10).

The inconclusive results observed in the fatty acid profile of the *B. carinata* seeds was inconsistent with work by Cakmak and Marschner (65), which reported a strong increase in fatty acids (both saturated and unsaturated) in Zn deficient cotton plants after 12 hours of deficiency treatments. Given the timeframe tested in the above study was much shorter than this study, after prolonged Zn deficiency occurs, the plant could potentially produce fewer fatty acids.

2.3.5. Molybdenum (Mo)

2.3.5.1. Mo Deficiency Symptoms

Visual deficiency symptoms of Mo did not manifest at any concentration or stage of development despite significant differences in leaf tissue levels. Molybdenum overall, resulted in a linear increase in plant biomass regarding concentration at the rosette stage, and no discernable trends occurred at the bolting or flowering stages. Regarding leaf tissue Mo concentration, however, a strong linear increase was found between increasing Mo concentrations and Mo leaf tissue concentrations in the rosette and bolting stages (Equations 2.3.5). However, in the flowering stage the model resulted in a platea regarding Mo accumulation.

2.3.5.2. Rosette Stage Mo Rates

Rosette plants varied in the distribution of their dry weights based on Mo fertility concentrations. Total plant dry weight when modeled against Mo concentrations displayed no discernable trend (Table 2.3.5, Graph 2.3.5). Leaf tissue Mo levels were

similar for all treatments with only the highest concentration showing higher Mo concentrations in leaf tissue as compared with 0.0 μmol • L^{-1} Mo (Table 2.3.5, Graph 2.3.5).

2.3.5.3. Bolting Stage Mo Rates

Bolting plants varied in the distribution of their dry weights and leaf tissue Mo based on fertility concentrations. The only statistical significance occurred between the 0.00 and 0.025 μmol • L^{-1} Mo treatments with the latter having a smaller dry weight than the former. From the 0.050 μmol • L^{-1} Mo to the highest concentration, no statistical differences occurred among concentrations (Table 2.3.5, Graph 2.3.5).

Leaf tissue Mo concentration exhibited an increasing trend as concentrations increased (Table 2.3.5, Graph 2.3.5). Leaf tissue Mo concentration increased with the lowest three concentrations (0.0, 0.025, and 0.05 μmol • L^{-1} Mo) being statistically similar (Table 2.3.5, Graph 2.3.5). The next two highest concentrations (0.075 and 0.088 μmol • L^{-1} Mo) were statistically similar to each other but were significantly higher in Mo leaf tissue levels when compared to the 0.00 μmol • L^{-1} Mo. The highest Mo concentration (0.10 μmol • L^{-1}) resulted in the highest Mo levels within the leaf tissue and were statistically significant from only the three lowest concentrations (Table 2.3.5, Graph 2.3.5).

2.3.5.4. Flowering Stage Mo Rates

In the flowering plants no significant increase or decrease in their flowering dry weights among Mo concentrations (Table 2.3.5, Graph 2.3.5).

Despite a lack of statistical significance in the plant dry weights, leaf tissue Mo concentration resulted in an increasing trend as Mo concentrations increased up to the 0.05 μmol • L^{-1} Mo treatment above which all leaf tissue values were statistically similar (Table 2.3.5, Graph 2.3.5). The similarity of the plant biomass production among Mo concentrations and life stages may indicate that only a minimal threshold of Mo is

required to benefit *B. carinata*. It has been reported that Mo mainly provides benefits to nodulating, and leguminous crops despite also being used in the xanthine oxidase/dehydrogenase reaction in plants (Vunkova-Radeva et al., (66)). While other crops receive great benefit from Mo, the extremely low concentrations required by the plant often dictate that Mo will be adequate from ambient sources within the soil.

2.3.5.5. Lipidome Impacts Mo Rates

Seed analysis resulted in no discernable difference in the lipidome and seed constituents except in the distribution of eicosenoic acid (20:1). The highest concentration of eicosenoic acid resulted in the seeds produced under 0.088 μmol • L^{-1} Mo (Graph 2.3.11). The lowest and highest fertility concentrations (0.0 and 0.10 μmol • L^{-1} Mo) resulted in the lowest values of eicosenoic acid and were statistically similar to each other. The eicosenoic acid content of the 0.025, 0.050, and 0.075 (μmol • L^{-1} Mo) fertility treatments were all statistically similar but were statistically different only from the 0.088 μmol • L^{-1} Mo which contained higher eicosenoic acid concentrations (Graph 2.3.11).

Given most micro elements explored in this study resulted in an increase in eicosenoic acid content with increasing fertility, the regulatory pathway for this fatty acid could simply be up regulated by increasing mineral resources. Alternatively, the regulation of eicosenoic acid could be genetically regulated as was postulated by Kondra and Stefansson (67) and thus not tied to mineral resources.

2.3.6. Manganese (Mn)

Results varied by life-stages and across Mn concentrations. Very little differences occurred among the dry weights for different growth stages and concentrations. Mn data overall, resulted in no discernable trend regarding plant dry weight at the rosette stage, and no differences were observed at the bolting or flowering stages. Regarding leaf tissue

Mn concentration, however, an increase up to the 13.50 and 15.75 μmol • L^{-1} occurred with the highest rate resulting in a lower Mn tissue level than the above two rates (Table 2.3.6, Graph 2.3.6). Regarding the increasing Mn fertility concentration and leaf tissue concentrations in the rosette and bolting stages, a plateau occurred in the bolting stage at the 9.00 μmol • L^{-1} Mn concentration. In the flowering stage, the plateau occurred at the 13.50 μmol • L^{-1} Mn (Table 2.3.6, Graph 2.3.6). The impacts of Mn deficiency were visible later in the rosette stage and were present at the two lowest concentrations tested.

2.3.6.1. Mn Deficiency Symptomatology

Deficiency symptoms of Mn were observed later in growth trials than most other nutrients. Manganese is an immobile element and thus cannot translocate from the lower foliage to the upper foliage and deficiency symptoms will manifest in the newer developing leaves. Plants were in the advanced stages of vegetative growth exhibiting a general paling of the entire plant when compared with the control (Fig. 2.3.10). This paling was more pronounced on the mid and upper foliage (Fig. 2.3.11).

2.3.6.2. Rosette Stage Mn Rates

Rosette plants varied in the distribution of their dry weights based on Mn fertility concentrations. Total plant dry weight exhibited no distinct trend with the increase of Mn fertility (Table 2.3.6, Graph 2.3.6).

Leaf tissue Mn concentrations displayed an increasing trend as Mn fertility increased. The lowest Mn values occurred at the 0.00 μmol • L^{-1} Mn concentration and were statistically smaller than all other treatments (Table 2.3.6, Graph 2.3.6). The highest Mn values were observed in the 15.75 μmol • L^{-1} Mn treatment and were statistically similar to the 13.50 μmol • L^{-1} Mn and significantly higher than the other Mn treatments (Table 2.3.6, Graph 2.3.6). Regression models indicated that a quadratic model accounted

for more variability in the dataset when Mn fertility concentration was treated as the independent variable (Equations 2.3.6). The decrease in Mn leaf tissue concentrations at 18.0 μmol • L^{-1} Mn may indicate that a sigmoidal model is present with the vertex being at the 13.5 and 15.75 μmol • L^{-1} Mn treatments (Table 2.3.6, Equations 2.3.6, Graph 2.3.6).

2.3.6.3. Bolting Stage Mn Rates

Bolting plants displayed no differences in dry weights among Mn concentrations. However, leaf tissue Mn concentration exhibited an increasing trend as Mn fertility increased (Table 2.3.6, Graph 2.3.6). Leaf tissue Mn concentration was lowest at 0.0 μmol • L^{-1} Mn and was statistically smaller than all other concentrations. The second lowest Mn leaf tissue later occurred at 4.50 μmol • L^{-1} Mn and was statistically smaller than the higher concentrations. The next four concentrations (9.00, 13.50, 15.75, and 18.00 μmol • L^{-1} Mn) were all statistically similar, indicating a plateau in leaf tissue Mn accumulation (Table 2.3.6, Graph 2.3.6). A polynomial regression model accounted for 88% of the variability of leaf tissue Mn concentration when Mn fertility concentration was treated as the independent variable (Equations 2.3.6)

These results may indicate that at earlier stages (rosette) of growth, Mn is more important to the plant. The low r^2 value (0.075) of the polynomial regression of plant biomass at the bolting stage may indicate that other factors regulate bolting more strongly than Mn concentrations. This makes sense given the role of Mn in the plant as the manganese-protein in photosystem II (PS II) as well as in the superoxide dismutase (MnSOD) (Jackson et al. (68)). This indicates that Mn may have a greater impact on photosynthesis and the resultant photosynthates produced in the plant rather than directly regulating plant cellular growth and expansion.

2.3.6.4. Flowering Stage Mn Rates

Flowering plant data did not report any statistical differences in their dry weights among concentrations (Table 2.3.6, Graph 2.3.6).

Leaf tissue Mn increased with increasing fertility concentrations with the lowest fertility treatment (0.0 μmol • L^{-1} M) leaf tissue Mn being statistically lower compared to the remaining treatments. The 4.50 μmol • L^{-1} Mn treatment had Mn tissue values which were 8.9x higher than 0.00 μmol • L^{-1} Mn and were significantly smaller than the upper four (9.0, 13.50, 15.75, and 18.0 μmol • L^{-1} Mn) concentrations (Table 2.3.6, Graph 2.3.6). The highest Mn concentration (18.0 μmol • L^{-1} Mn) resulted in the leaf tissue of the highest concentration and was statistically higher when compared to the lower three concentrations (9.00, 13.50, and 15.75 μmol • L^{-1} Mn), but not the upper concentrations of 13.50 and 15.75 μmol • L^{-1} Mn (Table 2.3.6, Graph 2.3.6). The quadratic regression model accounted for 91% of the variability of leaf tissue Mn concentration when Mn fertility concentration was treated as the independent variable (Equations 2.3.6).

The higher Mn leaf accumulation may indicate that as the developing sinks of the floral and subsequent reproductive structures increase in demand, more Mn resources are accumulated and utilized by the plants. This would make sense given Mn's role in the photosynthetic O_2 evolution in PS II and the role of Mn in the lignin content of plants (Nable et al., (69), and Brown et al., (70)). The impacts of the higher Mn rates would ensure that the photosynthate resources produced by PS II would be present in higher concentrations for the developing reproductive sinks.

2.3.6.5. Lipidome Impacts Mn Rates

Seed analysis resulted in no discernable difference in the lipidome and seed constituents except for erucic acid. While statistical differences were present within the distribution of oil content within the seeds, no discernable trend was observed to

correlate between Mn fertility treatments (Table 2.3.12). The lowest concentration of erucic acid was observed in the 4.50 μmol • L^{-1} Mn and was statistically smaller than the highest (18.0 μmol • L^{-1} Mn) concentration. The next three concentrations resulted in an increase in erucic acid when compared to 4.50 μmol • L^{-1} Mn treatment, but that increase was similar for all three concentrations and the highest concentration (Table 2.3.12). Despite an initial decrease of erucic acid concentration at the 4.50 μmol • L^{-1} Mn treatment, no discernable trend was observed regarding increasing or decreasing erucic acid content given the lowest and highest rates were statistically similar (Table 2.3.12). It was surprising to see no change in oleic acid content given this fatty acid typically increases with Mn concentrations (Wilson et al., (71)).

2.4. CONCLUSION

Different levels of micronutrients are required at different optimal concentrations over the life stages of *B. carinata*. The optimal fertility level can be extrapolated as the fertility concentration after which increasing the fertility does not result in a greater or lesser accumulation in leaf tissue. For each of the micronutrients tested, each of the tables (Tables 2.3.1, 2.3.2, 2.3.4, 2.3.5, 2.3.6, 2.3.7) compares tissue values to known *B. carinata* and *B. napus* tissue values from published literature as well as providing trends in leaf tissue mineral accumulation and biomass production based on life stage. The cells within these tables indicate the plateau value for leaf tissue accumulation when the statistical letters indicate no change above a certain fertility treatment.

Finally, little to no discernable impact or trend was observed regarding micronutrient rate and the fatty acid composition of the lipid profile of *B. carinata* seeds. This trend may indicate fatty acid composition and concentrations within *B. carinata* are regulated by other abiotic factors or genetic regulation rather than mineral nutrient fertility.

ACKNOWLEDGMENTS

This material is based on work that is supported by the National Institute of Food and Agriculture, USDA, under award number 2016-1123. Any opinions, findings, conclusions, or recommendations expressed in this publication are those of the author(s) and do not necessarily reflect the view of the U.S. Department of Agriculture.

LITERATURE CITED

1. Govardhan G, Sreedharan KS, Nanjundiah R, Moorthy KK, Surendran SB. Possible climatic implications of high-altitude black carbon emissions. Atmospheric Chemistry and Physics. 2017 Aug 1;17(15):9623.
2. Satheesh SK. High Altitude emissions of black carbon aerosols: potential climate implications. AGUFM. 2017 Dec; 2017 : U21D-01.
3. Craig H. The natural distribution of radiocarbon and the exchange time of carbon dioxide between atmosphere and sea. Tellus. 1957 Jan 1;9(1):1-7.
4. Friend AD, Lucht W, Rademacher TT, Keribin R, Betts R, Cadule P, Ciais P, Clark DB, Dankers R, Falloon PD, Ito A. Carbon residence time dominates uncertainty in terrestrial vegetation responses to future climate and atmospheric CO2. Proceedings of the National Academy of Sciences. 2014 Mar 4;111(9):3280-5.
5. U.S, Energy Information Administration. Monthly Energy Review. 2016 July. (accessed 8.11.16) http://www.eia.gov/totalenergy/data/monthly/pdf/mer.pdf.
6. Seepaul R, George S, Wright DL. Comparative response of *Brassica carinata* and *B. napus* vegetative growth, development and photosynthesis to nitrogen nutrition. Industrial Crops and Products. 2016 Dec 30;94:872-83.
7. United States, Federal Aviation Administration, and Pratt & Whitney. Evaluation of ARA catalytic hydrothermolysis (CH) fuel. Continuous Lower Energy, Emissions and Noise (CLEEN) Program, 2014. Federal Aviation Administration.
8. Gesch RW, Isbell TA, Oblath EA, Allen BL, Archer DW, Brown J, Hatfield JL, Jabro JD, Kiniry JR, Long DS, Vigil MF. Comparison of several Brassica species in the north central US for potential jet fuel feedstock. Industrial crops and products. 2015 Nov 30;75:2-7.
9. Marschner H. Marschner's mineral nutrition of higher plants. Academic press; 2011 Aug 8.
10. Gibson JL, Nelson PV, Pitchay DS, Whipker BE. Identifying nutrient deficiencies of Bedding plants. NC. State university floriculture research. Florex. 2001 ;4:1-4.
11. Grant CA, Bailey LD. Fertility management in canola production. Canadian Journal of Plant Science. 1993 Jul 1;73(3):651-70.
12. Seepaul R, Small IM, Marois J, George S, Wright DL. *Brassica carinata* and *Brassica napus* Growth, nitrogen use, seed, and oil productivity constrained by post-bolting nitrogen deficiency. Crop Science. 2019 Nov;59(6):2720-32.
13. Harper FR, Berkenkamp B. Revised growth-stage key for Brassica campestris and *B. napus*. Canadian Journal of Plant Science. 1975 Apr 1;55(2):657-8.
14. Matoh TB. Plant nutrition and cell wall development. In Plant Nutrient Acquisition 2001 (pp. 227-250). Springer, Tokyo.

15. Chebli Y, Geitmann A. Cellular growth in plants requires regulation of cell wall biochemistry. Current opinion in cell biology. 2017 Feb 1;44:28-35.
16. Ma BL, Biswas DK, Herath AW, Whalen JK, Ruan SQ, Caldwell C, Earl H, Vanasse A, Scott P, Smith DL. Growth, yield, and yield components of canola as affected by nitrogen, sulfur, and B application. Journal of Plant Nutrition and Soil Science. 2015 Aug;178(4):658-70.
17. Mei Yang, Lei Shi, Fang-Sen Xu, Jian-Wei Lu, Yun-Hua Wang. Effects of B, Mo, Zn, and their interactions on seed yield of rapeseed (*Brassica napus* L.). Pedosphere. 2009 Feb 1;19(1):53-9.
18. Gardner FP, Pearce RB, Mitchell RL. Physiology of crop plants. Scientific Publishers; 2017.
19. Shetty AS, Miller GW. Influence of Fe chlorosis on pigment and protein metabolism in leaves of Nicotiana tabacum L. Plant physiology. 1966 Mar 1;41(3):415-21.
20. Terry N, Abadía J. Function of Fe in chloroplasts. Journal of Plant Nutrition. 1986 Mar 1;9(3-7):609-46.
21. Rutherford AW. Photosystem II, the water-splitting enzyme. Trends in biochemical sciences. 1989 Jun 1;14(6):227-32.
22. Fei DI, Wang XF, Shi QH, Wang ML, Yang FJ, Gao QH. Exogenous nitric oxide alleviated the inhibition of photosynthesis and antioxidant enzyme activities in Fe-deficient Chinese cabbage (Brassica chinensis L.). Agricultural Sciences in China. 2008 Feb 1;7(2):168-79.
23. Sandmann G, Reck H, Kessler E, Böger P. Distribution of plastocyanin and soluble plastidic cytochrome c in various classes of algae. Archives of Microbiology. 1983 Jan 1;134(1):23-7.
24. Hopmans P. Stem deformity in Pinus radiata plantations in south-eastern Australia. Plant and Soil. 1990 Feb 1;122(1):97-104.
25. Coleman JE. Zn proteins: enzymes, storage proteins, transcription factors, and replication proteins. Annual review of biochemistry. 1992 Jan 1;61:897-946.
26. Moore Jr PA, Patrick Jr WH. Effect of Zn deficiency on alcohol dehydrogenase activity and nutrient uptake in rice. Agronomy Journal. 1988 Nov;80(6):882-5.
27. Sandmann G, Boger P. Enzymological function of heavy metals and their role in electron transfer processes of plants. Encyclopedia of plant physiology. New series. 1983.
28. O'sullivan M. Aldolase activity in plants as an indicator of Zn deficiency. Journal of the Science of Food and Agriculture. 1970 Dec;21(12):607-9.
29. Cakmak I, Marschner H. Enhanced superoxide radical production in roots of Zn-deficient plants. Journal of Experimental Botany. 1988 Oct 1;39(10):1449-60.

30. Çakmak İ, Marschner H. Zn-dependent changes in ESR signals, NADPH oxidase and plasma membrane permeability in cotton roots. Physiologia Plantarum. 1988 May;73(1):182-6.
31. Agarwala SC, Hewitt EJ. Mo as a Plant Nutrient: V. The interrelationships of molybdenum and nitrate supply in the concentration of sugars, nitrate and organic nitrogen in cauliflower plants grown in sand culture. Journal of Horticultural Science. 1955 Jan 1;30(3):151-62.
32. Hewitt EJ, Bolle-Jones EW. Mo as a plant nutrient: I. The influence of Mo on the growth of some Brassica crops in sand culture. Journal of Horticultural Science. 1952 Jan 1;27(4):245-56.
33. Eyster C, Brown TE, Tanner HA, Hood SL. Mn Requirement with Respect to Growth, Hill Reaction and Photosynthesis. Plant physiology. 1958 Jul;33(4):235.
34. Nable RO, Loneragan JF. Translocation of Mn in subterranean clover (Trifolium subterraneum L. Cv. Seaton Park) I. redistribution during vegetative growth. Functional Plant Biology. 1984 ;11(2):101-11.
35. Kriedemann PE, Graham RD, Wiskich JT. Photosynthetic dysfunction and in vivo changes in chlorophyll a fluorescence from Mn-deficient wheat leaves. Australian journal of agricultural research. 1985;36(2):157-69.
36. Constantopoulos G. Lipid metabolism of Mn-deficient algae: I. Effect of Mn deficiency on the greening and the lipid composition of Euglena gracilis Z. Plant physiology. 1970 Jan 1;45(1):76-80.
37. Wilson DO, Boswell FC, Ohki K, Parker MB, Shuman LM, Jellum MD. Changes in soybean seed oil and protein as influenced by Mn nutrition 1. Crop Science. 1982 Sep;22(5):948-52.
38. Henry JB, Vann M, McCall I, Cockson P, Whipker BE. Nutrient disorders of burley and flue-cured tobacco. Crops & Soils. 2018 Sep;51(5):44-52.
39. Taylor, D.C., Barton, D.L., Rioux, K.P., MacKenzie, S.L., Reed, D.W., Underhill, E.W., Pomeroy, M.K. and Weber, N., Biosynthesis of acyl lipids containing very-long chain fatty acids in microspore-derived and zygotic embryos of *Brassica napus* L. cv Reston. Plant Physiology. 1992. 99(4), pp.1609-1618.
40. Hoagland DR, Arnon DI. The water-culture method for growing plants without soil. Circular. California agricultural experiment station. 1950;347(2nd edit).
41. Barnes J, Whipker B, McCall I, Frantz J. Nutrient disorders of 'Evolution' mealy-cup sage. HortTechnology. 2012 Aug 1;22(4):502-8.
42. Bariya H, Bagtharia S, Patel A. B: A promising nutrient for increasing growth and yield of plants. In Nutrient use efficiency in plants 2014 (pp. 153-170). Springer, Cham.
43. Henry JB. Beneficial and adverse effects of low phosphorus fertilization of floriculture species. 2017. NCSU Library Repository.

44. Matoh T. B in plant nutrition and cell wall development. InPlant Nutrient Acquisition 2001 (pp. 227-250). Springer, Tokyo.
45. Nuttall WF, Ukrainetz H, Stewart JW, Spurr DT. The effect of nitrogen, sulphur and B on yield and quality of rapeseed (*Brassica napus* L. and B. campestris L.). Canadian Journal of Soil Science. 1987 Aug 1;67(3):545-59.
46. Chebli Y, Geitmann A. Cellular growth in plants requires regulation of cell wall biochemistry. Current opinion in cell biology. 2017 Feb 1;44:28-35.
47. Yang M, Shi L, Xu FS, Wang YH. Effect of B on dynamic change of seed yield and quality formation in developing seed of *Brassica napus*. Journal of Plant Nutrition. 2009 Apr 13;32(5):785-97.
48. Mulvaney MJ, Leon RG, Seepaul R, Wright DL, Hoffman TL. *Brassica carinata* seeding rate and row spacing effects on morphology, yield, and oil. Agronomy Journal. 2019 Mar;111(2):528-35.
49. Bao X, Pollard M, Ohlrogge J. The biosynthesis of erucic acid in developing embryos of *Brassica rapa*. Plant Physiology. 1998 Sep 1;118(1):183-90.
50. Ecke W, Uzunova M, Weissleder K. Mapping the genome of rapeseed (*Brassica napus* L.). II. Localization of genes controlling erucic acid synthesis and seed oil content. Theoretical and Applied Genetics. 1995 Nov 1;91(6-7):972-7.
51. Bryson, G.M. Mills, H.A., Sasseville, D.N., Jones Jr., J.B., and Barker, A.V. Plant analysis handbook IV. Athens, GA, USA: Micro-Macro Publ. 2014.
52. Chen G, Clark A, Kremen A, Lawley Y, Price A, Stocking L, Weil R. Brassicas and mustards: Managing cover crops profitably. 2007 Dec 12:81-9.
53. Wu J, Schat H, Sun R, Koornneef M, Wang X, Aarts MG. Characterization of natural variation for Zn, Fe and Mn accumulation and Zn exposure response in *Brassica rapa* L. Plant and Soil. 2007 Feb 1;291(1-2):167-80.
54. Marschner H. Marschner's mineral nutrition of higher plants. Academic press; 2011 Aug 8.
55. Ayala MB, Sandmann G. Activities of Cu-containing proteins in Cu-depleted pea leaves. Physiologia Plantarum. 1988 Apr;72(4):801-6.
56. Khan NA, Singh S, Nazar R, Lone PM. The source–sink relationship in mustard. Asian Aust J Plant Sci Biotechnol. 2007;1:10-8.
57. Ayala MB, Gorgé JL, Lachica M, Sandmann G. Changes in carotenoids and fatty acids in photosystem II of Cu deficient pea plants. Physiologia Plantarum. 1992 Jan;84(1):1-5.
58. Droppa M, Terry N, Horvath G. Variation in photosynthetic pigments and plastoquinone contents in sugar beet chloroplasts with changes in leaf Cu content. Plant Physiology. 1984 Mar 1;74(3):717-20.
59. Wahle KW, Davies NT. Involvement of Cu in microsomal mixed-function oxidase reactions: A review. Journal of the Science of Food and Agriculture. 1977 Jan;28(1):93-7.

60. Vallee BL, Auld DS. Zn coordination, function, and structure of Zn enzymes and other proteins. Biochemistry. 1990 Jun 1;29(24):5647-59.
61. Vallee BL, Falchuk KH. The biochemical basis of Zn physiology. Physiological reviews. 1993 Jan 1;73(1):79-118.
62. Kochian LV. Mechanisms of micronutrient uptake and translocation in plants. Micronutrients in agriculture. 1991 Jan 1;4:229-96.
63. Ajisaka H, Kuginuki Y, Yui S, Enomoto S, Hirai M. Identification and mapping of a quantitative trait locus controlling extreme late bolting in Chinese cabbage (*Brassica rapa* L. ssp. pekinensis syn. campestris L.) using bulked segregant analysis. Euphytica. 2001 Mar 1;118(1):75.
64. Cakmak I, Marschner H. Increase in membrane permeability and exudation in roots of Zn deficient plants. Journal of Plant physiology. 1988 Apr 1;132(3):356-61.
65. Cakmak I, Marschner H. Decrease in nitrate uptake and increase in proton release in Zn deficient cotton, sunflower and buckwheat plants. Plant and Soil. 1990 Dec 1;129(2):261-8.
66. Vunkova-Radeva R, Schiemann J, Mendel RR, Salcheva G, Georgieva D. Stress and activity of Mo-containing complex (Mo cofactor) in winter wheat seeds. Plant physiology. 1988 Jun 1;87(2):533-5.
67. Kondra ZP, Stefansson BR. Inheritance of erucic and eicosenoic acid content of rapeseed oil (*Brassica napus*). Canadian Journal of Genetics and Cytology. 1965 Sep 1;7(3):505-10.
68. Jackson C, Dench J, Moore AL, Halliwell B, Foyer CH, Hall DO. Subcellular localisation and identification of superoxide dismutase in the leaves of higher plants. European journal of Biochemistry. 1978 Nov;91(2):339-44.
69. Nable RO, Loneragan JF. Translocation of Mn in subterranean clover (Trifolium subterraneum L. Cv. Seaton Park) I. redistribution during vegetative growth. Functional Plant Biology. 1984;11(2):101-11.
70. Brown PH, Graham RD, Nicholas DJ. The effects of Mn and nitrate supply on the levels of phenolics and lignin in young wheat plants. Plant and soil. 1984 Oct 1;81(3):437-40.
71. Wilson DO, Boswell FC, Ohki K, Parker MB, Shuman LM, Jellum MD. Changes in soybean seed oil and protein as influenced by Mn nutrition 1. Crop Science. 1982 Sep;22(5):948-52.

TABLES AND FIGURES

Table 2.2.1: Calculations for modified Hoagland's solution utilized to explore the impacts of varying micronutrients on the growth of *Brassica carinata* over its life stages.

Fertility Rate (%)[1]	0.00		25.00		50.00		75.00		87.50		100.00	
	μmol • L^{-1}	ppm	μmol • L^{-1}	ppm	μmol • L^{-1}	ppm	μmol • L^{-1}	ppm	μmol • L^{-1}	ppm	μmol • L^{-1}	ppm
Fe (Fe) (μmol • L^{-1})[2]	0.00	0.00	18.00	1.01	36.00	2.01	54.00	3.02	63.00	3.52	72.00	4.02
Mn (Mn) (μmol • L^{-1})[2]	0.00	0.00	4.50	0.25	9.00	0.50	13.50	0.74	15.75	0.87	18.00	0.99
Zn (Zn) (μmol • L^{-1})[2]	0.00	0.00	0.75	0.05	1.50	0.10	2.25	0.15	2.63	0.18	3.00	0.20
Cu (Cu) (μmol • L^{-1})[2]	0.00	0.00	0.75	0.05	1.50	0.10	2.25	0.14	2.63	0.17	3.00	0.19
B (B) (μmol • L^{-1})[2]	0.00	0.00	11.25	0.12	22.50	0.25	33.75	0.37	39.38	0.43	45.00	0.49
Mo (Mo) (μmol • L^{-1})[2]	0.00	0.00	0.025	0.0025	0.050	0.005	0.075	0.0075	0.088	0.0088	0.100	0.01

[1] Values indicate the adjusted fertility rate provided from a modified Hoagland's solution with all elements held constant except the adjusted microelement being studied. These values are expressed as a percentage of the standard Hoagland's solution.

[2] Values given for each element listed in μmol • L^{-1}. To convert μmol • L^{-1} to parts per million (ppm) multiply by the molecular weight and divide by 1000.

Table 2.3.1: *Brassica carinata* plant dry weights (g) and leaf tissue concentration (mg · kg^{-1}) based on boron (B) fertility treatments.

B Fertility (µmol • L^{-1})[1]	0.00	11.25	22.50	33.75	39.38	45.00
Plant Dry Weight (g)						
Rosette	1.35 A ***	5.44 B ***	5.20 B ***	5.55 B ***	9.33 C ***	8.53 C ***
Bolting	11.26 A **	26.28 AB **	38.21 B **	30.10 B **	35.56 B **	31.51 B **
Flowering	3.73 A ***	32.96 B ***	39.10 B ***	36.08 B ***	36.73 B ***	40.68 B ***
	B Leaf Tissue Nutrient Concentrations (mg · kg^{-1})					
Rosette	9.39 A ***	47.20 B ***	48.46 B ***	49.40 B ***	49.45 B ***	50.00 B ***
Bolting	3.63 A ***	41.84 B ***	59.82 C ***	65.50 C ***	92.52 D ***	91.20 D ***
Flowering	11.41 A ***	70.10 B ***	79.20 BC ***	86.70 BC ***	111.64 D ***	98.52 CD ***
	Comparison Boron Leaf Tissue Values (mg · kg^{-1})[3]					
	Brassica carinata[3]			*Brassica napus*[4]		
Rosette[3]	13.4 – 26.2			15.0 – 54.0		
Bolting[3]	10.0 – 18.8					
Flowering[3]	6.5 – 19.1					

[1] Values indicate the adjusted fertility rate provided from a modified Hoagland's Solution with all elements held constant except the adjusted microelement being studied.
[2] *, **, or *** Indicates statistically significant differences between sample means based on F-test (proc GLM) at $P \leq 0.05$, $P \leq 0.01$, or $P \leq 0.001$, respectively. NS (not significant) indicates the F-test difference between sample means was $P > 0.05$. Values with the same letter indicate a lack of statistical significance while values with different letters indicate statistically significant results.
[4] Reference values from Seepaul et al., 2019. Values given are based on *Brassica carinata* leaf tissue samples from two growing seasons with samples taken based on plant life stages.
[5] Reference values based on 50 mature leaves without petioles taken throughout the season from rosette stage to pod set. Values taken from *Brassica napus* leaf tissue values from Bryson et al. (51).

Equations 2.3.1: Regression models for linear and quadratic for *Brassica carinata* plant dry weights (g) and leaf tissue nutrient concentrations (mg · kg^{-1}) based on boron (B) fertility treatments.

Boron Regression Models	Power & Significance[1]	Regression Equation[3]	R^2 [4]	Adj-R^2 [4]
Plant Dry Weight (g)				
Rosette[2]	L ***	2.19 + 0.147x	0.73	0.72
	Q ***	1.20 + 0.198x – 0.00073x^2	0.73	0.71
Bolting[2]	L **	18.46 + 0.411x	0.34	0.31
	Q ***	11.57 + 1.664x - 0.02822x^2	0.57	0.53
Flowering[2]	L ***	2.19 + 0.147x	0.73	0.72
	Q ***	1.20 + 0.180x - 0.00073x^2	0.73	0.71
Boron Leaf Tissue Nutrient Concentrations (%)				
Rosette[2]	L ***	25.14 + 0.678x	0.51	0.48
	Q ***	14.17 + 2.625x - 0.04297x^2	0.80	0.78
Bolting[2]	L ***	11.27 + 1.194x	0.93	0.92
	Q ***	7.11 + 2.671x - 0.01703x^2	0.94	0.93
Flowering[2]	L ***	30.03 + 1.826x	0.76	0.75
	Q ***	16.69 + 4.19x - 0.05225x^2	0.85	0.84

[1] Regression models (L = linear regression model, Q = quadratic regression model) were subjected to linear and higher power polynomial modeling to determine a model of fit. Model fits above the second power resulted in no greater interpretation of data for all models tested, consequently the above models only compare linear and second order polynomials.*, **, or *** Indicates the model's statistical significance at $p \leq 0.05$, $P \leq 0.01$, or $P \leq 0.001$, respectively. NS (not significant) indicates the model resulted in $p > 0.05$.

[2] *Brassica carinata* life stage.

[3] Models were calculated using PROC REG on SAS v 9.4. Determination of best model was accomplished by selecting the model with the best R^2 value and had the lowest p-value.

[4] Best fit statistics: R^2 = coefficient of determination, Adj-R^2 = adjusted coefficient of determination.

Graph 2.3.1: Polynomial regression models for boron (B) fertility impacts on *Brassica carinata* plant dry weights (g) and leaf tissue nutrient concentrations (mg · kg^{-1}).

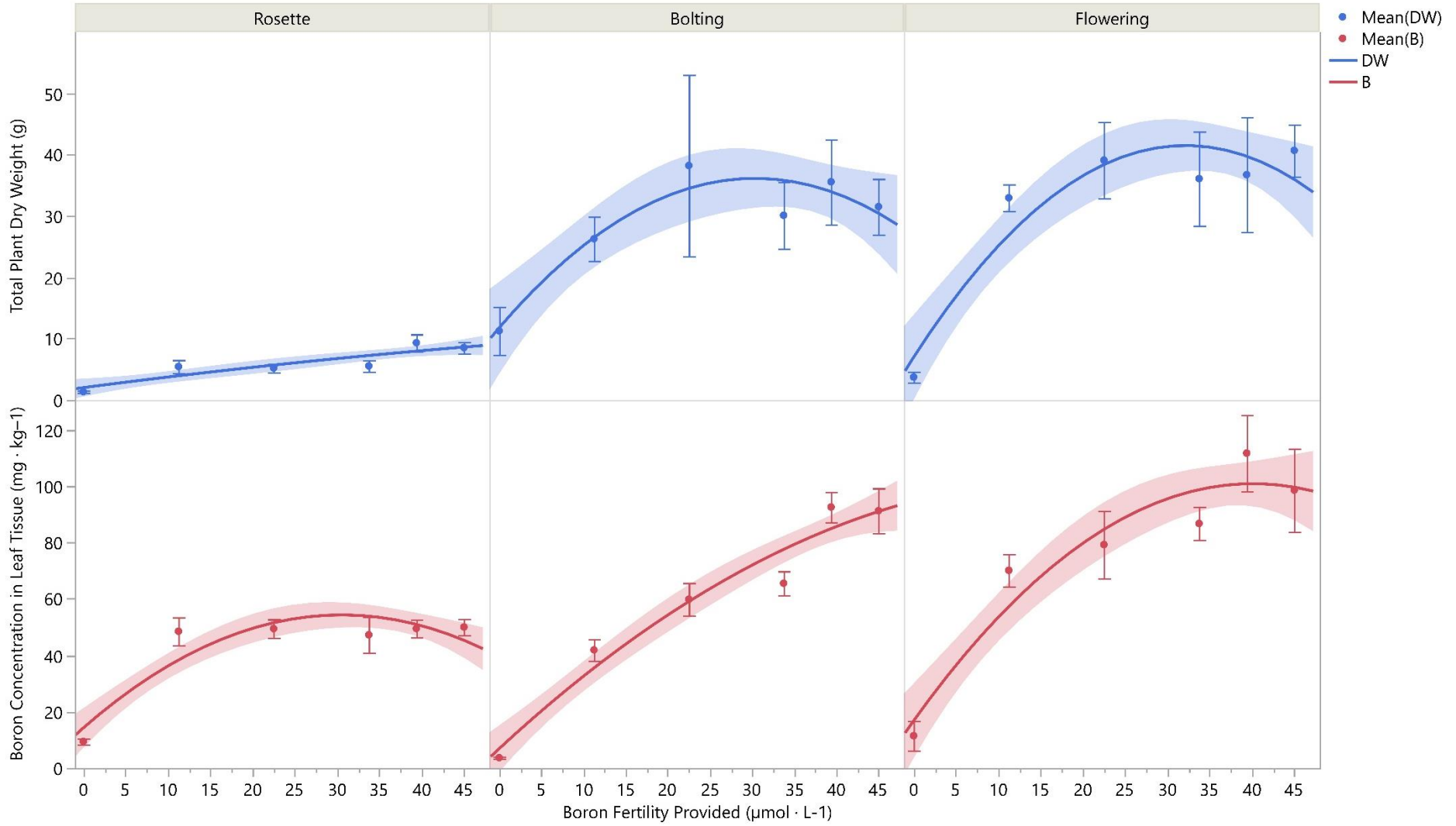

Table 2.3.2: *Brassica carinata* plant dry weights (g) and leaf tissue concentration (mg · kg^{-1}) based on iron (Fe) fertility treatments.

Fe Fertility (µmol • L^{-1})[1]	0.00	18.00	36.00	54.00	63.00	72.00
Plant Dry Weight (g)						
Rosette[2]	0.97 A ***	5.80 B ***	7.58 BC ***	5.62 B ***	8.92 C ***	8.53 C ***
Bolting[2]	26.91 AB **	33.85 A **	13.00 B **	23.91 AB **	30.48 A **	31.51 A **
Flowering[2]	31.47 A NS	41.06 A NS	27.16 A NS	40.30 A NS	36.82 A NS	40.68 A NS
	Fe Leaf Tissue Nutrient Concentrations (mg · kg^{-1})					
Rosette[2]	73.73 C ***	60.64 A ***	64.77 AB ***	69.35 BC ***	65.03 AB ***	74.83 C ***
Bolting[2]	46.07 A ***	49.19 A ***	49.98 A ***	59.18 A ***	113.77 B ***	66.00 A ***
Flowering[2]	43.67 A **	57.97 A **	53.57 A **	70.72 AB **	83.53 B **	56.40 A **
	Comparison Fe Leaf Tissue Values (mg · kg^{-1})[3]					
	Brassica carinata[3]			*Brassica napus*[4]		
Rosette[3]	67.6 – 595.3			30.0 – 200.0		
Bolting[3]	51.9 – 226.0					
Flowering[3]	38.4 – 172.2					

[1] Values indicate the adjusted fertility rate provided from a modified Hoagland's Solution with all elements held constant except the adjusted microelement being studied.
[2] *, **, or *** Indicates statistically significant differences between sample means based on F-test at $P \leq 0.05$, $P \leq 0.01$, or $P \leq 0.001$, respectively. NS (not significant) indicates the F-test difference between sample means was $P > 0.05$. Values with the same letter indicate a lack of statistical significance while values with different letters indicate statistically significant results.
[3] Reference values from Seepaul et al., 2019. Values given are based on *Brassica carinata* leaf tissue samples from two growing seasons with samples taken based on plant life stages.
[4] Reference values based on 50 mature leaves without petioles taken throughout the season from rosette stage to pod set. Values taken from *Brassica napus* leaf tissue values from Bryson et al. (51).

Equations 2.3.2: Regression models for linear and quadratic for *Brassica carinata* plant dry weights (g) and leaf tissue nutrient concentrations (mg · kg^{-1}) based on iron (Fe) fertility treatments.

Fe Regression Models	Power & Significance[1]	Regression Equation[3]	R^2 [4]	Adj-R^2 [4]
Plant Dry Weight (g)				
Rosette[2]	L ***	2.93 + 0.084x	0.61	0.60
	Q ***	1.74 + 0.199x – 0.00154x^2	0.70	0.67
Bolting[2]	L NS	25.64 + 0.023x	0.00	-0.04
	Q NS	30.54 - 0.520x + 0.00750x^2	0.18	0.11
Flowering[2]	L NS	28.07 – 0.170x	0.14	0.10
	Q NS	26.98 + 0.291x – 0.00167x^2	0.15	0.06
Iron Leaf Tissue Nutrient Concentrations (%)				
Rosette[2]	L NS	65.65 – 0.051x	0.05	0.003
	Q **	71.67 – 0.532x + 0.00783x^2	0.50	0.45
Bolting[2]	L **	40.45 + 0.582x	0.29	0.26
	Q *	44.04 + 0.184x + 0.00549x^2	0.30	0.23
Flowering[2]	L *	47.96 + 0.326x	0.25	0.22
	Q *	42.47 + 0.859x – 0.00716x^2	0.30	0.23

[1] Regression models (L = linear regression model, Q = quadratic regression model) were subjected to linear and higher power polynomial modeling to determine a model of fit. Model fits above the second power resulted in no greater interpretation of data for all models tested, consequently the above models only compare linear and second order polynomials.*, **, or *** Indicates the model's statistical significance at p $\leq$ 0.05, P $\leq$ 0.01, or P $\leq$ 0.001, respectively. NS (not significant) indicates the model resulted in p > 0.05.

[2] *Brassica carinata* life stage.

[3] Models were calculated using PROC REG on SAS v 9.4. Determination of best model was accomplished by selecting the model with the best R^2 value and had the lowest p-value.

[4] Best fit statistics: R^2 = coefficient of determination, Adj-R^2 = adjusted coefficient of determination.

Graph 2.3.2: Polynomial regression models for Iron (Fe) fertility impacts on *Brassica carinata* plant dry weights (g) and leaf tissue nutrient concentrations (mg · kg^{-1}).

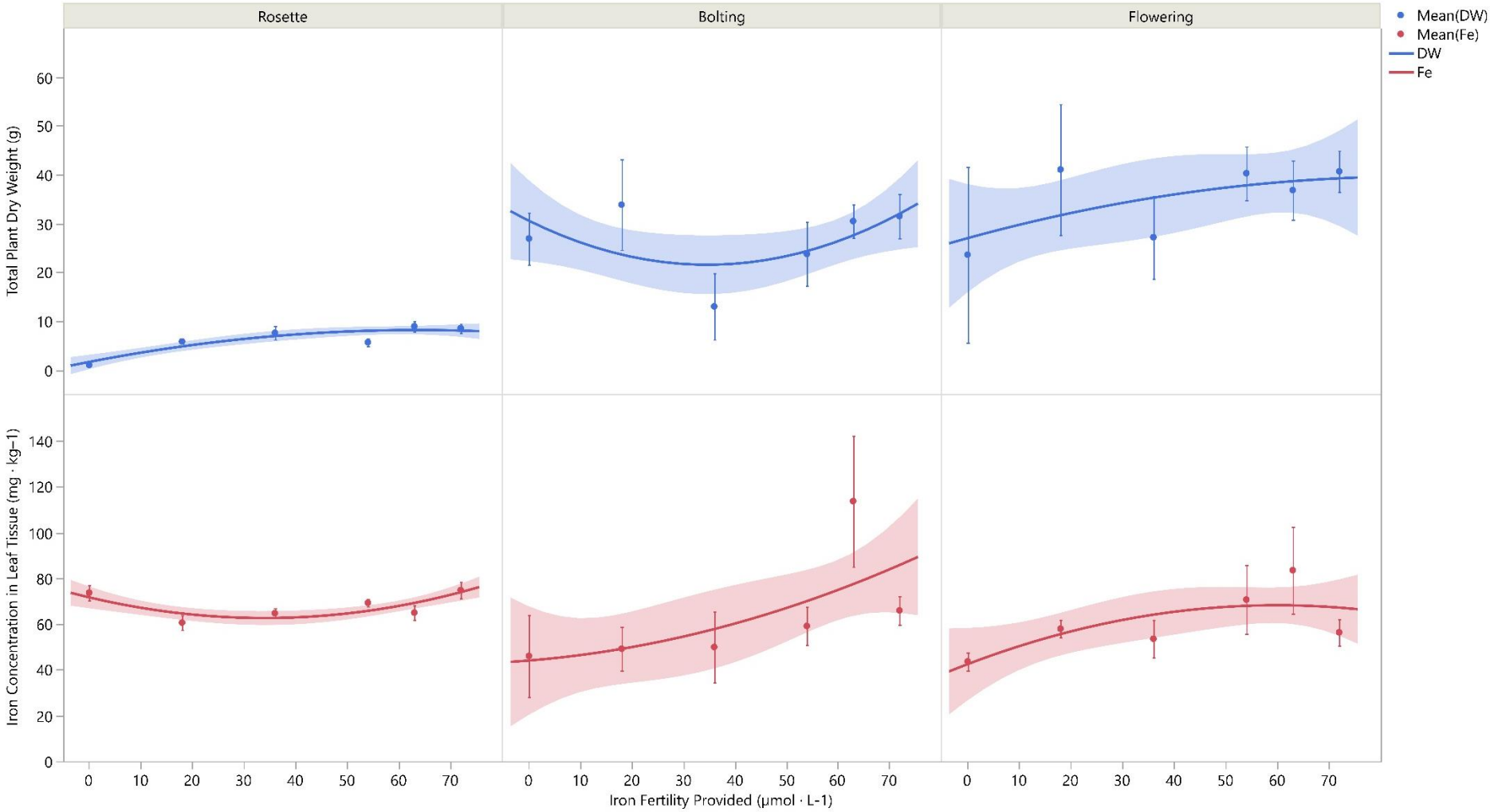

Table 2.3.3: *Brassica carinata* plant dry weights (g) and leaf tissue concentration (mg · kg^{-1}) based on copper (Cu) fertility treatments.

Cu Fertility (µmol • L^{-1})[1]	0.00	0.75	1.50	2.25	2.63	3.00
Plant Dry Weight (g)						
Rosette	7.26 BCD ***	10.26 A ***	9.38 AB ***	6.63 CD ***	5.67 D ***	8.53 ABC ***
Bolting	22.89 A ***	46.56 B ***	37.22 BC ***	29.14 AB ***	33.51 ABC ***	31.51 AB ***
Flowering	27.54 AB ***	21.67 A ***	48.29 C ***	40.56 BC ***	37.63 BC ***	40.68 BC ***
	Cu Leaf Tissue Nutrient Concentrations (mg · kg^{-1})					
Rosette	2.75 A ***	5.91 B ***	7.85 C ***	6.06 B ***	7.63 C ***	8.03 C ***
Bolting	1.22 A ***	3.91 B ***	6.12 BC ***	7.98 C ***	6.62 C ***	7.57 C ***
Flowering	4.14 A **	7.88 AB **	8.96 B **	10.92 B **	9.52 B **	10.37 B **
	Comparison Cu Leaf Tissue Values (mg · kg^{-1})[3]					
	Brassica carinata[3]			*Brassica napus*[4]		
Rosette[3]	1.9 – 3.2			4.0 – 25.0		
Bolting[3]	3.4 – 3.6					
Flowering[3]	2.3 – 3.2					

[1] Values indicate the adjusted fertility rate provided from a modified Hoagland's Solution with all elements held constant except the adjusted microelement being studied.
[2] *, **, or *** Indicates statistically significant differences between sample means based on F-test at $P \leq 0.05$, $P \leq 0.01$, or $P \leq 0.001$, respectively. NS (not significant) indicates the F-test difference between sample means was $P > 0.05$. Values with the same letter indicate a lack of statistical significance while values with different letters indicate statistically significant results.
[3] Reference values from Seepaul et al., 2019. Values given are based on *Brassica carinata* leaf tissue samples from two growing seasons with samples taken based on plant life stages.
[4] Reference values based on 50 mature leaves without petioles taken throughout the season from rosette stage to pod set. Values taken from *Brassica napus* leaf tissue values from Bryson et al. (51).

Equations 2.3.3: Regression models for linear and quadratic for *Brassica carinata* plant dry weights (g) and leaf tissue nutrient concentrations (mg · kg^{-1}) based on copper (Cu) fertility treatments.

Cu Regression Models	Power & Significance[1]	Regression Equation[3]	R^2 [4]	Adj-R^2 [4]
Plant Dry Weight (g)				
Rosette[2]	L NS	8.81 – 0.5079x	0.09	0.04
	Q NS	8.15 + 1.233x – 0.57626x^2	0.16	0.07
Bolting[2]	L NS	33.50 – 0.015x	0.00	-0.05
	Q *	27.56 + 15.777x – 5.227x^2	0.25	0.18
Flowering[2]	L ***	27.06+ 5.330x	0.30	0.26
	Q ***	23.71+ 14.240x – 2.94890x^2	0.36	0.29
Copper Leaf Tissue Nutrient Concentrations (%)				
Rosette[2]	L ***	3.98+ 1.414x	0.61	0.59
	Q ***	3.10 + 3.765x – 0.77801x^2	0.73	0.70
Bolting[2]	L ***	2.09 + 2.058x	0.73	0.72
	Q ***	1.12 + 4.654x – 0.85893x^2	0.82	0.80
Flowering[2]	L ***	5.44 + 1.887x	0.49	0.47
	Q ***	4.30 + 4.931x – 1.00753x^2	0.59	0.55

[1] Regression models (L = linear regression model, Q = quadratic regression model) were subjected to linear and higher power polynomial modeling to determine a model of fit. Model fits above the second power resulted in no greater interpretation of data for all models tested, consequently the above models only compare linear and second order polynomials.*, **, or *** Indicates the model's statistical significance at $p \leq 0.05$, $P \leq 0.01$, or $P \leq 0.001$, respectively. NS (not significant) indicates the model resulted in $p > 0.05$.

[2] *Brassica carinata* life stage.

[3] Models were calculated using PROC REG on SAS v 9.4. Determination of best model was accomplished by selecting the model with the best R^2 value and had the lowest p-value.

[4] Best fit statistics: R^2 = coefficient of determination, Adj-R^2 = adjusted coefficient of determination.

Graph 2.3.3: Polynomial regression models for copper (Cu) fertility impacts on *Brassica carinata* plant dry weights (g) and leaf tissue nutrient concentrations (mg · kg^{-1}).

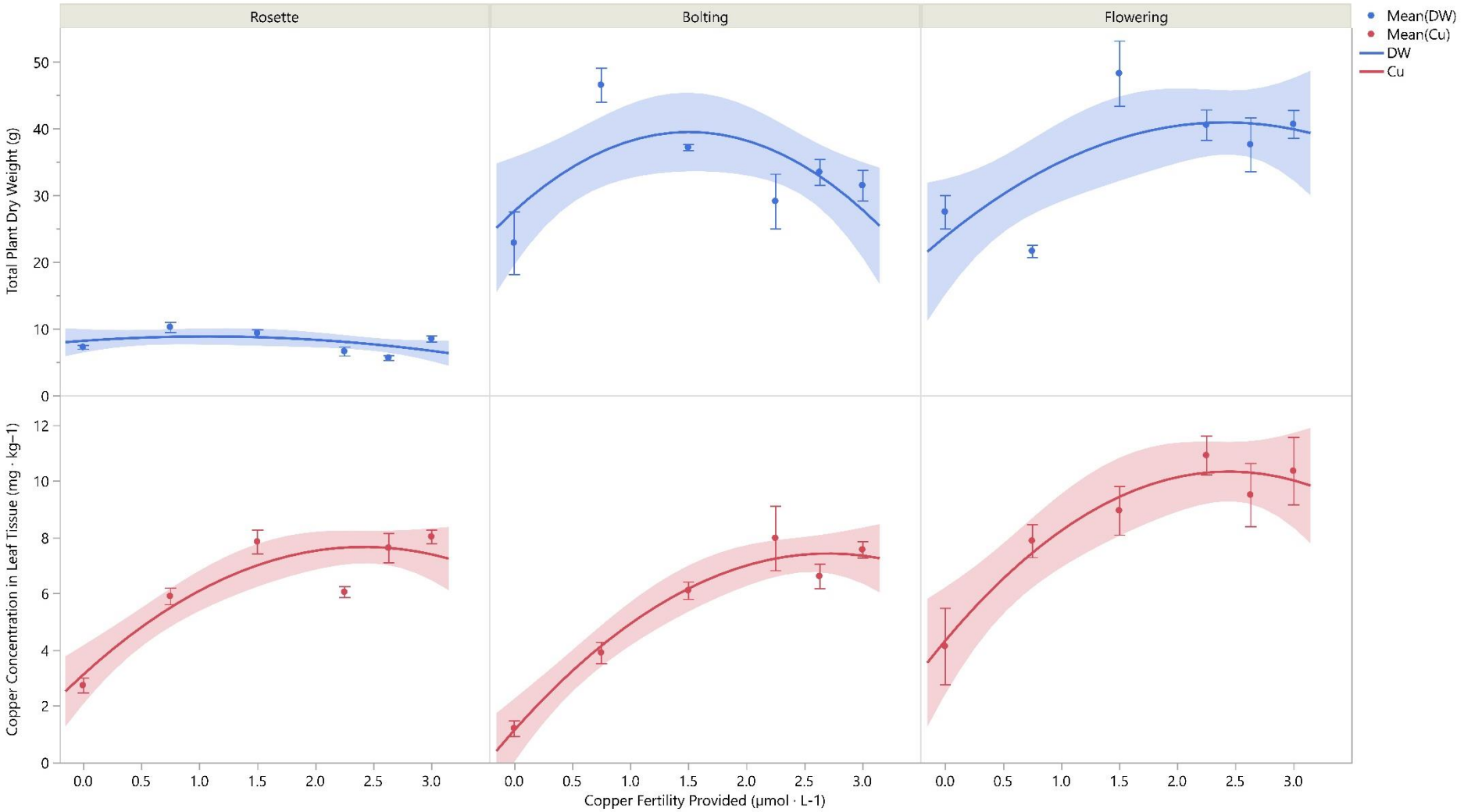

Table 2.3.4: *Brassica carinata* plant dry weights (g) and leaf tissue concentration (mg · kg^{-1}) based on zinc (Zn) fertility treatments.

Zn Fertility (µmol • L^{-1})[1]	0.00	0.75	1.50	2.25	2.63	3.00
Plant Dry Weight (g)						
Rosette	5.84 A ***	5.72 A ***	6.74 AB ***	7.46 BC ***	5.61 A ***	8.53 C ***
Bolting	32.21 A **	15.42 B **	24.96 AB **	32.91 A **	16.06 B **	31.51 A **
Flowering	34.15 AB ***	22.11 B ***	37.40 AB ***	38.03 AB ***	36.80 AB ***	40.68 AB ***
	Zn Leaf Tissue Nutrient Concentrations (mg · kg^{-1})					
Rosette	14.66 A ***	13.18 A ***	19.07 B ***	23.22 C ***	21.02 BC ***	22.65 C ***
Bolting	9.17 A ***	27.47 B ***	34.92 B ***	39.61 B ***	39.87 B ***	29.10 B ***
Flowering	15.50 A *	33.98 B *	42.26 B *	43.41 B *	43.50 B *	43.43 B *
	Comparison Zn Leaf Tissue Values (mg · kg^{-1})[3]					
	Brassica carinata[3]			*Brassica napus*[4]		
Rosette[3]	21.9 – 25.3			22.0 – 49.0		
Bolting[3]	20.9 – 25.7					
Flowering[3]	22.7 – 28.0					

[1] Values indicate the adjusted fertility rate provided from a modified Hoagland's Solution with all elements held constant except the adjusted microelement being studied.
[2] *, **, or *** Indicates statistically significant differences between sample means based on F-test at $P \leq 0.05$, $P \leq 0.01$, or $P \leq 0.001$, respectively. NS (not significant) indicates the F-test difference between sample means was $P > 0.05$. Values with the same letter indicate a lack of statistical significance while values with different letters indicate statistically significant results.
[3] Reference values from Seepaul et al., 2019. Values given are based on *Brassica carinata* leaf tissue samples from two growing seasons with samples taken based on plant life stages.
[4] Reference values based on 50 mature leaves without petioles taken throughout the season from rosette stage to pod set. Values taken from *Brassica napus* leaf tissue values from Bryson et al. (51).

Equations 2.3.4: Regression models for linear and quadratic for *Brassica carinata* plant dry weights (g) and leaf tissue nutrient concentrations (mg · kg^{-1}) based on zinc (Zn) fertility treatments.

Zn Regression Models	Power & Significance[1]	Regression Equation[3]	R^2 [4]	Adj-R^2 [4]
Plant Dry Weight (g)				
Rosette[2]	L ***	13.45 + 3.265x	0.72	0.71
	Q ***	13.42 + 3.346x – 0.02688x^2	0.72	0.70
Bolting[2]	L NS	25.16 + 0.207x	0.00	-0.05
	Q NS	28.98 – 9.951x + 3.36205x^2	0.10	0.001
Flowering[2]	L *	28.83 + 3.577x	0.18	0.14
	Q NS	30.88 – 1.903x + 1.81364x^2	0.21	0.13
Zinc Leaf Tissue Nutrient Concentrations (%)				
Rosette[2]	L ***	5.60 + 0.621x	0.29	0.26
	Q ***	5.84 -0.008x + 0.20806x^2	0.31	0.25
Bolting[2]	L **	17.38 + 7.493x	0.44	0.41
	Q ***	8.81+ 30.277x – 7.54088x^2	0.73	0.71
Flowering[2]	L ***	22.81 + 8.415x	0.52	0.49
	Q ***	16.42 + 25.397x – 5.62037x^2	0.67	0.64

[1] Regression models (L = linear regression model, Q = quadratic regression model) were subjected to linear and higher power polynomial modeling to determine a model of fit. Model fits above the second power resulted in no greater interpretation of data for all models tested, consequently the above models only compare linear and second order polynomials.*, **, or *** Indicates the model's statistical significance at $p \leq 0.05$, $P \leq 0.01$, or $P \leq 0.001$, respectively. NS (not significant) indicates the model resulted in $p > 0.05$.

[2] *Brassica carinata* life stage.

[3] Models were calculated using PROC REG on SAS v 9.4. Determination of best model was accomplished by selecting the model with the best R^2 value and had the lowest p-value.

[4] Best fit statistics: R^2 = coefficient of determination, Adj-R^2 = adjusted coefficient of determination.

Graph 2.3.4: Polynomial regression models for zinc (Zn) fertility impacts on *Brassica carinata* plant dry weights (g) and leaf tissue nutrient concentrations (mg · kg^{-1}).

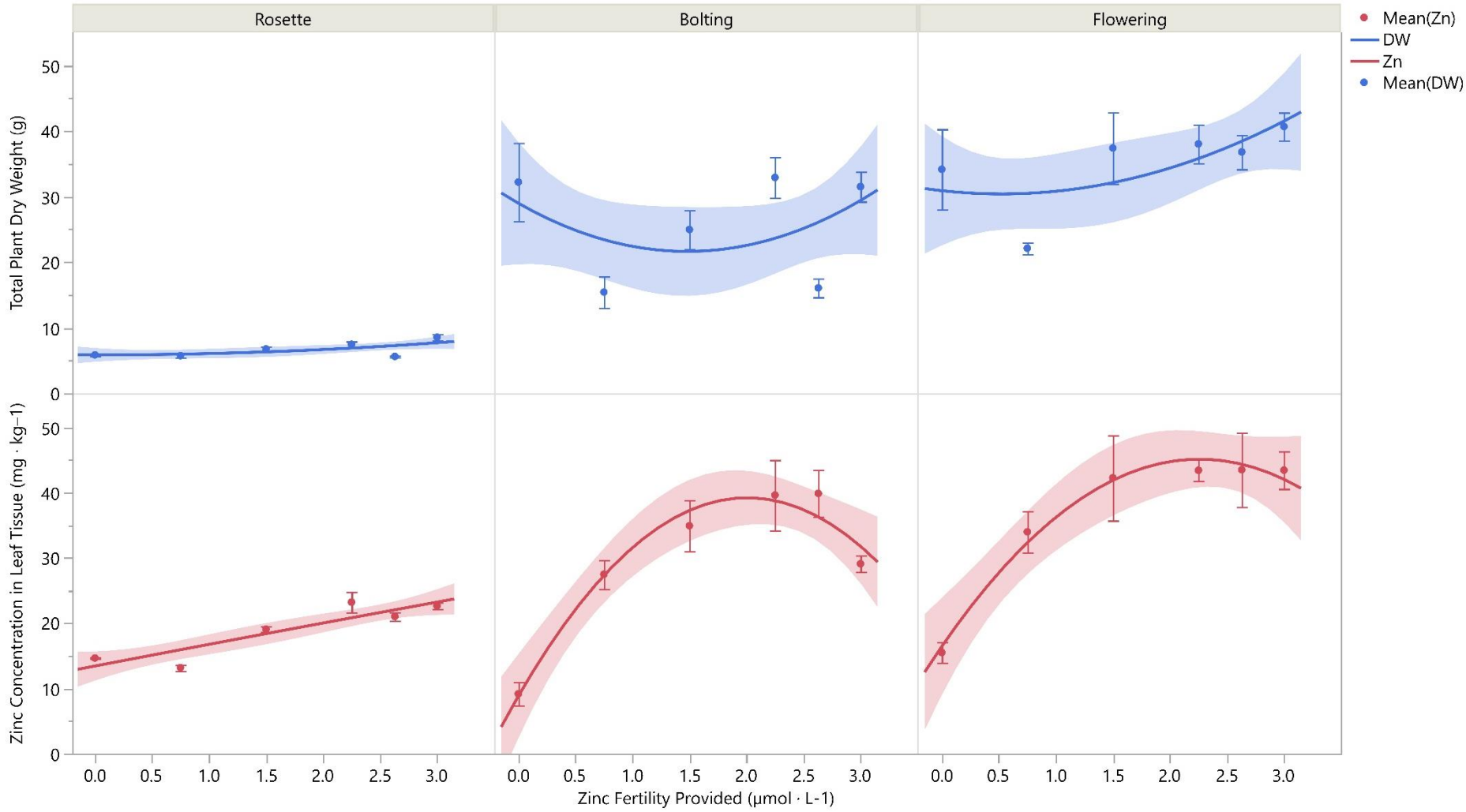

Table 2.3.5: *Brassica carinata* plant dry weights (g) and leaf tissue concentration (mg · kg^{-1}) based on molybdenum (Mo) fertility treatments.

Mo Fertility (µmol • L^{-1})[1]	0.00	0.025	0.050	0.075	0.088	0.100
Plant Dry Weight (g)						
Rosette	5.62 A ***	7.59 AB ***	7.06 AB ***	6.54 AB ***	12.18 C ***	8.53 B ***
Bolting	42.78 A **	19.99 B **	33.17 AB **	30.74 AB **	30.02 AB **	31.51 AB **
Flowering	50.69 A NS	30.51 A NS	44.26 A NS	38.00 A NS	55.52 A NS	40.68 A NS
	Mo Leaf Tissue Nutrient Concentrations (mg · kg^{-1})					
Rosette	0.39 A ***	0.31 A ***	1.61 A ***	1.21 A ***	1.03 A ***	14.53 B ***
Bolting	0.31 A ***	1.17 AB ***	1.28 AB ***	1.93 BC ***	2.21 BC ***	3.15 C ***
Flowering	0.80 A ***	1.59 AB ***	2.89 C ***	3.00 C ***	3.23 C ***	2.42 C ***
	Comparison Mo Leaf Tissue Values (mg · kg^{-1})[3]					
	Brassica carinata[3]			*Brassica napus*[4]		
Rosette[3]	N/A[3]			0.25 – 0.60		
Bolting[3]	N/A[3]					
Flowering[3]	N/A[3]					

[1] Values indicate the adjusted fertility rate provided from a modified Hoagland's Solution with all elements held constant except the adjusted microelement being studied.

[2] *, **, or *** Indicates statistically significant differences between sample means based on F-test at $P \leq 0.05$, $P \leq 0.01$, or $P \leq 0.001$, respectively. NS (not significant) indicates the F-test difference between sample means was $P > 0.05$. Values with the same letter indicate a lack of statistical significance while values with different letters indicate statistically significant results.

[3] Reference values from Seepaul et al., 2019. Values given are based on *Brassica carinata* leaf tissue samples from two growing seasons with samples taken based on plant life stages. N/A indicates values were not present for the above work.

[4] Reference values based on 50 mature leaves without petioles taken throughout the season from rosette stage to pod set. Values taken from *Brassica napus* leaf tissue values from Bryson et al. (51).

Equations 2.3.5: Regression models for linear and quadratic for *Brassica carinata* plant dry weights (g) and leaf tissue nutrient concentrations (mg · kg^{-1}) based on Molybdenum (Mo) fertility treatments.

Mo Regression Models	Power & Significance[1]	Regression Equation[3]	R^2 [4]	Adj-R^2 [4]
Plant Dry Weight (g)				
Rosette[2]	L **	5.86 + 37.04x	0.33	0.30
	Q *	5.98 + 27.673x + 92.92428x^2	0.33	0.27
Bolting[2]	L NS	33.98 – 46.392x	0.03	0.00
	Q NS	38.52 – 407.991x + 3586.43172x^2	0.20	0.12
Flowering[2]	L NS	39.75 – 29.880x	0.00	-0.04
	Q NS	47.22 – 565.55x + 5905.6487x^2	0.12	0.03
Molybdenum Leaf Tissue Nutrient Concentrations (%)				
Rosette[2]	L *	-1.72 + 86.885x	0.25	0.22
	Q **	1.68 – 183.692x + 2683.6461x^2	0.43	0.38
Bolting[2]	L ***	0.51 + 20.635x	0.51	0.49
	Q ***	0.23 + 43.270x – 224.4981x^2	0.56	0.52
Flowering[2]	L ***	1.14 + 20.383x	0.55	0.53
	Q ***	0.63 + 63.260x – 426.4652x^2	0.72	0.69

[1] Regression models (L = linear regression model, Q = quadratic regression model) were subjected to linear and higher power polynomial modeling to determine a model of fit. Model fits above the second power resulted in no greater interpretation of data for all models tested, consequently the above models only compare linear and second order polynomials.*, **, or *** Indicates the model's statistical significance at $p \leq 0.05$, $P \leq 0.01$, or $P \leq 0.001$, respectively. NS (not significant) indicates the model resulted in $p > 0.05$.

[2] *Brassica carinata* life stage.

[3] Models were calculated using PROC REG on SAS v 9.4. Determination of best model was accomplished by selecting the model with the best R^2 value and had the lowest p-value.

[4] Best fit statistics: R^2 = coefficient of determination, Adj-R^2 = adjusted coefficient of determination.

Graph 2.3.5: Polynomial regression models for molybdenum (Mo) fertility impacts on *Brassica carinata* plant dry weights (g) and leaf tissue nutrient concentrations (mg · kg^{-1}).

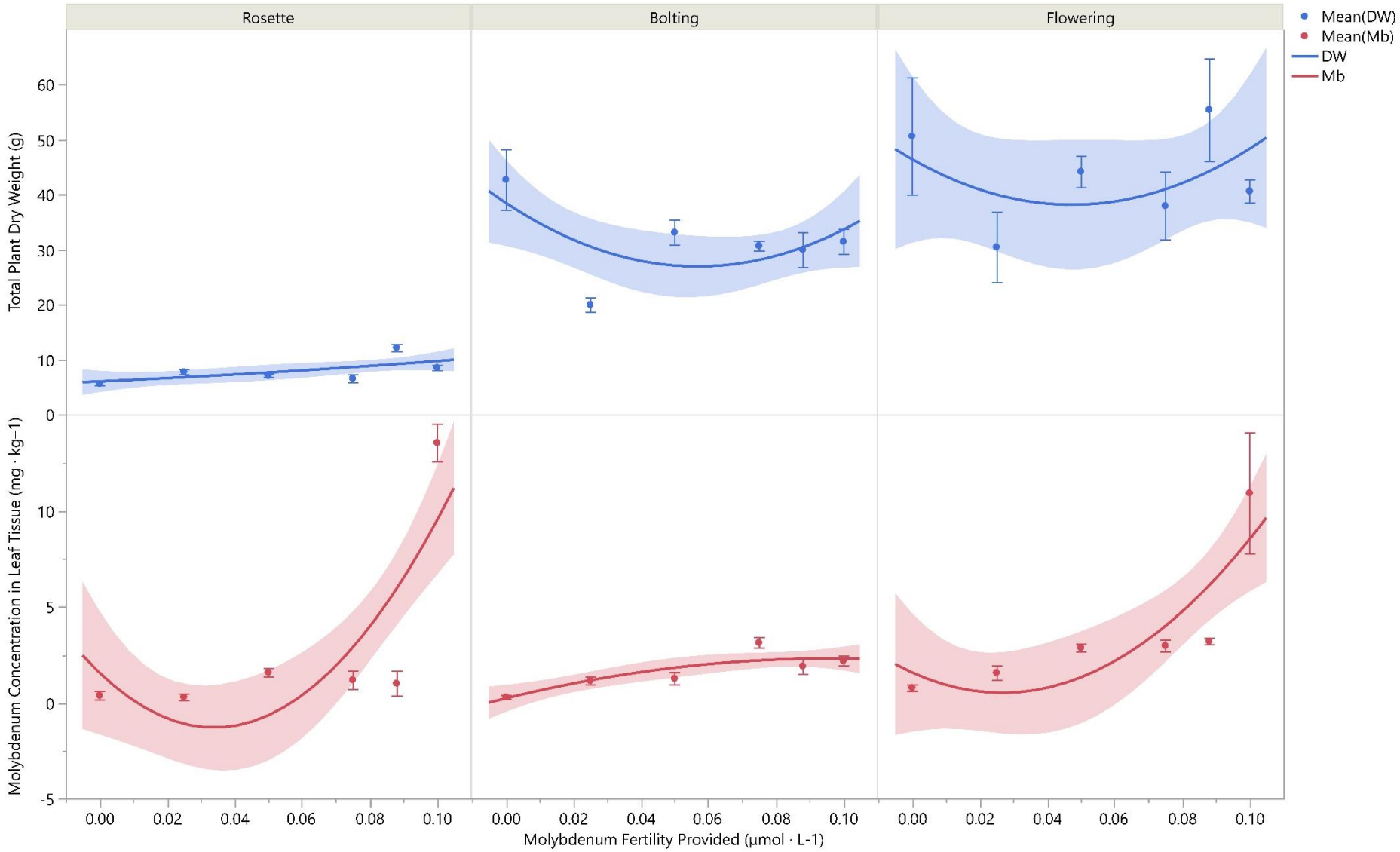

Table 2.3.6: *Brassica carinata* plant dry weights (g) and leaf tissue concentration (mg · kg^{-1}) based on manganese (Mn) fertility treatments.

Mn Fertility Rate (µmol • L^{-1})[1]	0.00	4.50	9.00	13.50	15.75	18.00
Plant Dry Weight (g)						
Rosette	6.29 CD ***	8.71 AB ***	10.65 A ***	5.81 D ***	6.41 BCD ***	8.53 ABC ***
Bolting	23.34 A NS	29.85 A NS	33.30 A NS	24.93 A NS	25.94 A NS	31.51 A NS
Flowering	24.33 A NS	49.08 A NS	51.16 A NS	30.45 A NS	39.00 A NS	40.68 A NS
	Mn Leaf Tissue Nutrient Concentrations (mg · kg^{-1})					
Rosette	14.70 A ***	74.31 B ***	112.11 C ***	149.36 D ***	155.93 D ***	103.25 C ***
Bolting	8.77 A ***	65.21 B ***	117.03 C ***	149.87 C ***	137.09 C ***	161.63 C ***
Flowering	6.90 A ***	61.56 B ***	105.20 C ***	132.17 CD ***	139.14 CD ***	145.70 D ***
	Comparison Mn Leaf Tissue Values (mg · kg^{-1})[3]					
	Brassica carinata[3]			*Brassica napus*[4]		
Rosette	17.1 – 22.6			25.0 – 250.0		
Bolting	9.5 – 17.1					
Flowering	11.6 – 18.7					

[1] Values indicate the adjusted fertility rate provided from a modified Hoagland's Solution with all elements held constant except the adjusted microelement being studied.
[2] *, **, or *** Indicates statistically significant differences between sample means based on F-test at $P \leq 0.05$, $P \leq 0.01$, or $P \leq 0.001$, respectively. NS (not significant) indicates the F-test difference between sample means was $P > 0.05$. Values with the same letter indicate a lack of statistical significance while values with different letters indicate statistically significant results.
[3] Reference values from Seepaul et al., 2019. Values given are based on *Brassica carinata* leaf tissue samples from two growing seasons with samples taken based on plant life stages.
[4] Reference values based on 50 mature leaves without petioles taken throughout the season from rosette stage to pod set. Values taken from *Brassica napus* leaf tissue values from Bryson et al., (51).

Equations 2.3.6: Regression models for linear and quadratic for *Brassica carinata* plant dry weights (g) and leaf tissue nutrient concentrations (mg · kg^{-1}) based on manganese (Mn) fertility treatments.

Manganese Regression Models	Power & Significance[1]	Regression Equation[3]	R^2 [4]	Adj-R^2 [4]
Plant Dry Weight (g)				
Rosette[2]	L NS	7.81 – 0.008x	0.00	-0.05
	Q NS	6.88 + 0.407x – 0.02288x^2	0.13	0.05
Bolting[2]	L NS	26.61 + 0.152x	0.02	-0.01
	Q NS	24.82 + 0.945x – 0.04120x^2	0.07	-0.01
Flowering[2]	L NS	36.48 + 0.260x	0.01	-0.03
	Q NS	28.98 + 3.588x – 0.18367x^2	0.18	0.09
Manganese Leaf Tissue Nutrient Concentrations (%)				
Rosette[2]	L ***	17.38 + 7.493x	0.44	0.41
	Q ***	8.81 + 30.277x – 7.54088x^2	0.73	0.71
Bolting[2]	L ***	23.97 + 8.16x	0.84	0.84
	Q ***	7.85 + 15.31x – 0.39452x^2	0.89	0.88
Flowering[2]	L ***	20.90+ 7.659x	0.87	0.87
	Q ***	6.60+ 14.000x – 0.34998x^2	0.92	0.91

[1] Regression models (L = linear regression model, Q = quadratic regression model) were subjected to linear and higher power polynomial modeling to determine a model of fit. Model fits above the second power resulted in no greater interpretation of data for all models tested, consequently the above models only compare linear and second order polynomials.*, **, or *** Indicates the model's statistical significance at $p \leq 0.05$, $P \leq 0.01$, or $P \leq 0.001$, respectively. NS (not significant) indicates the model resulted in $p > 0.05$.

[2] *Brassica carinata* life stage.

[3] Models were calculated using PROC REG on SAS v 9.4. Determination of best model was accomplished by selecting the model with the best R^2 value and had the lowest p-value.

[4] Best fit statistics: R^2 = coefficient of determination, Adj-R^2 = adjusted coefficient of determination.

Graph 2.3.3.6: Polynomial regression models for manganese (Mn) fertility impacts on *Brassica carinata* plant dry weights (g) and leaf tissue nutrient concentrations (mg · kg^{-1}).

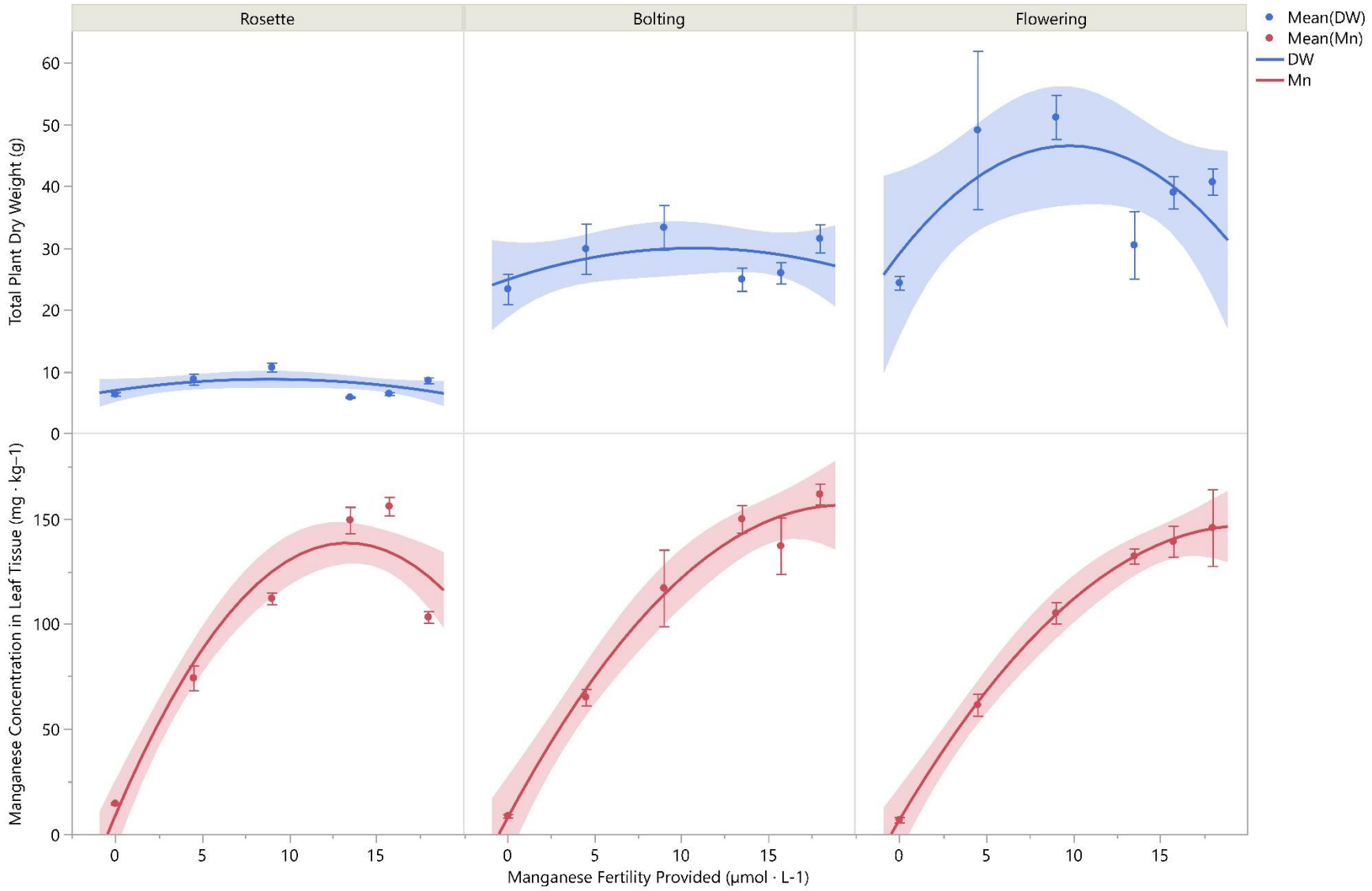

Figure 2.3.1 Boron deficiency first manifested as a general distortion of the upper leaves. Note that the distortion resulted in a folding of the leaves rather than as a curling, cupping, or withering of the leaf surface. This folding was concentrated along the margin and midrib similar to the leaf was being folded in half lengthwise.

Figure 2.3.2: As boron deficiency symptomology progressed, the folding became more severe, especially on new foliage. The newest foliage appeared rolled on itself like a tube of paper. This rolling is different than the cupping of the leaves observed in calcium because the whole leaf curls from the midrib to the margin whereas calcium deficiency results in only the leaf margin curling in and downward.

Figure 2.3.3: As symptoms progressed, the new leaves showed signs of cracking along the midrib and petiole. This leaf curling along with the cracking are classical boron deficiency symptoms.

Figure 2.3.4: In the advanced stages of boron deficiency, the growing tip eventually dies. You can see here the necrotic center of the plant where the growing tip should be. This results in the proliferation of axillary shoots as the plant continues to grow.

Figure 2.3.5: Boron deficiency will eventually result in the death of the growing tip. This sudden loss of apical dominance results in the axillary shoots to begin growing in earnest, resulting in many side shoots. Note the dense cluster of side shoots around the dead growing tip.

Figure 2.3.6: Iron deficiency symptoms were present in the rosette stage for *Brassica carinata* and were quite severe in the lowest fertility treatment resulting in newer and developing leaves which had interveinal chlorosis.

Figure 2.3.7: Symptoms of iron deficiency were present at the lowest fertility treatment at both the flowering (top) and pod set (bottom) stages.

Figure 2.3.8: The above carinata plant appeared healthy and vigorous. It had moved out of its rosette phase and into the beginning phases of elongation/bolting before zinc deficiency symptoms began to appear.

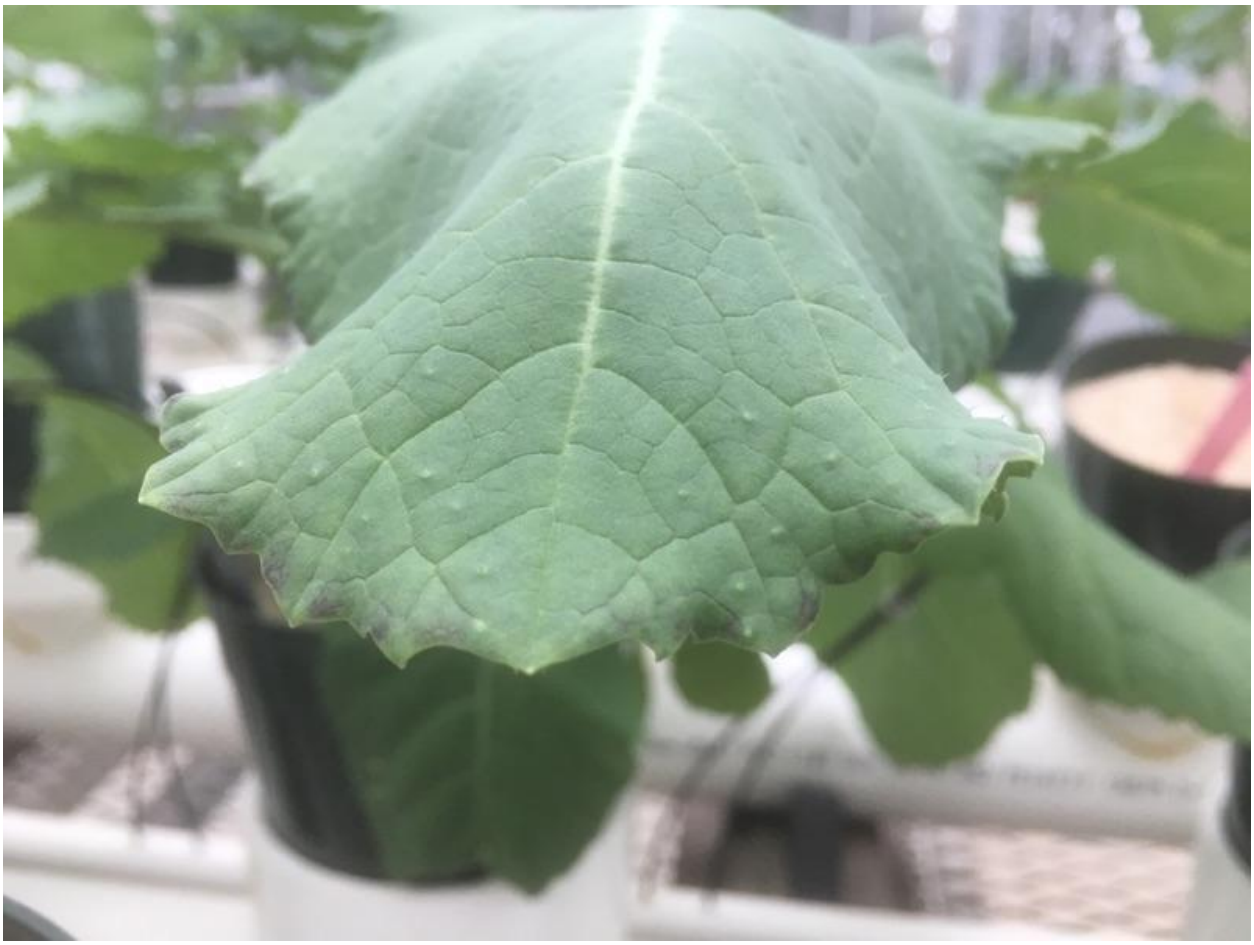

Figure 2.3.9: The beginning stages of zinc deficiency very late in the experiment as a marginal paleness and purpling of the leaf margin especially of the leaf tip. Also note the gall like structures on the leaf surface. When diagnosing Zn deficiency these two symptoms may be unique symptomologies.

Figure 2.3.10: The plant on the left received all its essential macro and micronutrients while the plant on the right is experience manganese deficiency. Note specifically the pale coloration of the plant especially along the upper portions.

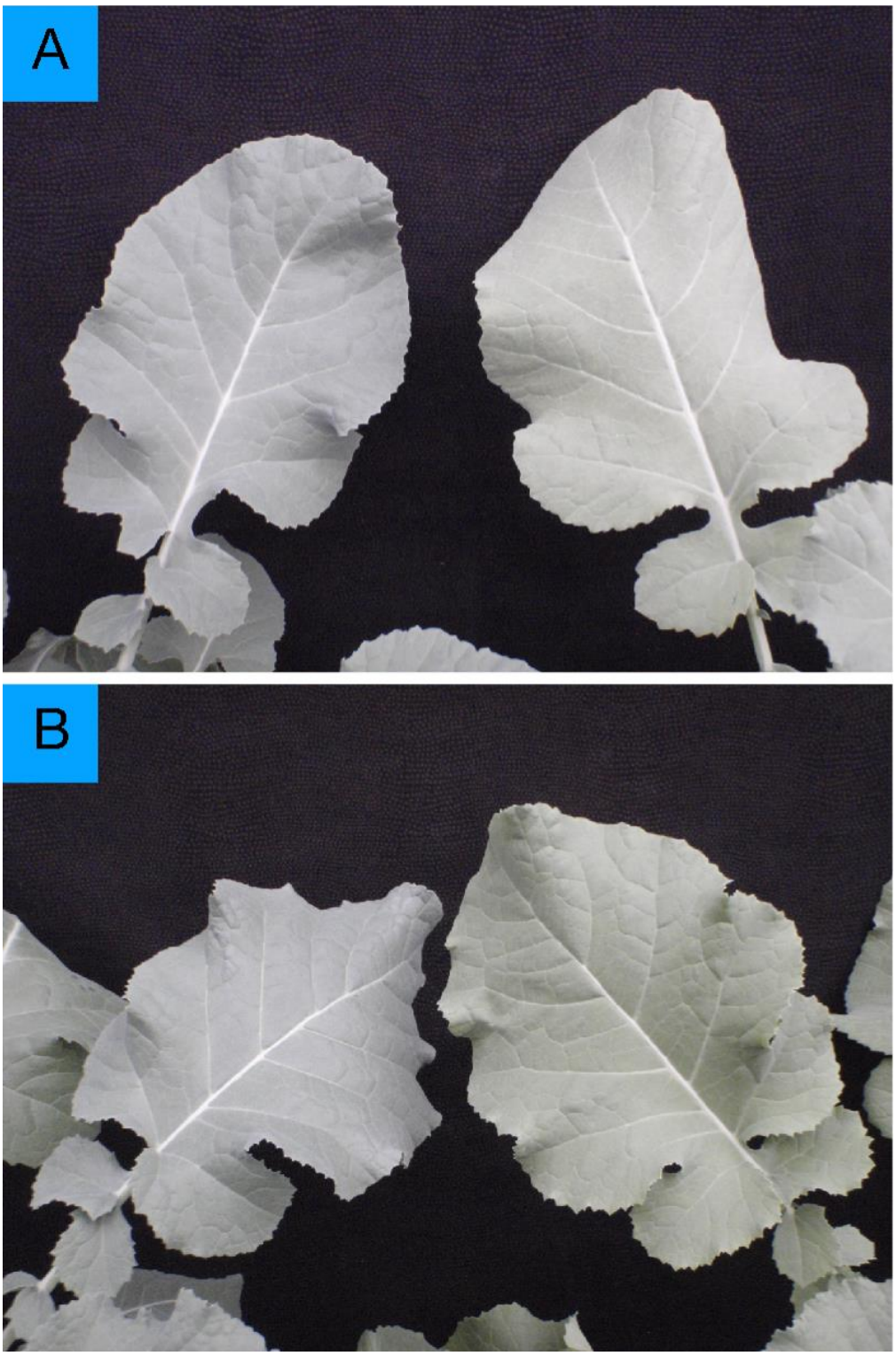

Figure 2.3.11: Mn deficient plants showed a paling coloration (right leaf, A and B). You can see this coloration was more developed in the upper (A) and mid (B) foliage.

Table 2.3.7: *Brassica carinata* plant lipidome metrics based on boron (B) fertility treatments.

Nutrient	Fertility Rate [1]	Oil Content [2]	Protein Content [3]	Glucosinolates [4]	Erucic Acid [5]	Saturated [6]	Monounsaturated [6]	Polyunsaturated [6]	18 : 1 [7]	18 : 2 [7]	18 : 3 [7]	20 : 1 [7]	LCFA [7]	VLCFA [7]
Boron	0.00	N/A	N/A	N/A	N/A	N/A	N/A	N/A	N/A	N/A	N/A	N/A	N/A	N/A
	11.25	25.91 A	41.74 A	122.81 AB	40.81 A	6.77 A	50.87 A	39.81 A	9.21 A	19.97 A	15.14 A	4.31 A	50.44 A	49.56 A
	22.50	26.83 A	42.03 A	112.33 BC	44.91 A	6.46 A	52.26 A	39.60 A	5.97 A	19.31 A	15.82 A	4.08 AB	51.40 A	48.60 A
	33.75	25.30 A	41.49 A	121.39 AB	41.68 A	7.03 A	52.23 A	38.87 A	9.40 A	20.79 A	14.37 A	3.87 AB	46.22 A	53.78 A
	39.38	22.75 A	45.39 A	135.32 A	37.68 A	6.93 A	49.15 A	40.28 A	12.00 A	21.27 A	14.55 A	4.20 A	56.20 A	43.80 A
	45.00	26.16 A	41.14 A	102.89 C	43.18 A	7.38 A	52.41 A	39.79 A	8.16 A	21.47 A	15.11 A	2.06 B	47.03 A	52.97 A
Analysis [8]		NS	NS	*	NS	NS	NS	NS	NS	NS	NS	*	NS	NS

[1] Fertility rate applied to plants with concentrations in μmol • L^{-1}. For details on rates and solutions see Table 1.
[2] Oil content calculated by percentage (%) dry weight.
[3] Protein content calculated by percentage (%) dry weight.
[4] Glucosinolate values in μmol • g based on seed/seeds dry weight.
[5] Erucic Acid content within the seed (%) dry weight.
[6] Saturated fatty acids are defined as fatty acids with no double bonded carbons (C=C) within the aliphatic chain. Monounsaturated fatty acids are defined as fatty acids with one double bonded carbon (C=C) within the aliphatic chain. Polyunsaturated fatty acids are defined as fatty acids with more than one double bonded carbon (C=C) within the aliphatic chain. All fatty acid values are reported based on percentage (%) of total fatty acids.
[7] Individual fatty acids and fatty acid types are presented in annotated form, with the first two numbers corresponding to the total number of carbons in the carbon chain (aliphatic portion), and the second number corresponding to the number of double bonded carbons (C=C). Long chain fatty acids (LCFA) are defined as fatty acid chains with 14-18 carbon bonds within the aliphatic portion of the chain. Very long chain fatty acids are defined as a fatty acid chain with >19 carbon bonds within the aliphatic portion of the chain. Fatty acids are listed as follows with their associated annotation (18:1 = Oleic Acid; 18:2 = Linoleic Acid; 18:3 = α-Linoleic Acid; 20:1 = Eicosenoic acid).
[8] *, **, or *** Indicates statistically significant differences between sample means based on F-test (GLM) at $P \leq 0.05$, $P \leq 0.01$, or $P \leq 0.001$, respectively. NS (not significant) indicates the F-test difference between sample means was $P > 0.05$. Values with the same letter indicate a lack of statistical significance while values with different letters indicate statistically significant results.

Table 2.3.8: *Brassica carinata* plant lipidome metrics based on iron (Fe) fertility treatments.

Nutrient	Fertility Rate [1]	Oil Content [2]	Protein Content [3]	Glucosinolates [4]	Erucic Acid [5]	Saturated [6]	Monounsaturated [6]	Polyunsaturated [6]	18 : 1 [7]	18 : 2 [7]	18 : 3 [7]	20 : 1 [7]	LCFA [7]	VLCFA [7]
Iron	0.00	25.66 A	40.08 B	113.10 A	43.17 A	7.14 A	53.82 A	36.91 A	9.23 A	19.96 A	13.20 A	4.99 A	42.67 A	57.33 A
	18.00	26.95 A	40.95 AB	108.98 A	44.61 A	6.90 A	54.50 A	37.60 A	7.10 A	19.71 A	14.92 A	3.59 AB	46.98 A	53.02 A
	36.00	23.59 A	44.50 A	116.08 A	42.30 A	7.27 A	50.82 A	39.57 A	9.46 A	20.62 A	14.71 A	3.44 AB	49.77 A	50.23 A
	54.00	26.99 A	40.00 B	106.13 A	42.20 A	6.60 A	53.92 A	37.75 A	8.13 A	19.42 A	14.77 A	5.05 A	52.72 A	47.28 A
	63.00	24.78 A	43.05 AB	130.20 A	38.03 A	6.79 A	50.90 A	39.85 A	11.83 A	21.36 A	13.88 A	4.91 A	55.16 A	44.84 A
	72.00	26.16 A	41.14 AB	102.90 A	43.16 A	7.38 A	52.42 A	39.79 A	8.16 A	21.47 A	15.11 A	2.06 B	47.03 A	52.97 A
Analysis [8]		NS	*	NS	NS	NS	NS	NS	NS	NS	NS	*	NS	NS

[1] Fertility rate applied to plants with concentrations in μmol • L^{-1}. For details on rates and solutions see Table 1.

[2] Oil content calculated by percentage (%) dry weight.

[3] Protein content calculated by percentage (%) dry weight.

[4] Glucosinolate values in μmol • g based on seed/seeds dry weight.

[5] Erucic Acid content within the seed (%) dry weight.

[6] Saturated fatty acids are defined as fatty acids with no double bonded carbons (C=C) within the aliphatic chain. Monounsaturated fatty acids are defined as fatty acids with one double bonded carbon (C=C) within the aliphatic chain. Polyunsaturated fatty acids are defined as fatty acids with more than one double bonded carbon (C=C) within the aliphatic chain. All fatty acid values are reported based on percentage (%) of total fatty acids.

[7] Individual fatty acids and fatty acid types are presented in annotated form, with the first two numbers corresponding to the total number of carbons in the carbon chain (aliphatic portion), and the second number corresponding to the number of double bonded carbons (C=C). Long chain fatty acids (LCFA) are defined as fatty acid chains with 14-18 carbon bonds within the aliphatic portion of the chain. Very long chain fatty acids are defined as a fatty acid chain with >19 carbon bonds within the aliphatic portion of the chain. Fatty acids are listed as follows with their associated annotation (18:1 = Oleic Acid; 18:2 = Linoleic Acid; 18:3 = α-Linoleic Acid; 20:1 = Eicosenoic acid).

[8] *, **, or *** Indicates statistically significant differences between sample means based on F-test (GLM) at $P \leq 0.05$, $P \leq 0.01$, or $P \leq 0.001$, respectively. NS (not significant) indicates the F-test difference between sample means was $P > 0.05$. Values with the same letter indicate a lack of statistical significance while values with different letters indicate statistically significant results.

Table 2.3.9: *Brassica carinata* plant lipidome metrics based on copper (Cu) fertility treatments.

Nutrient	Fertility Rate [1]	Oil Content [2]	Protein Content [3]	Glucosinolates [4]	Erucic Acid [5]	Saturated [6]	Monounsaturated [6]	Polyunsaturated [6]	18 : 1 [7]	18 : 2 [7]	18 : 3 [7]	20 : 1 [7]	LCFA [7]	VLCFA [7]
Copper	0.00	27.22 A	40.07 AB	110.10 A	43.82 A	8.32 A	56.74 A	36.63 A	8.66 A	22.45 A	14.80 A	0.56 B	32.60 C	67.40 A
	0.75	26.07 A	41.40 AB	119.01 A	40.03 A	6.80 A	51.38 AB	39.66 A	10.24 A	20.75 A	14.20 A	4.93 A	51.82 AB	48.18 BC
	1.50	25.35 A	44.43 A	118.87 A	38.77 A	6.58 A	50.34 B	40.39 A	11.07 A	20.78 A	15.11 A	4.48 A	56.78 A	43.23 C
	2.25	26.90 A	40.63 AB	121.81 A	39.18 A	6.73 A	52.59 AB	39.04 A	10.82 A	21.23 A	14.64 A	4.52 A	49.60 AB	50.41 BC
	2.63	28.38 A	39.23 B	109.60 A	43.40 A	7.46 A	54.62 AB	37.84 A	7.82 A	20.76 A	15.39 A	1.74 AB	38.14 BC	61.87 BA
	3.00	26.15 A	41.14 AB	102.90 A	43.16 A	7.38 A	52.42 AB	39.79 A	8.16 A	21.47 A	15.12 A	2.06 AB	47.03 ABC	52.97 ABC
Analysis [8]		NS	*	NS	NS	NS	*	NS	NS	NS	NS	*	*	*

[1] Fertility rate applied to plants with concentrations in μmol • L^{-1}. For details on rates and solutions see Table 1.
[2] Oil content calculated by percentage (%) dry weight.
[3] Protein content calculated by percentage (%) dry weight.
[4] Glucosinolate values in μmol • g based on seed/seeds dry weight.
[5] Erucic Acid content within the seed (%) dry weight.
[6] Saturated fatty acids are defined as fatty acids with no double bonded carbons (C=C) within the aliphatic chain. Monounsaturated fatty acids are defined as fatty acids with one double bonded carbon (C=C) within the aliphatic chain. Polyunsaturated fatty acids are defined as fatty acids with more than one double bonded carbon (C=C) within the aliphatic chain. All fatty acid values are reported based on percentage (%) of total fatty acids.
[7] Individual fatty acids and fatty acid types are presented in annotated form, with the first two numbers corresponding to the total number of carbons in the carbon chain (aliphatic portion), and the second number corresponding to the number of double bonded carbons (C=C). Long chain fatty acids (LCFA) are defined as fatty acid chains with 14-18 carbon bonds within the aliphatic portion of the chain. Very long chain fatty acids are defined as a fatty acid chain with >19 carbon bonds within the aliphatic portion of the chain. Fatty acids are listed as follows with their associated annotation (18:1 = Oleic Acid; 18:2 = Linoleic Acid; 18:3 = α-Linoleic Acid; 20:1 = Eicosenoic acid).
[8] *, **, or *** Indicates statistically significant differences between sample means based on F-test (GLM) at $P \leq 0.05$, $P \leq 0.01$, or $P \leq 0.001$, respectively. NS (not significant) indicates the F-test difference between sample means was $P > 0.05$. Values with the same letter indicate a lack of statistical significance while values with different letters indicate statistically significant results.

Table 2.3.10: *Brassica carinata* plant lipidome metrics based on zinc (Zn) fertility treatments.

Nutrient	Fertility Rate [1]	Oil Content [2]	Protein Content [3]	Glucosinolates [4]	Erucic Acid [5]	Saturated [6]	Monounsaturated [6]	Polyunsaturated [6]	18 : 1 [7]	18 : 2 [7]	18 : 3 [7]	20 : 1 [7]	LCFA [7]	VLCFA [7]
Zinc	0.00	23.80 B	41.13 A	116.25 A	38.14 A	7.15 A	51.01 A	39.14 AB	11.17 A	20.66 A	14.79 A	4.34 ABC	47.21 A	52.79 A
	0.75	27.98 A	41.21 A	115.05 A	43.01 A	7.06 A	53.79 A	37.62 B	8.71 A	20.09 A	15.19 A	2.34 BC	38.86 A	61.14 A
	1.50	24.55 AB	42.87 A	130.47 A	40.86 A	6.75 A	50.30 A	39.77 AB	9.41 A	20.47 A	14.97 A	4.90 AB	47.03 A	51.66 A
	2.25	25.41 AB	39.05 A	108.67 A	37.94 A	7.14 A	52.31 A	38.65 AB	11.13 A	20.95 A	13.52 A	5.06 AB	46.89 A	53.11 A
	2.63	27.96 A	40.52 A	113.09 A	40.47 A	6.50 A	50.66 A	40.81 A	9.09 A	21.19 A	15.38 A	5.11 A	49.77 A	50.23 A
	3.00	26.16 AB	41.14 A	102.90 A	43.16 A	7.38 A	52.42 A	39.79 AB	8.16 A	21.47 A	15.11 A	2.06 C	47.03 A	52.97 A
Analysis [8]		*	NS	NS	NS	NS	NS	*	NS	NS	NS	*	NS	NS

[1] Fertility rate applied to plants with concentrations in µmol • L^{-1}. For details on rates and solutions see Table 1.
[2] Oil content calculated by percentage (%) dry weight.
[3] Protein content calculated by percentage (%) dry weight.
[4] Glucosinolate values in µmol • g based on seed/seeds dry weight.
[5] Erucic Acid content within the seed (%) dry weight.
[6] Saturated fatty acids are defined as fatty acids with no double bonded carbons (C=C) within the aliphatic chain. Monounsaturated fatty acids are defined as fatty acids with one double bonded carbon (C=C) within the aliphatic chain. Polyunsaturated fatty acids are defined as fatty acids with more than one double bonded carbon (C=C) within the aliphatic chain. All fatty acid values are reported based on percentage (%) of total fatty acids.
[7] Individual fatty acids and fatty acid types are presented in annotated form, with the first two numbers corresponding to the total number of carbons in the carbon chain (aliphatic portion), and the second number corresponding to the number of double bonded carbons (C=C). Long chain fatty acids (LCFA) are defined as fatty acid chains with 14-18 carbon bonds within the aliphatic portion of the chain. Very long chain fatty acids are defined as a fatty acid chain with >19 carbon bonds within the aliphatic portion of the chain. Fatty acids are listed as follows with their associated annotation (18:1 = Oleic Acid; 18:2 = Linoleic Acid; 18:3 = α-Linoleic Acid; 20:1 = Eicosenoic acid).
[8] *, **, or *** Indicates statistically significant differences between sample means based on F-test (GLM) at $P \leq 0.05$, $P \leq 0.01$, or $P \leq 0.001$, respectively. NS (not significant) indicates the F-test difference between sample means was $P > 0.05$. Values with the same letter indicate a lack of statistical significance while values with different letters indicate statistically significant results.

Table 2.3.11: *Brassica carinata* plant lipidome metrics based on molybdenum (Mo) fertility treatments.

Nutrient	Fertility Rate [1]	Oil Content [2]	Protein Content [3]	Glucosinolates [4]	Erucic Acid [5]	Saturated [6]	Monounsaturated [6]	Polyunsaturated [6]	18 : 1 [7]	18 : 2 [7]	18 : 3 [7]	20 : 1 [7]	LCFA [7]	VLCFA [7]
Molybdenum	0.00	26.03 A	43.07 A	122.01 A	46.63 A	7.32 A	52.98 A	39.14 A	5.91 A	20.21 A	15.72 A	1.91 B	40.20 A	59.80 A
	0.025	28.01 A	41.07 A	109.79 A	42.29 A	6.48 A	51.89 A	39.80 A	8.24 A	19.83 A	14.79 A	4.78 AB	50.25 A	49.75 A
	0.050	26.36 A	40.60 A	120.07 A	37.94 A	6.73 A	51.46 A	39.29 A	11.54 A	21.10 A	14.41 A	5.37 AB	49.09 A	50.91 A
	0.075	24.29 A	42.95 A	117.87 A	40.19 A	6.82 A	49.80 A	40.16 A	10.30 A	20.56 A	14.65 A	5.04 AB	52.67 A	47.33 A
	0.088	25.38 A	40.24 A	128.30 A	35.60 A	6.56 A	52.11 A	38.22 A	12.64 A	20.42 A	14.27 A	6.00 A	45.94 A	54.06 A
	0.100	26.16 A	41.14 A	102.90 A	43.16 A	7.38 A	52.42 A	39.79 A	8.16 A	21.47 A	15.11 A	2.06 B	47.03 A	52.97 A
Analysis [8]		NS	NS	NS	NS	NS	NS	NS	NS	NS	NS	*	NS	NS

[1] Fertility rate applied to plants with concentrations in µmol • L^{-1}. For details on rates and solutions see Table 1.
[2] Oil content calculated by percentage (%) dry weight.
[3] Protein content calculated by percentage (%) dry weight.
[4] Glucosinolate values in µmol • g based on seed/seeds dry weight.
[5] Erucic Acid content within the seed (%) dry weight.
[6] Saturated fatty acids are defined as fatty acids with no double bonded carbons (C=C) within the aliphatic chain. Monounsaturated fatty acids are defined as fatty acids with one double bonded carbon (C=C) within the aliphatic chain. Polyunsaturated fatty acids are defined as fatty acids with more than one double bonded carbon (C=C) within the aliphatic chain. All fatty acid values are reported based on percentage (%) of total fatty acids.
[7] Individual fatty acids and fatty acid types are presented in annotated form, with the first two numbers corresponding to the total number of carbons in the carbon chain (aliphatic portion), and the second number corresponding to the number of double bonded carbons (C=C). Long chain fatty acids (LCFA) are defined as fatty acid chains with 14-18 carbon bonds within the aliphatic portion of the chain. Very long chain fatty acids are defined as a fatty acid chain with >19 carbon bonds within the aliphatic portion of the chain. Fatty acids are listed as follows with their associated annotation (18:1 = Oleic Acid; 18:2 = Linoleic Acid; 18:3 = α-Linoleic Acid; 20:1 = Eicosenoic acid).
[8] *, **, or *** Indicates statistically significant differences between sample means based on F-test (GLM) at $P \leq 0.05$, $P \leq 0.01$, or $P \leq 0.001$, respectively. NS (not significant) indicates the F-test difference between sample means was $P > 0.05$. Values with the same letter indicate a lack of statistical significance while values with different letters indicate statistically significant results.

Table 2.3.12: *Brassica carinata* plant lipidome metrics based on manganese (Mn) fertility treatments.

Nutrient	Fertility Rate [1]	Oil Content [2]	Protein Content [3]	Glucosinolates [4]	Erucic Acid [5]	Saturated [6]	Monounsaturated [6]	Polyunsaturated [6]	18 : 1 [7]	18 : 2 [7]	18 : 3 [7]	20 : 1 [7]	LCFA [7]	VLCFA [7]
Manganese	0.00	27.33 A	40.56 A	114.48 A	43.60 A	7.23 A	53.29 A	38.90 A	8.17 A	21.09 A	15.29 A	2.51 A	43.42 A	56.58 A
	4.50	23.58 A	41.41 A	124.63 A	36.76 B	7.06 A	51.38 A	38.97 A	12.07 A	20.97 A	14.42 A	4.72 A	48.67 A	51.33 A
	9.00	23.77 A	41.79 A	122.98 A	38.44 AB	7.03 A	52.57 A	38.61 A	11.20 A	21.00 A	14.11 A	4.45 A	52.41 A	47.59 A
	13.50	27.99 A	41.79 A	118.59 A	42.57 AB	7.07 A	53.77 A	38.49 A	8.78 A	21.34 A	14.73 A	3.39 A	44.01 A	55.99 A
	15.75	28.02 A	39.38 A	118.68 A	41.59 AB	6.45 A	53.25 A	38.71 A	8.71 A	20.08 A	14.79 A	4.98 A	44.95 A	55.05 A
	18.00	26.16 A	41.14 A	102.90 A	43.16 A	7.38 A	52.42 A	39.79 A	8.16 A	21.47 A	15.11 A	2.06 A	47.03 A	52.97 A
Analysis [8]		NS	NS	NS	*	NS	NS	NS	NS	NS	NS	NS	NS	NS

[1] Fertility rate applied to plants with concentrations in µmol • L^{-1}. For details on rates and solutions see Table 1.
[2] Oil content calculated by percentage (%) dry weight.
[3] Protein content calculated by percentage (%) dry weight.
[4] Glucosinolate values in µmol • g based on seed/seeds dry weight.
[5] Erucic Acid content within the seed (%) dry weight.
[6] Saturated fatty acids are defined as fatty acids with no double bonded carbons (C=C) within the aliphatic chain. Monounsaturated fatty acids are defined as fatty acids with one double bonded carbon (C=C) within the aliphatic chain. Polyunsaturated fatty acids are defined as fatty acids with more than one double bonded carbon (C=C) within the aliphatic chain. All fatty acid values are reported based on percentage (%) of total fatty acids.
[7] Individual fatty acids and fatty acid types are presented in annotated form, with the first two numbers corresponding to the total number of carbons in the carbon chain (aliphatic portion), and the second number corresponding to the number of double bonded carbons (C=C). Long chain fatty acids (LCFA) are defined as fatty acid chains with 14-18 carbon bonds within the aliphatic portion of the chain. Very long chain fatty acids are defined as a fatty acid chain with >19 carbon bonds within the aliphatic portion of the chain. Fatty acids are listed as follows with their associated annotation (18:1 = Oleic Acid; 18:2 = Linoleic Acid; 18:3 = α-Linoleic Acid; 20:1 = Eicosenoic acid).
[8] *, **, or *** Indicates statistically significant differences between sample means based on F-test (GLM) at $P \leq 0.05$, $P \leq 0.01$, or $P \leq 0.001$, respectively. NS (not significant) indicates the F-test difference between sample means was $P > 0.05$. Values with the same letter indicate a lack of statistical significance while values with different letters indicate statistically significant results.

CHAPTER 3. The Impacts of Differing Fertility Concentrations of Macronutrients on Leaf Tissue Accumulation and Growth of *Brassica carinata* During Different Life Stages.

Paul Cockson [1,*], Patrick Veazie[1], David Logan[1], Matthew Davis[1], Gabby Barajas[1], Angela Post[2], Carl Crozier[2], Ramone Leon[2], Bob Patterson[2], and Brian E. Whipker [1]

[1] Department of Horticultural Science, North Carolina State University, Raleigh, NC 27695, USA; bwhipker@ncsu.edu (B.E.W.)

[2] Department of Crop and Soil Science, North Carolina State University, Raleigh, NC 27695, USA;

* Correspondence: pncockso@ncsu.edu

Abstract: Many abiotic factors impact the yield and growth of *Brassica carinata* (commonly referred to as carinata). Very little is known about carinata and how mineral nutrients impact its growth, and more specifically the sufficiency values for fertility over the plant's growth cycle and life stages. Thus, this study explored the impact plant nutrients, specifically macronutrients, have on the growth and development of carinata over its distinct life stages (rosette, bolting, flowering, and pod set). Additionally, this study sought to explore the adequate ranges for fertility by regressing nutrient curves to find the concentration at which leaf tissue mineral concentrations plateaued. Plants were grown under varying macronutrient concentrations (0.0, 25.0, 50.0, 75.0, 87.5, and 100.0%) utilizing the concentrations of a modified Hoagland's solution. This experiment took data on plant height, diameter, leaf tissue mineral nutrient concentrations, and biomass. The results demonstrated that macronutrient fertility can have profound impacts on the production of *B. carinata* during different life stages. Additionally, optimal concentrations of macronutrients and the maximization of biomass production can vary dramatically based on the macronutrient fertility provided.

Keywords: oilseed, *Brassica carinata*, fatty acids, lipidome, fertility, life-cycle, micronutrients, symptomology, foliar, aviation biofuel

3.1. INTRODUCTION

Increasingly, concerns of a rapidly changing global climate have garnered increased attention and produced policies directly related toward CO_2 emissions regulation, sequestration, and alternative energy resources. The changes to the energy landscape and carbon conscious mentality has resulted in many countries and nations seeking to mitigate carbon emissions. In particular, the diversification of fuel sources in the transportation, utilities, and industry sectors has garnered more attention as government and private industry bodies seek to diversify fuel and energy sources to create a more robust and secure energy portfolio.

Globally, and especially in European countries and the West Coast of the United States, alternative and more carbon neutral aviation fuel have gained attention. Aviation engine emissions produce CO_2 at high altitudes (Govardhan et al., [1]; Satheesh, [2]) which is problematic given the carbon's longer residency time due to poor carbon cycling (Craig, [3]; Friend et al., [4]). Additionally, carbon emissions produced at higher altitudes are physically separated from carbon sequestering plants. Thus, an aviation system by default deposits CO_2 out of reach of the organisms which traditionally sequester carbon. To help mitigate this system of high altitude emissions, one alternative would be to source aviation fuel from a renewable biofuel. This could potentially reduce the carbon impacts on aviation emissions.

One such biofuel option is plant lipid sourced biofuels. These fatty acid derived biofuels already have an established precedent in soybean and corn source fuels such as ethanol and biodiesels (U.S. Energy Information Administration, [5]; Seepaul et al., [6]). These biofuels are often more competitive against traditional fuel markets during increases in petroleum prices. However, as we continue to grow in population and the energy demands of the global energy system increase, a diversification of energy sources and systems will be needed.

Aviation fuel, much like other fuel sources, requires a certain chemical and physical consistency and constituency for optimal functionality in a turbine engine (Federal Aviation Administration, [7]). Consequently, any biofuel seeking to supplement or replace traditional petroleum based aviation fuels will have to mimic or improve upon the chemical and physical properties of these fuels. One biofuel source, which can potentially supplement or replace aviation petroleum after refinement, comes from the fatty acid profile of the seeds of *Brassica carinata*, also known as Ethiopian mustard, and commonly referred to as simply carinata. This oilseed crop has a unique fatty acid, lipid, and protein profile (Gesch et al., [8]) which has a higher distribution of mid chain (MCFA), long chain (LCFA), and very long chain fatty acids (VLCFA) which after refinement produce a fuel source very similar to the physical and chemical properties of petroleum derived aviation fuel (U.S. Energy Information Administration, [5]). The biofuel derived from carinata has been tested in a flight in 2012 and shown to decrease particle emissions, black carbon emissions, aerosol emissions, and increased specific fuel consumption (Govardhan et al., [1]; Satheesh, [2]; Federal Aviation Administration, [7]).

Despite the success already observed in aviation biofuels produced from carinata, challenges remain. Traditionally, variations in quality and consistency of the product sourced from a biological organism is not as consistent as petroleum sources. These raw resources produced from living organisms are subject to deleterious impacts abiotic stresses can have on yield, plant growth, and reproduction. Specifically, in carinata, fatty acids, oil content, and protein distribution of the seeds can result in a less than uniform product which can cause challenges in the supply chain of a bio-derived fuel. One such abiotic stress is plant nutrients and fertility.

Plants require certain micro and macronutrients to optimize growth, yield, and complete their lifecycle (Marschner, [9]). These nutrients have direct impacts on yield, especially in brassicas (Gibson et al., [10]; Grant and Bailey, [11]). Additionally,

brassicas have distinct life stages (rosette, bolting, flowering, pod set, and pod fill) each requiring different levels of mineral nutrients to ensure adequate development and yield.

Brassicas undergo distinct phases of growth after germination (SPARC, Appendix 1; Seepaul et al. [6, 12]; Harper and Berkenkamp, [13]). The first stage of growth is the rosette stage. During this stage, plants remain vegetative and low to the ground producing mainly vegetative biomass and root biomass. The next stage is bolting when, plants initiate their reproductive phase and produce ahighy-branched vertical flower spikelet. The next stage of development is flowering and reproduction. During this phase, resources are poured into the developing flowers and siliques. The next stage is pod fill and seed set when plants direct resources into developing embryos and seeds. Finally, the plants will defoliate and desiccate.

Given different sources and sinks will be present at each life stage, carinata will have different mineral nutrient requirements at different stages. Other abiotic factors will impact growth and yield such as water and temperature in addition to fertilization (Ahmadi and Bahrani, [14]; Angadi et al., [15]; Polowick and Sawhney, [16]; Tayo and Morgan, [17]). However, macro and micronutrients are among the most yield-limiting factor to oilseed brassicas (Berry and Spink, [18]). If an essential macro or microelement is limited, this can impact the yield and production of quality oil in brassica species (Miller et al., [19]; Govahi and Saffari, [20]; Gao et al., [21]; Durenne et al., [22]; Nuttall et al., [23]; Fismes et al., [24]; Ma et al., [25]).

The primary macronutrients (nitrogen (N), phosphorous (P), and potassium (K)) are present in the greatest quantities within plants as compared to the secondary macronutrients (calcium (Ca), magnesium (Mg), and sulfur (S)). The work by Yousaf et al. ([26]) explored the impacts of the primary macronutrients on the productivity and

quality of *Brassica napus* L. This work inquired specifically into N, P, and K and their impacts on yield, oil production, and protein content. Their findings showed that N was the most limiting element followed by P and K, and that yield increased by 61-72% under an NPK fertility regime when compared to just a PK treatment. Protein and oil constituents and other fatty acids were not influenced significantly by the application of P and K fertilizer even though oil and protein yields were affected. An increase in N fertilizer resulted in a reduction of oil concentration and an increase in protein content. This inverse relationship between protein and oils has been studied in other works (Brennan et al., [27]; Krauze and Bowszys, [28]). These studies show the three essential macronutrients have an impact on the growth, oil production, and protein content in oilseed brassicas.

Work out of the University of Florida has shown a strong correlation between *Brassica napus* and *B. carinata* and photosynthetic activity and concentration based on nitrogen fertility concentrations (Seepaul et al., [6]). This work used differing N concentrations and studied the impacts on both brassicas showing that when N was limited, biomass accumulation, total dry matter, and leaf area were all less when compared to the highest N treatments. Another work by Seepaul et al. ([12]) studied the dry matter accumulation of *B. carinata* under different nitrogen fertilizer regimes. This work showed that life stage of *B. carinata* impacted N uptake as well, with the greatest uptake occurring in the bolting and flower stages of the plant's lifecycle.

In another work completed by Govahi and Saffari ([20]), who studied K and S fertilization on yield, seed quality, and yield components of *Brassica napus* L. By varying both concentrations of K and S, the group was able to determine that an increase in S resulted in an increase in biomass production, primary and secondary branching, and average seed/pod number. Their results also indicated that increasing S concentrations from 0 to 40 and 40 to 80 kg/ha resulted in an increase in seed oil content of 3.89% and 6.0% respectively. However, at the highest concentrations of 80 and 120 kg/ha of S applied, there was no significant increase in seed oil content. Increasing K concentrations had no impact on seed oil content. The highest protein yield was observed at the highest S concentration of 120 kg/ha.

Sulfur is needed at much higher levels in brassicas than in other row crops. Varényiová et al. ([29]) explored the impacts of varying S nutrition in the yield, oiliness, oil production, seed nutrient content, and plant nutrient content in *Brassica napus* L. By varying the rates of S applied (0, 15, 40, 65 kg/ha), they sought to determine the impacts of S on plant growth and yield. Their results however, showed no significant impacts on oil content among all treatments. This is interesting given that Ahmad et al. ([30]), saw a significant increase in oil content at a dose of 20 kg/ha. More research is needed to further understand the complex relations of S nutrition on plant physiology and yield metrics.

Two works by Nuttall et al. ([23]) and Ma et al. ([25]) examined the impacts of N, S, and boron (B) on the yield and quality of oilseed brassicas. Nuttall et al. ([23]) found S fertilizer increased the glucosinolate concentration of rape meal and increased oil concentrations. Nitrogen fertility increased the content of protein while N plus B treatments resulted in a decrease of protein and an increase in oil percentage. In these studies Sulfur remedied poor seed set and B improved pod development and decreased the number of sterile florets. Ma et al. ([25]) found a foliar application of B resulted in a 10 percent increase in yield when applied at the early flowering stage. They also showed a strong correlation (r^2=0.99) between N rates and yield. Sulfur applications resulted in an increase of canola yields of 3-31% varying by location. Additionally, work completed by Ali et al., ([31]) showed direct impacts on irrigation and nitrogen fertility to oil yield in canola plants.

In addition to different fertility needs based on life stage, different macronutrient needs exist in brassicas. For example, during the bolting phase, rapid cell polarization and expansion necessitates a higher use of elements which aid the expansion and stabilization of the cell wall. Boron and Ca are primarily found in the cell wall contained within the B-dimeric rhamnogalacturonan II (RG-II) complex (Matoh, [32]). Within this complex, both B and Ca help to stabilize the structure, and allow the complex to create Ca ion bridges between the pectin chains within the cell wall (Chebli and Geitmann, [33]; Matoh, [32]). When B was limited, the RG-II complex was monomeric and the cell walls swelled rather than differentiating polarly (Matoh, [32]). The cells may not be able to expand properly or directionally given the stabilizing nature the RG-II complex plays within the cell wall and stabilizing the pectin matrix. Given the bolting phase

produces the flower spikelet, any limitation of this process will have a direct impact on flower formation, siliques, and seeds.

When levels of a macroelement fall below a certain range, negative impacts are observed on plant growth and development, physiological functions and pathways, metabolites, and seed and embryo development (Taylor et al., [34]). To rectify or avoid these negative impacts, proper fertility must be administered to plants during all stages of development. This work seeks to explore the impacts of macronutrients on the growth and development of a new and emerging biofuel oilseed crop Brassica carianata. The optimal macronutrient fertility ranges will be explored by supplying each macronutrient at differing fertility levels based on a modified Hoagland's solution. The impacts on total plant above ground biomass as well as leaf tissue concentration were cataloged, at each of the four distinct life stages of the crop (rosette, bolting, flowering, and pod set).

3.2 MATERIALS AND METHODS

B. carinata 'Avanza 641' (Agrisoma, Gatineau, Quebec) seeds were sown on 20 November 2019 into 72-cell plug trays filled with a substrate mix of 80:20 (v:v) Canadian sphagnum peat moss (Conrad Fafard, Agawam, MA) and horticultural grade perlite (Perlite Vermiculite Packaging Industries, Inc., North Bloomfield, OH). The substrate mix was amended with dolomitic lime at 8.875 kg/m^3 (Rockydale Agricultural, Roanoke, VA) and wetting agent (Aquatrols, Cherry Hill, NJ) at 600 g/m^3. The premade substrate mix ensured no macronutrient charge or contaminants were present in the seeding substrate. Seedlings were then grown at 22.8 ± 2.8°C day/night (D/N) temperatures (73.0 ± 5.0°F) in a glass greenhouse in Raleigh, NC (35.8°N Latitude) under a mist bench set at irrigation intervals (5 sec. every 3 minutes). After the second

true leaves emerged, the plants were removed from mist and hand irrigated with a nurse fertilizer solution (33.4 g KNO_3, 33.4 g Ca $(NO_3)_2 \bullet H_2O$, 6.6 g KH_2PO_4, 13.2 g $MgSO_4 \bullet 7H_2O$ in 20L H_2O per 100L deionized (DI) H_2O).

Plugs were then grown out and hardened until they developed four true leaves after which time, they were transplanted on 18 December 2019 into 15.24-cm diameter (1.76 L) plastic pots filled with acid washed silica-sand [Millersville #2 (0.8 to 1.2 mm diameter) from Southern Products and Silica Co., Hoffman, NC] (Henry et al., [35]). Each pot received one rooted plug. At transplant fertility treatment regimens started.

After transplant, the plants were grown at 15.5/12.8 ± 2.8°C D/N temperatures (59.9/55.0 ± 5.04°F) day/night temperatures. On, 17 January 2020 the day temperature and night temperature were increased to 18.3/15.5 ± 3.1°C D/N temperatures (65/60 ± 5.58°F) respectively to encourage bolting and the bolting harvest occurred on 14 February. Plants were grown out until 6 March at which point the flowering harvest occurred. Finally, pod set stage harvest was completed on 25 March.

Plants were grown in an automated, recirculating irrigation system made from 10.2-cm diameter PVC pipe (Charlotte Plastics, Charlotte, NC), fit with 12.7-cm diameter openings to hold the pots (Henry et al., [34]). Plants were distributed into rows capable of holding either 8 or 6 pots with 6 rows blocked per group and 4 groups per bench with a total of four benches in the greenhouse. Each row received a different macronutrient fertility treatment with treatments distributed among benches, blocks, and lines using a randomized block design. Fertility macronutrient treatments were sub-divided into different concentrations (0, 25, 50, 75, 87.5, and 100%) of a modified Hoagland's solution (Hoagland and Arnon, [36]; Henry et al., [34]; Barnes et al., [37]). Control plants were grown with (macronutrient concentrations in mM) 15 nitrate-nitrogen (NO_3^-), 1.0 phosphate-phosphorus ($H_2PO_4^-$), 6.0 potassium (K^+), 5.0 calcium (Ca^{2+}), 2.0 magnesium (Mg^{2+}), and 2.0 sulfate-sulfur (SO_4^{2-}) plus (micronutrient concentrations in μM) 72 iron (Fe^{2+}), 18 manganese (Mn^{2+}), 3.0 copper (Cu^{2+}), 3.0 zinc

(Zn^{2+}), 45 boron (BO_3^{3-}), and 0.1 molybdenum (MoO_4^{2-}) (Hoagland and Arnon, [36]). Macronutrients were altered based on the above baselines. Complete breakouts of nutrients and concentrations can be observed in Table 3.2.1. All nutrient solutions were tested and confirmed for concentrations using the North Carolina Department of Agriculture & Consumer Services (NCDA) testing lab using 50 mLs of the solutions after letting the concentrations sit for 48 hours after mixing (Raleigh, NC). Upon mixing more fertilizer solutions, each new batch was visually inspected for precipitates and the pH and EC were tested to ensure the values were within the desired values.

Plants were drip irrigated utilizing their assigned modified macronutrient solutions using a sump-pump (model 1A, Little Giant Pump Co., Oklahoma City, OK) system. Irrigations occurred every hour and ran for one minute between 6:00 and 19:00 hours. Irrigation solution drained from the pot and was captured for reuse with solutions being emptied and replenished weekly (Henry et al., [34]). For more details on the modified Hoagland's solution and the setup, please refer to Barnes et al., ([37]). Macronutrient concentration solutions were replaced weekly to ensure fertilizer concentrations stayed within acceptable ranges.

Plants were grown in their respective macronutrient treatments until either visual nutritive deficiency symptoms were observed, or the respective physiological stage was observed in over 50% of the control plants (100% Modified Hoagland's solution). Physiological stages for harvest were set at the rosette, bolting, flowering, and pod-set stages. Stages were determined using the decimal code (1.5-1.9: rosette, 3.0-3.3: bolting, 6.5: full flowering, 8.9-9.5: pod-set) developed by the SPARC working group (Appendix 1).

After the onset of initial visual deficient symptoms of each macronutrient treatment occurred, four symptomatic plants were selected and sampled. If visual symptoms did not develop, plants were harvested when over 50% of control plants reached physiological and morphological changes based on life cycle (SPARC,

Appendix 1). After sampling of the four replicates, the remaining plants (n=12) were grown to document symptomological and nutritive stresses into the remaining physiological stages. Thus, four more replicates were harvested when 50% of the control plants (100% of the concentration of the modified Hoagland's solution) reached bolting stage (SPARC, Appendix 1), and so on for the other physiological stages listed above.

For the four harvested replicates, most recently matured leaves were sampled to evaluate the critical macronutrient tissue concentrations for each fertility treatment and concentration. Plants were destructively harvested, and the most recently matured leaves were initially rinsed with deionized water, then washed in a solution of 0.1 M HCl for 1 min and again rinsed with DI water (Henry et al., [34]). The remaining shoot tissue was harvested separately, and roots were discarded.

Each harvest followed the above protocol. Upon sampling, the plant tissues were dried at 70 °C for 96 hours, and the dry mass was weighed and recorded. After drying, leaf tissue was ground in a Foss Tecator Cyclotec™ 1093 sample mill (Analytical Instruments, LLC; Golden Valley, MN; $\leq$0.5 mm sieve). The ground tissue was then placed in vials containing ~8 g of tissue and sent off for analysis to AgSource Laboratories (Lincoln, NE). A composite sample was taken from the vial (0.250 g $\pm$ 0.003 g) and digested with nitric acid (12 M) at 60 °C. After the nitric acid digestion, 3 mLs of 30% hydrogen peroxide was added to the sample and further digestion took place at 120 °C. Upon cooling, the sample then was then diluted to 25 mLs using a 20% hydrochloric acid solution. Analysis took place using an ICP-OES machine (Agilent 5110; Santa Clara, CA) using a 0.5 mL loop.

Data were analyzed using SAS program (version 9.4; SAS inst., Cary, NC). All leaf tissue mineral nutrition values and plant dry weights (tissue + rest of above ground plant biomass) were subjected to GLM using PROC GLM. The GLM procedure calculated the differences in means of the total plant dry weight and element and

utilized the concentration as the predictor. Means were adjusted utilizing Tukey's multiple comparison test. The resultant report indicated which samples were statistically different from each other and are reported in the summary tables.

Data were subjected to first and second order polynomial regression using PROC REG. Regression models treated the element as the y variable, and the concentration of fertility as the x variable. Each element was analyzed separately from the rest to eliminate any competition or enhancement that may have resulted due to nutrient antagonisms or synergisms of uptake (see Mudler's Chart Appendix 1; Baryia et al., [38]). Regression models were compared, and the polynomial model which resulted in the greatest statistical significance (α = 0.05, 0.01, 0.001) and the greatest adjusted r^2 values were selected.

Additionally, if data displayed a non-linear pattern in which a maximum values for leaf tissue or dry weights was obtained, PROC NLIN was utilized to determine the values of the maximum values contained within the plateau. The equations for the non-linear models can be found in Appendix 1. The corresponding X_0 values indicated the predicted concentration at which the plant dry weight or leaf tissue nutrients were obtained, and the associated average dry weight or leaf tissue corresponding to that value (Henry, [39]).

Tables were populated with the means from the statistical outputs above. Figures were created using JMP (version 14.2.0; SAS inst., Cary, NC). Data is organized by element with concentrations showing impacts on both dry weights and leaf tissue element concentrations. Data is reported with the means of each dataset and the associated r^2 and adjusted r^2 and regression equations (linear and polynomial).

3.3. RESULTS

3.3.1. Nitrogen (N)

Results varied by life-stage in carinata and across N concentrations. Nitrogen leaf tissue concentrations at all life stages, except the pod set stage, indicated that above 7.50 (mM • L^{-1}) no greater accumulation of leaf tissue N levels. Additionally, plant biomass production increased in plant dry weights as N concentrations increased. No differences occurred in plant biomass production at the higher N concentrations at the pod set stage.

3.3.1.1. N Deficiency Symptomology

Deficiency symptoms of N were only present at the 0.00, 3.75, and 7.50 mM • L^{-1} concentrations for the rosette stage and only the 0.00 and 3.75 mM • L^{-1} displayed visual symptoms in the bolting and flowering stages. As symptoms progressed, nutritive stress became more acute with lower leaves abscising until only the floral spikelet remained. Consequently, little to no vegetative material was present at the pod set stage for the 0.0 and 3.75 mM • L^{-1} concentrations.

Nitrogen deficiency first manifested as a general stunting of the plant (Fig. 3.3.1). The lower leaves appeared yellow or pale. As plants continued to grow, symptomology progressed rapidly, and the plant's overall growth rate decreased. During the rosette stage, the most mature leaves developed an interveinal chlorosis where the leaf veins developed a pink to red coloration (Fig. 3.3.2).

In the bolting stage at the lowest N concentrations, the lower foliage paled and bleached resulting in a yellow to white appearance (Fig. 3.3.3). Additionally, new and developing leaves yellowed. This resulted in a tri-level discoloration where lower foliage was bleached white, the mid foliage turned yellow or light green, and the upper foliage was dark green (Fig. 3.3.4). Eventually, the older leaves abscised and the next node

toward the terminal end of the plant displayed signs of N stress. This trend continued until no foliage remained at the pod set stage for the two lowest fertility concentrations.

3.3.1.2. Rosette Stage N Rates

Plants in the rosette stage increased in plant dry weight as N concentrations increased (Table 3.3.1, Graph 3.3.1). The greatest dry weight and the greatest leaf tissue N concentrations were observed at the highest fertility concentration (15.0 mM • L^{-1}). The highest concentration of N fertility resulted in a 26x increase of plant dry weight and a 6x increase in leaf tissue N when compared to the 0 mM • L^{-1} concentration. Additionally, plant dry weights for the two highest concentrations (13.13 and 15.0 mM • L^{-1}) were statistically similar and greater than the remaining values (Table 3.3.1, Graph 3.3.1).

At the rosette growth stage, plant dry weight showed a positive correlation to N concentrations. The linear and second order polynomial regression models accounted for 81.0% and 88.0%, respectively, of the variance explained for plant dry weight when N concentration was treated as the independent variable (Equations 3.3.1).

Leaf tissue N concentration increased up to 7.50 mM • L^{-1} N after which, increasing N did not result in any statistically greater leaf tissue accumulation. The greatest N leaf tissue value was observed at the highest fertility concentration (15.0 mM • L^{-1}) (Table 3.3.1, Graph 3.3.1).

At the rosette growth stage, leaf tissue N concentrations showed a positive correlation to increasing N fertility concentrations. The second order polynomial regression models accounted for 91.0% of the variance explained for the percentage of leaf tissue N when N fertility concentration was treated as the independent variable (Equations 3.3.1).

Recent studies have explored *B. carinata* and N fertility. Work completed by Seepaul et al. [6] explored N rates of 0, 5, 10, and 16 mg N • L^{-1}. These concentrations fall

well below the upper range of this study with the maximum value falling below the 3.75 mM • L^{-1} concentration explored here. Their work mirrored an increase of biomass and leaf tissue accumulation as N concentrations increased. Additionally, their work showed little differences between linear or quadratic regression models when exploring plant height, total leaf area, leaf dry weight, stem dry weight, total plant dry weight and main stem node number at the sub-optimal N levels provided. This study also demonstrated that different brassica species (*Brassica napus* and *Brassica carinata*) vary in accumulating leaf tissue N and plant biomass (Seepaul et al., [6]). Finally, our models for leaf tissue N accumulation and biomass production resulted in a plateau as compared to the lack of maximal leaf tissue observed in Seepaul et al. [6] (Table 3.3.1, Graph 3.3.1). This is most likely due to lower N concentrations utilized given the plateau model for both leaf tissue occurs at the 7.5 mM • L^{-1} which would be ≈ 100 ppm N (Equations 3.3.1).

Another work completed by Seepaul et al., [40] explored the impacts of N fertility on carinata dry matter accumulation. These data indicate that dry matter accumulation increased as N fertility increased from 0 to 135 kg • ha^{-1}. These data indicated that even when no N resources were provided, dry matter accumulated through the pod development stage after which, increases in mass and leveled off during seed maturation. There was little to no difference observed in plant dry mass production with linear or quadratic models when N rate was treated as the independent variable, confirming our results (Table 3.3.1, Graph 3.3.1).

3.3.1.3. Bolting Stage N Rates

Plants in the bolting stage showed a linear increase in dry weight as N concentrations increased (Table 3.3.1, Graph 3.3.1). The greatest plant dry weight and the greatest leaf tissue N concentrations were observed at the highest fertility concentration

(15.0 mM • L^{-1}). The lowest concentration of N fertility resulted in 97.9% less plant biomass when compared to the 15.0 mM • L^{-1} concentration (Table 3.3.1, Graph 3.3.1).

At the bolting growth stage, plant dry weight showed a positive correlation to N concentrations. The linear and second order polynomial regression models accounted for 73.0% and 72.0% of the variance explained for the plant dry weight when N concentration was treated as the independent variable.

Leaf tissue N concentration increased up to the 7.50 mM • L^{-1} fertility concentration after which increasing N did not result in any statistically greater accumulation. The greatest N leaf tissue value was observed at the second highest fertility concentration (13.13 mM • L^{-1}) and contained > 4x the leaf tissue N when compared to the lowest concentration (0.00 mM • L^{-1}).

At the bolting growth stage, leaf tissue N concentrations had a positive correlation to increasing N fertility. The second order polynomial regression models accounted for 93.0% of the variance explained for leaf tissue N concentration when N fertility treatment was treated as the independent variable.

Results from Seepaul et al., [40] indicate that during times of rapid cell growth and expansion, such as bolting, dry matter increasing 107%. From bolting onward, biomass production is maximized and any N resource scarcity during this stage will negatively impact biomass production and yield due to decreased branching. We found N needs are met at the 7.50 mM • L^{-1} for the rosette, bolting, and flowering stages which resulted in leaf tissue N concentrations of 5.82, 5.91, and 5.52% respectively (Table 3.3.1, Graph 3.3.1). However, maximum N concentration in above ground tissue sampled (2.33%) resulted from the second highest fertility application (90 kg • ha^{-1}) from Seepaul et al., [40]. More research is needed to further explore optimal N rates with regard to leaf tissue accumulation given plants grown under field conditions resulted in much lower N concentrations, and included values at some life stages, which were much lower than values observed in *Brassica napus* (Bryson et al, [41]).

3.3.1.4. Flowering Stage N Rates

During flowering, carinata plants showed an increase in plant dry weight as N concentrations increased (Table 3.3.1, Graph 3.3.1). The greatest plant dry weight occurred at 15.0 mM • L^{-1} N. Nitrogen fertility at 13.13 mM • L^{-1} resulted in the greatest leaf tissue N concentration though not statistically different from the remaining three concentrations (7.50, 11.25, and 15 mM • L^{-1}). Additionally, leaf tissue N concentration increased with N fertility concentrations up to 7.50 (mM • L^{-1}) after which point increasing N did not result in any statistically greater accumulation. The lowest concentration of N (0.0 mM • L^{-1}) fertility contained 77% less leaf tissue N when compared to the 15.0 mM • L^{-1} concentration (Table 3.3.1, Graph 3.3.1).

There was no difference in adjusted r^2 value between the linear and second order polynomial regression models for dry weights. Both models accounted for 83.0% of the variance explained for plant dry weight. For leaf tissue N concentrations, the quadratic model accounted for 84% of variation when N fertility was treated as the independent variable.

Drawing upon the work done by Seepaul et al., [40], a decrease in above ground tissue N concentration resulted during the flowering stage and pod set stage. During these life stages, N resources in leaf tissues were most likely reduced through translocation from vegetative portions to developing seeds (Taylor et al., [34]). The results presented by Seepaul et al., [12] highlight the importance of adequate N resources to the plant during pre and post bolting stages of *B. carinata* development.

3.3.1.5. Pod Set Stage N Rates

At pod set, plant dry weight increased as N fertilization increased with the greatest plant dry weight corresponding to the highest N fertilization (15.0 mM • L^{-1}) (Table 3.3.1, Graph 3.3.1). Plants grown with 0.0 and 3.75 mM • L^{-1} N were completely defoliated and

no datapoints exist for these lower concentrations. The 13.13 mM • L^{-1} resulted in the greatest leaf tissue N concentration when compared to 7.50 mM • L^{-1} values. The datapoints present resulted in a best fit to a second order polynomial regression for total plant dry weight (adj. r^2=0.52), and leaf tissue N accumulation (adj. r^2=0.40). Pod set stage models presented here were produced from a truncated dataset and are not as robust in their explanatory power as other models we present.

For N fertilization no further increase in leaf tissue accumulation occurred after 7.50 mM • L^{-1} for the rosette, bolting, and flowering stages of carinata growth and this concentration of N will result in adequate leaf tissue concentrations. Care should be taken when translating these results to field production given the growth habit of carinata is different in a greenhouse environment compared to the field. Additionally, these plants were grown with plant available water soluble N resources which results in much greater availability and uptake by the plant.

3.3.2. Phosphorus (P)

Phosphorus concentrations produced similar trends as N rates, with the plant dry weights increasing with P fertility. However, the leaf tissue P concentrations resulted in slightly different plateaus based on life stages (Table 3.3.2, Graph 3.3.2).

3.3.2.1. P Deficiency Symptomology

Deficiency symptoms of P were only present at the 0.0 and 0.25 mM • L^{-1}, concentrations for the rosette stage and bolting stages. Phosphorus deficiency first manifested as a general stunting of the plant (Fig. 3.3.5). The lower leaves appeared yellow or olive green in color (Fig. 3.3.6). There was a gradation of leaf color with the

most recently mature and expanding leaves appearing dark green, the older leaves appearing olive-yellow, and the oldest leaves appearing yellow and necrotic (Fig 3.3.7).

As plants continued to grow, symptomology progressed rapidly, and the plant's overall growth rate was less at 0.0 mM • L^{-1} and especially during the bolting stage when compared to 1.0 mM • L^{-1} (Fig. 3.3.8). The above tri-coloration patterning continued. The older leaves started abscising and the next node toward the terminal end of the plant displayed signs of P deficiency. The flowering stage resulted in stunted floral development when compared to the control at the lowest P fertility treatment (0.0 mM • L^{-1}) (Fig. 3.3.8).

3.3.2.2. Rosette Stage P Rates

Rosette stage plants within the P treatments increased in dry weights as P concentrations increased (Table 3.3.2, Graph 3.3.2). The greatest plant dry weight occurred with the highest P fertility (1.0 mM • L^{-1}). The linear and second order polynomial regression models accounted for 62.0% and 82.0% of the variance for plant dry weight when P concentration was treated as the independent variable (Equations 3.3.1).

Leaf tissue P increased up to 0.50 mM • L^{-1} after which increasing P fertility resulted in the same leaf tissue concentrations for the upper four treatments (0.50, 0.75, 0.875, and 1.0 mM • L^{-1}) (Table 3.3.2, Graph 3.3.2). The greatest leaf P was observed at the highest fertility concentration (1.0 mM • L^{-1}) and contained 3.2x more leaf tissue P than the lowest fertility treatment (0.0 mM • L^{-1}). The quadratic model accounted for 20% more of the variance explained in the leaf tissue P concentrations when P fertility treatments were used as the independent variable (Equations 3.3.2).

Plant dry weights increased quadratically, but leaf tissue P concentrations plateaued at 0.50 (mM • L^{-1}) concentration indicating P resources may be allocated to

biomass production and later reallocated to developing sinks during other life stages. Madani et al., [42] demonstrated that regardless of phosphate concentration, reproductive portions of the plant always contained significantly greater P resources than vegetative portions due to translocation of these resources within the plant.

Additionally, as plant biomass increased, the leaf tissue concentration remained relatively similar. Often an increase in plant biomass will result in a decrease in leaf tissue mineral concentrations due to a dilution effect as was observed in some of the species explored in Henry's work [39]. Since leaf tissue P concentrations remained relatively constant despite increasing plant biomass production, P fertility requirements may be greater at the rosette stage.

3.3.2.3. Bolting Stage P Rates

Bolting plants within the P treatments increased linearly in dry weights with the highest treatment (1.0 mM • L^{-1}) producing over 4x the biomass when compared to the lowest treatment (0.0 mM • L^{-1}) (Table 3.3.2, Graph 3.3.2). When regression models were applied, both the linear and quadratic models accounted for only approximately 58 and 59% respectively of the variance in plant dry weight (Equations 3.3.2).

Leaf tissue P increased up to 0.50 mM • L^{-1} after which point increasing P fertility resulted in similar leaf tissue concentrations for the upper three treatments (0.50, 0.75, and 0.875 mM • L^{-1}) (Table 3.3.2, Graph 3.3.2). The greatest leaf P was observed at the second highest fertility concentration (0.875 mM • L^{-1}). The highest P fertility treatment (1.0 mM • L^{-1}) resulted in statistically lower leaf tissue values than the 0.875 mM • L^{-1} rates. These results indicate this concentration (1.00 mM • L^{-1}) may be too high. Alternatively, the decrease could be the result of the greater plant biomass produced and a resultant dilution effect (Table 3.3.2, Graph 3.3.2). The quadratic model had greater

explanatory power than the linear model for variance in leaf tissue P concentrations (Equations 3.3.2).

The above results may be best interpreted in the context of Seepaul et al. [40] and Jullien et al. [43]. The work completed by Seepaul et al. [40] indicated that P concentration within the straw (stems and leaf petioles) was much lower (0.07% of plant DW) than the whole plant P concentrations (0.33% of plant DW) at the bolting stage. Thus, demonstrating that during the bolting stage, the P concentration within developing stem architecture may be much lower than in leaf tissue. These results may indicate another P demand at the bolting stage other than leaves and stems such as the development of floral material.

Work by Jullien et al. [43] tracked the interactions between plant architecture via source-sink relations in *Brassica napus* using the GreenLab model. Their work indicated that the greatest increase in plant dry weight occurs at the bolting stage and results in a stem dry weight accumulation of over 70x. The data from the above two studies indicate during the bolting phase greater P resources are required and plant architecture will increase despite not being a large P repository. These results suggest P resources should remain higher to help fulfill needs during bolting .

3.3.2.4. Flowering Stage P Rates

At the flowering stage, plants increased in biomass with increasing P treatments with the exception of the 0.25 mM • L^{-1} P treatment which produced the second greatest biomass. The greatest plant dry weights were observed at the highest concentration of P fertility (1.0 mM • L^{-1}) and was statistically greater than the remaining fertility concentrations (Table 3.3.2, Graph 3.3.2). When regression models were applied, both the linear and quadratic models accounted for little of the variance in plant dry weight with very low adjusted r^2 values of 0.31 and 0.28, respectively (Equations 3.3.2).

Leaf tissue P increased up to 0.50 mM • L^{-1} after which increasing P fertility resulted in the same leaf tissue concentrations for the upper four treatments (0.50, 0.75, 0.875, and 1.0 mM • L^{-1}) and the upper three concentrations being similar to the 0.25 mM • L^{-1} concentration (Table 3.3.2, Graph 3.3.2). The greatest leaf P was observed at the second highest fertility concentration (0.875 mM • L^{-1}) and contained 9.5x more leaf tissue P than the lowest fertility treatment (0.0 mM • L^{-1}). The quadratic model accounted for more variance in leaf tissue P concentrations when compared to the linear model (Equations 3.3.2). After the bolting stage, all leaf tissue values for all P fertility treatments resulted in lower values (Table 3.3.2). This may indicate that P resources after the bolting stage are taken from the leaves and translocated to developing sinks such as flowers and seeds.

In a study completed by Su et al., [44] proved that at different fertility depths, plant uptake of P resources was impacted. While this study mainly explored the impacts of different depths of P fertility, this work highlights that at different life stages (seedling, flowering, maturity, seed, and straw) different levels of P resources are contained within the plant. Interestingly, this study showed that P resources increase during the seed fill stage with 5.5% whole plant P being reported. These results help to interpret the overall decrease in leaf tissue P concentration by proving that during the reproductive phase of brassicas, the whole plant P content remains constant, but reallocate due to leaf translocation. Thus, it would be reasonable to assume that the decrease in leaf tissue P resources indicates that other sinks such as the reproductive structures have a greater draw on P resources after the rosette stage.

3.3.3.5. Pod Set Stage P Rates

At the final data collection (pod set), plant dry weights were similar after the 0.50 mM • L^{-1} with all P treatments above this rate being statistically similar. The exception

being the 0.75 (mM • L^{-1}) treatment, which was similar to the lowest two treatments (0.0 and 02.5 mM • L^{-1}) (Table 3.3.2, Graph 3.3.2). Regression models indicated both the linear model was statistically insignificant while the quadratic model accounted for 51% of the variance in plant dry weight (Equations 3.3.2). These results indicate that much like the flowering stage, P fertility impacts plant biomass production, however that impact is minimal and other factors may play a greater role.

Leaf tissue P increased up to the 0.50 and 0.75 mM • L^{-1} concentrations which were statistically greater than the lower two treatments (0.0 and 0.25 mM • L^{-1}) and similar to the 0.875 (mM • L-1) treatment. The two highest fertility concentration (0.875 and 1.0) were statistically similar to the 0.25 (mM • L^{-1}) treatment (Table 3.3.2, Graph 3.3.2). and the upper two concentrations being similar to the 0.25 mM • L^{-1} concentration (Table 3.3.2, Graph 3.3.2). These results may indicate that at the pod fill stage, the optimal fertility concentration may be between 0.50 and 0.75 (mM • L^{-1}) considering leaf tissue values after these treatments decreased.

Drawing upon the work of Seepaul et al. [40] one can surmise that the P resources within the developing reproductive sinks (seeds and siliques) resulted in a much greater demand sink for P given that levels of 0.91% seed P were reported. This indicates that the seeds and siliques result in a huge P demand, thus, greater P concentrations may help in providing adequate P resources.

3.3.4. Potassium (K)

Potassium fertility treatments produced regression trends with the plant dry weights increasing and the flowering stage resulting in a plateau after the 3.0 mM • L^{-1} treatment. Leaf tissue K values varied in their peak concentration for the various sampling stages (Table 3.3.3, Graph 3.3.3).

3.3.4.1. K Deficiency Symptomology

Deficiency symptoms of K stress occurred at the 0.0 and 1.50 mM • L^{-1}, concentrations for all stages with symptoms becoming more advanced as plants continued growing. Potassium deficiency first manifested as a slight interveinal yellowing of large regions of the leaf especially of the margin (Fig. 3.3.9). The leaf margin then became necrotic and started to distort causing the leaves to curl inward (Fig. 3.3.10). The necrotic regions continued to expand across the leaf toward the midrib eventually resulting in extremely necrotic and chlorotic leaves (Fig 3.3.11). The lower leaves eventually became completely necrotic and abscised, this resulted in the next leaf upward toward the terminal node to display symptoms. This upward symptomological progression continued until even the new and expanding leaves became severely distorted (Fig. 3.3.12).

3.3.4.2. Rosette Stage K Rates

Rosette plants dry weights were similar across all rates except at the highest treatment (6.0 mM • L^{-1}) (Table 3.3.2, Graph 3.3.2). The only other statistical increase occurred between 3.0 (mM • L^{-1} K) which was lower in dry weight when compared to the 5.25 (1.0 mM • L^{-1} K) treatment. The linear and second order polynomial regression models accounted for 28.0% and 73.0% of the variance explained for the plant dry weight when K concentration was treated as the independent variable (Equations 3.3.2).

Leaf tissue K increased up to 1.50 mM • L^{-1} after which point increasing K fertility resulted in similar mineral concentrations for the upper four treatments (3.0, 4.5, 5.25, and 6.0 mM • L^{-1}) (Table 3.3.3, Graph 3.3.3). Between the 0.0 and 1.50 (mM • L^{-1} K) leaf tissue K concentrations increased 8x. Regression indicated a quadratic model explained more of the variance in the leaf tissue K concentrations when K fertility treatments were used as the independent variable (Equations 3.3.3).

Given the role of potassium as an enzymatic activator (Suelter, [45]), it is to be expected that during the rosette stage a low level of K resources are maintained within the plant. The rosette stage represents lowest organ demand compared to later stages of plant development due to the stronger sinks of the internodal stem tissue production (bolting) and the seed development occurs in *Brassica napus* (Jullien et al., [43]). Additionally, greater leaf area and respiration rates were observed in the bolting stage given an increase in leaf area (Jullien et al., [43], Seepaul et al., [6]). Thus, when enzymatic activity is lower, plant biomass production is relatively stable, and photosynthetic rates are lessened, the low impact of K on biomass and the early K leaf tissue plateau would be expected.

3.3.4.3. Bolting Stage K Rates

The bolting stage resulted in the lowest plant dry weight at the 0.0 (mM • L^{-1} K) fertility was only statistically smaller than the 3.0 and 6.0 (mM • L^{-1} K) treatments (Table 3.3.3, Graph 3.3.3). Plant variation at the initiation of bolting had a major impact on plant dry weight among treatments and would account for this lack of response. Given the statistically similar data distribution, neither the linear nor the quadratic regression models accounted for much of the variance in plant dry weight (Equations 3.3.3).

Leaf tissue K increased up to 4.50 mM • L^{-1} after which point increasing K fertility resulted in similar leaf tissue concentrations for the remaining treatments (5.25 and 6.0 mM • L^{-1}) (Table 3.3.3, Graph 3.3.3). The linear model supplied marginally greater explanatory power for the variance in leaf tissue K concentrations when compared to the quadratic model (Equations 3.3.3). These data may indicate that the upper range of K fertility was not reached within treatments tested.

The internodes and internode production represents a large organ demand within *B. napus* (Jullien et al., [43]) for K. Additionally, photosynthetic rates increase during the

bolting stage within *B. carinata* (Seepaul et al., [6]). Thus, the lower leaf tissue concentrations observed at the bolting stage for the 1.5 and 3.0 mM • L^{-1} rates may indicate that K is being allocated towards developing sinks and enzymatic activity to produce the flowering spikelet. Work completed by Ecke et al. [46] and Ajisaka et al. [47] demonstrated that genetic controls and the cultivars can greatly impact bolting vigor, timing, and other biological functions within brassicas.

3.3.4.4. Flowering Stage K Rates

Plant dry weights at the flowering stage increased as K fertility increased. The greatest plant dry weights were observed at the 3.0 and 6.0 (mM • L^{-1} K) treatments and were statistically greater when compared to the two lowest treatments (0.0 and 1.50 mM • L^{-1} K) (Table 3.3.3, Graph 3.3.3). When regression models were applied, a quadratic model accounted for marginally greater variances in plant dry weight (Equations 3.3.3).

Potassium leaf tissue increased with K fertility rates (Table 3.3.3, Graph 3.3.3). The upper three fertility concentrations (4.5, 5.25, and 6.0 mM • L^{-1} K) were similar, but the quadratic regression model indicated that an upper range may not have been reached regarding maximum K leaf tissue fertility (Equations 3.3.2).

The greatest leaf tissue K concentrations were observed in the rosette stage after which point the remaining stages were lower or equal (Table 3.3.3). The presence of lower K leaf tissue could indicate that the flowering stage and pod-set stage produces the largest sink strengths in brassicas, Jullien et al., [43] and Khan et al. [48]. Thus, K resources would be in much higher demand during this time.

Additionally, work done by White et al. [46] indicated that genetics and the growing environment (greenhouse versus field conditions) influence K uptake. Their work indicated that in a greenhouse environment higher shoot K concentration are observed as opposed to field conditions which were lower.

3.3.4.5. Pod Set Stage K Rates

During pod set, plant dry weights increased with K rate, with the greatest dry weight present in the highest fertility treatment (6.0 mM • L^{-1} K) (Table 3.3.3, Graph 3.3.3). Regression models (linear or quadratic) interpreted very little of the variance in plant dry weight regarding K treatments (Equations 3.3.3). Due to a wide plant to plant variability, these results indicate that K fertility at later stages of growth may be only one factor which regulates plant biomass production.

Despite the linear increase of plant dry weights, leaf tissue K increased up to the 4.5 mM • L^{-1} concentration after which K concentrations were statistically similar (Table 3.3.3, Graph 3.3.3). The quadratic model supplied the greatest explanatory power for the variance in leaf tissue K concentrations when compared to the linear model (Equations 3.3.3).

As observed above, the developing reproductive sinks draw upon massive resources (Jullien et al., [43], Khan et al. [48]). Additional work completed by Inamullah et al. [50] observed greater silique number, grains per silique, and 1000 grain seed weight as K level increased. This work was supported again with results from Mozaffari et al. [51] which observed an increase in thousand seed wight as K increased. The above comprehensive results indicate that K may not greatly impact plant biomass production due to plant to plant variability, but K leaf tissue level more adequately induce the nutrient stress and demand for K by *B. carinata*.

3.3.5. Calcium (Ca)

Increasing Ca fertility resulted in an increase in biomass at the rosette, bolting, and flowering stages. Within the rosette and bolting stages, a leaf tissue concentration plateau occurred at 3.75 mM • L^{-1} Ca. The pod set stages did not produce a maximal leaf tissue concentration even at the highest fertility treatments (Table 3.3.4, Graph 3.3.4). Fertility

provided at 0.0 mM • L^{-1} Ca did not produce a reproductive structure and consequently did not produce flowers or siliques.

3.3.5.1. Ca Deficiency Symptomology

Deficiency symptoms of Ca deficiency were only present at the 0.0 and 1.25 mM • L^{-1} concentrations. Little plant growth differences were observed at the above two Ca rates in the rosette stage when compared to the control. Calcium deficiency first manifested as a general downward cupping and distortion of the leaf margin of the new and developing leaves (Fig. 3.3.13). As symptoms continued and during rapid cell division during bolting, the new and expanding leaves become severely distorted resulting in tan speckling of the leaf surface (Fig. 3.3.14). Plants in the bolting stage were severely dwarfed when compared to their controls (Fig. 3.3.15). This is due to a lack of cellular development at the apical meristem which eventually resulted in the death of the apical meristematic region (Fig. 3.3.16). Consequently, at the 0.0 mM • L^{-1} rate, floral development did not occur and consequently no siliques were produced. In advanced stages, the apical meristem died, and the axillary shoots tried to expand resulting in a highly distorted and branched architecture (Fig. 3.3.16).

3.3.5.2. Rosette Stage Ca Rates

Rosette plants dry weights did not show any discernable trend regarding Ca fertility treatments (Table 3.3.4, Graph 3.3.4). The second order polynomial regression models accounted for 62.0% of the variance explained for the plant dry weight when Ca fertility concentrations were treated as the independent variable (Equations 3.3.4).

Leaf tissue Ca increased up to 3.75 mM • L^{-1} after which point increasing fertility resulted in similar mineral concentrations for the upper two treatments (4.38 and 5.0 mM

• L^{-1}) (Table 3.3.4, Graph 3.3.4). Regression indicated a quadratic model explained more of the variance in the leaf tissue Ca (Equations 3.3.4).

Calcium is primarily utilized in the maintenance of cell wall structures where they help stabilize the pectin chains by creating Ca ion bridges (Chebli and Geitmann, [32]; Matoh, [33]). Thus, the Ca leaf tissue plateau at the 3.75 mM • L^{-1} is unsurprising given the slower growth rate present in the rosette stage as compared to the bolting stage.

3.3.5.3. Bolting Stage Ca Rates

Plant dry weight at the bolting stage resulted in an increasing trend as Ca fertility increased (Table 3.3.4, Graph 3.3.4). Calcium leaf tissue concentrations increased by 3x between the lowest and highest (0.0 and 5.0 mM • L^{-1}) fertility treatments. The linear model accounted for 37% of the variance in plant dry weight (Equations 3.3.4).

Calcium leaf tissue increased up to 3.75 mM • L^{-1} treatment after which point increasing Ca produced similar leaf tissue concentrations for the remaining treatments (4.38 and 5.0 mM • L^{-1}) (Table 3.3.4, Graph 3.3.4). Regarding regression, the quadratic model accounted for 91% of the variance in leaf tissue Ca concentrations (Equations 3.3.4). The rosette and bolting stages both had a similar trend of optimal Ca fertility at 3.75 mM • L^{-1}.

The bolting stage internodes rapidly lengthen and consequently represents a large organ demand within *B. napus* (Jullien et al., [43]). The Ca leaf tissue trend was expected given the balance between the plant mass demand and the variable Ca in plans seems to have been met. During times of increased photosynthetic rates and rapid internode lengthening, it would be reasonable to assume Ca demands would increase (Jullien et al., [43], Seepaul et al., [6]). The tissue Ca values present in this study were higher than other works completed (Seepaul et al. [6], Bryson et al. [41]). Additionally, the leaf tissue Ca values during bolting were less than the other life stages (excepting the 0 and 1.88 mM •

L^{-1} flowering values) for most of the fertility rates. The lower leaf tissue Ca concentrations could indicate Ca resources were being utilized more in the stems and branches within the peptide matrix. This is supported given high values of Ca (2.96 – 5.17%) are observed within the stems and branches of *B. carinata* in previous works (Seepaul et al., [6], [12]).

3.3.5.4. Flowering Stage Ca Rates

Plant dry weights at the flowering stage showed an increase as Ca fertility increased (Table 3.3.4, Graph 3.3.4). Both linear and quadratic regression models accounted for only 56 and 54% respectively of the variances in plant dry weight (Equations 3.3.4).

Calcium leaf tissue increased with increasing fertility (Table 3.3.4, Graph 3.3.4). The highest Ca treatment (5.0 mM • L^{-1}) contained over 6.8 times the leaf tissue Ca when compared to the lowest treatment (0.0 mM • L^{-1}) (Table 3.3.4, Graph 3.3.4). A plateau in leaf tissue Ca accumulation also occurred with 5.0 Ca based on the quadratic regression (Equations 3.3.4).

The plateau regarding leaf tissue Ca suggests that Ca demands are met with 5.0 mM • L^{-1} fertility at the flower stage for *B. carinata*. This could be related to the reproductive structures being formed. Calcium is often required for pollen germination, pollen tube elongation, and synergid receptivity (Ge et al., [52]). This is in contrast with work by Seepaul et al. [40] who also modeled a Ca decrease in the flowering and pod development stages of growth. Thus, some external effect such as weather or another abiotic condition may have negatively impacted Ca uptake in their filed study.

3.3.5.5. Pod Set Stage Ca Rates

During pod set the plant dry weights varied amongst the fertility treatments and resulting in a low degree of predictability associated with the quadratic regression model (Table 3.3.4, Graph 3.3.4, Equations 3.3.4).

Leaf tissue Ca increased up to the 3.75 mM • L^{-1} concentration after which Ca concentrations were statistically similar (Table 3.3.4, Graph 3.3.4). The quadratic model supplied a greater explanatory power than the linear model for the variance in leaf tissue Ca concentrations, though neither model strongly interpreted the variance (Equations 3.3.4).

As stated above, lower Ca leaf tissue values at the bolting and flowering stages were present in previous works with *B. carinata* (Seepaul et al., [40]). This work ([40]) also indicated that seeds contained between 0.42 – 0.44 % Ca which indicates that the developing seeds require certain levels of Ca. While this does not fully explain the lack of a leaf tissue Ca plateau at the rosette and pod set stage, it does demonstrate that in addition to flower Ca needs, seed Ca content is also required by *B. carinata*.

3.3.6. Sulfur (S)

Increase in S fertility generally increased plant dry weights excepting the pods set stage (Table 3.3.5, Graph 3.3.5). Sulfur leaf tissue concentration increased with increasing S fertility rates however levels were lower during the rosette and bolting stage when compared to the flowering and pod set stages (Table 3.3.5, Graph 3.3.5).

3.3.6.1. S Deficiency Symptomology

Sulfur deficiency manifested early in the rosette stage. Plants appeared pale yellow when compared to the control (Fig. 3.3.17). This overall yellowing was difficult to detect without a control for comparison. As symptoms progressed into the bolting stage, the

leaf morphology of the upper leaves along the reproductive structure changed to become more upright in orientation and slightly stunted. The middle foliage developed a paling and yellowing when compared to control leaves (Fig. 3.3.18). Additionally, these leaves resulted in an overall purple coloration of the lower leaf surface (Fig. 3.3.19). During the flowering stage, the leaves along the reproductive spikelet produced severely stunted leaves and smaller flowers when compared to the control (Fig. 3.3.20).

3.3.6.2. Rosette Stage S Rates

Rosette plants dry weights had a slight quadratic increase with the increase of S fertility (Table 3.3.5, Graph 3.3.5). The second order polynomial regression models accounted for 73.0% of the variance explained for the plant dry weight when S fertility concentrations were treated as the independent variable (Equations 3.3.5).

Leaf tissue S increased up to 1.5 mM • L^{-1} treatment after which point increasing fertility resulted in similar mineral concentrations for the upper two treatments (1.75 and 2.0 mM • L^{-1}) (Table 3.3.5, Graph 3.3.5). Quadratic regression modeling explained a greater amount of the variance in the leaf tissue S when compared to the linear model (Equations 3.3.5).

Brassicas typically demand greater S than other crops (Jez [53], Marschner [9]). In brassicas, the high levels of glucosinolates attribute part of this increased demand (Jez, [53]). Additionally, given *B. carinata* is an oilseed crop, the increased production of amino acids necessitates an increased demand for S resources (Marschner [9], Stansly et al., [54], Govahi and Saffari, [20]). Given the biomass present in the rosette stage is much less than other stages, the lower S plateau in leaf tissue values were expected due to the lack of biomass and seed sinks.

3.3.6.3. Bolting Stage S Rates

Plant dry weight at the bolting stage resulted in an increasing trend as S fertility increased (Table 3.3.5, Graph 3.3.5). The linear and quadratic models accounted for 65 and 72% of the same variance in plant dry weight (Equations 3.3.5). The plants grown at the 0.0 mM • L^{-1} S fertility resulted in visual symptoms of overall paling and produced 72% less dry matter than with the highest fertility (2.0 mM • L^{-1}).

Sulfur leaf tissue increased as S fertility increased, and plateaued between 1.5 and 2.0 mM • L^{-1} S (Table 3.3.5, Graph 3.3.5). Quadratic modeling accounted for 83% of the variance in leaf tissue S concentrations (Equations 3.3.5).

As *B. carinata* plants increased in biomass production, the glucosinolate resources also increased (Jez, [53]). Additionally, S uptake increases as plants develop (Mobin et al., [55]). The plateau value observed within the leaf tissue accumulation indicates the fertility treatments tested may have adequately provided the needs for *B. carinata* at the bolting stage.

3.3.6.4. Flowering Stage S Rates

Plant dry weights at flowering resulted in dry weights similar at the lower five S fertility treatments (0.0, 0.5, 1.0, 1.5, and 1.75 mM • L^{-1}) with only the highest (2.0 mM • L^{-1}) S fertility resulting in a statistically greater dry weight (Table 3.3.5, Graph 3.3.5). Regression indicated the quadratic model accounted for the greatest variances in plant dry weight (0.55 adj. r^2) (Equations 3.3.5).

Sulfur leaf tissue increased with increasing fertility though no plateau value was established within the ranges tested (Table 3.3.5, Graph 3.3.5). The highest S treatment (2.0 mM • L^{-1}) contained 12x more leaf tissue S when compared to the lowest treatment (0.0 mM • L^{-1}) (Table 3.3.4, Graph 3.3.4). These data may indicate that greater S resources are required during the flowering stage in *B. carinata*.

With the development of reproductive sinks, S demand and dynamics change dramatically in brassicas (Jullien et al., [43]). Previous works showed an enhancement of the reproductive growth and associated reproductive tissues increased with increasing S (McGrath et al., [56]). Sulfur uptake increases greatly during the maturation stage of canola and can increase almost 2x when compared to the rosette stage (Fismes et al., [24]).

3.3.6.5. Pod Set Stage S Rates

Plants in the pod set stage, displayed a wide variation in values regarding dry weights and S fertility treatments but followed an overall increase in dry weight as S fertility rate increased (Table 3.3.5, Graph 3.3.5). Both the quadratic and linear regression models were similar in predicting the variance in plant dry weight regarding S treatments (Equations 3.3.5).

Leaf tissue S increased with increasing S concentrations and did not result in a plateau value (Table 3.3.5, Graph 3.3.5). Both the linear and quadratic models supplied excellent explanatory power for the variance in leaf tissue S concentrations indicating that the rates tested need to be increased to see optimal leaf tissue accumulation of S resources at this growth stage (Equations 3.3.5).

Given the role S plays in amino fatty acid synthesis, the lack of a leaf tissue accumulation plateau was expected given S demands would be greater during this life stage (Varényiová et al., [57], Malhi et al., [58], Rehman et al., [59], Govahi and Saffari, [20], Ma et al., [25]). In the pod set stage, the developing sink of the seeds and fatty acid resources contained within are present and result in a massive demand of S resources. A limitation of S fertility will result in fewer seeds per siliques and a decrease in oil content per seed in brassicas (Varényiová et al., [57], Malhi et al., [58], Rehman et al., [59], Govahi and Saffari, [20], Ma et al., [25]). The fertility treatments explored above indicate *B. carinata* may have a much higher demand during the pod set stage. This may be partly

due to the high concentrations of LC and VLC fatty acids and erucic acid content found within *B. carinata* seeds (Seepaul et al., [6, 12, 40], Mulvaney et al., [60]).

3.3.7. Magnesium (Mg)

Magnesium leaf tissue values increased with increasing fertility across all stages of growth. The plant dry weights indicated an increase in biomass production at the rosette and bolting stage, but the flower and pod set stage resulted in variable results among fertility treatments (Table 3.3.6, Graph 3.3.6).

3.3.7.1. Mg Deficiency Symptomology

Deficiency symptoms of Mg were only present at the 0.0 and 0.25 mM • L^{-1}, concentrations for the rosette stage and bolting stages. Magnesium deficiency resulted in the interveinal regions becoming yellow and tan (Fig. 3.3.21). These regions expanded to become interveinal yellowing regions with necrotic, slightly sunken centers and a yellow halo (Fig. 3.3.22). As deficiencies continued, the sunken necrotic regions expanded to become large necrotic tan regions (Fig. 3.3.23). In advanced symptoms, the interveinal and necrotic regions expanded to produce a severely necrotic leaf (Fig. 3.3.24). Additionally, these necrotic leaves displayed an interveinal purpling of the leaf underside (Fig. 3.3.25). Eventually lower leaves became completely necrotic and abscised.

3.3.7.2. Rosette Stage Mg Rates

Rosette plants dry weights increased with increasing of Mg fertility (Table 3.3.6, Graph 3.3.6). There was little difference between linear and quadratic regression models despite the low r^2 values (0.62 and 0.63 respectively) (Equations 3.3.6).

Leaf tissue Mg increased as fertility treatments increased with no plateau in leaf tissue values even at the highest fertility concentration (2.0 mM • L^{-1} Mg) (Table 3.3.6,

Graph 3.3.6). Quadratic regression modeling explained only 1% more of the variance in the leaf tissue Mg when compared to the linear model (Equations 3.3.6). These results may indicate that during the rosette stage, Mg demands are higher.

Work done by Kopsell et al. [61], indicated as the Ca:Mg ratio increased, an increase in leaf tissue Mg content also increased. Additionally, a linear rather than quadratic model accounted for more of the variability when exploring the orthogonal contrasts. This work showed a continued increase in leaf tissue Mg with no plateau value indicated.

3.3.7.3. Bolting Stage Mg Rates

Bolting carinata plants produced variable results when Mg fertility treatments were treated as the explanatory variable (Table 3.3.6, Graph 3.3.6). The linear and quadratic models accounted for only 29.0 and 27.0% of the variance in plant dry weight (Equations 3.3.6).

Leaf tissue increased and displayed a maximum leaf tissue plateau at the 1.5 mM • L^{-1} Mg treatment with the upper two treatments (1.75 and 2.0 mM • L^{-1} Mg) containing statistically similar values (Table 3.3.6, Graph 3.3.6). The highest leaf tissue Mg concentration was observed at the highest fertility treatment and contained 4.6x more leaf tissue Mg than the lowest (0 mM • L^{-1} Mg) treatment (Table 3.3.6, Graph 3.3.6). Both quadratic and linear modeling accounted for 90% of the variance in leaf tissue Mg concentrations (Equations 3.3.6). Given the high explanatory power of the Mg treatments regarding leaf tissue Mg, yet the low explanatory power regarding dry weights, Mg may only be one regulating factor in bolting time and vigor.

When exploring varying sub taxa regarding shoot Ca and Mg concentrations, Martin et al. [62] indicated that Ca varied from 1.7 – 3.3% of shoot dry weight and Mg varied from 0.35 – 0.80%. Their data also indicated that in B. oleracea, the traits for Ca

and Mg accumulation were very heritable and differed significantly among sub taxa. Finally, their work indicated that Ca and Mg shoot content based on differing fertility treatments were highly correlated between field and greenhouse conditions. These results may indicate that with further experimental inquiry, the models found within this work for both Ca and Mg may be useful as a guide or field uptake.

3.3.7.4. Flowering Stage Mg Rates

Plant dry weights at the flowering stage produced no discernable trends regarding the variance within that life stage (Table 3.3.6, Graph 3.3.6). Regression and linear modeling both were statically insignificant predictors of the variance observed in the plant dry weights (Equations 3.3.6). However, regression (linear and quadratic adjusted r^2 values of 0.91) modeling of leaf tissue Mg concentrations increased in a quadratic fashion with increasing Mg concentrations (Table 3.3.6, Graph 3.3.6). These data indicate that *B. carinata* may utilize greater Mg resources during the flowering stage.

Work by Rios et al. [63] explored the distribution of Ca and Mg in the leaves of *B. rapa*. Their work focused specifically on the distribution of mineral contents within the different types of foliar cells (adaxial epidermal, palisade mesophyll, spongy mesophyll, and abaxial epidermal). They found that within 21 day old *B. rapa* leaves the distribution of leaf Ca and Mg depended heavily on exogenous Ca and Mg supply, but the type of cell also contained higher concentrations of each cation. Thus, at different life stages and within different plant parts, different Ca and Mg content and demands are present regarding mineral nutrients.

3.3.7.5. Pod Set Stage Mg Rates

During pod set, a wide variation in results were observed in dry weights with only the greatest fertility treatment (2.0 mM • L^{-1} Mg) being statistically greater than the

remaining treatments (Table 3.3.6, Graph 3.3.6). Neither the quadratic regression nor the linear resulted in a reliable model for the variance in plant dry weight regarding Mg treatments (Equations 3.3.6).

Leaf tissue Mg during pod set however showed an increasing trend in leaf tissue Mg as fertility treatments increased (Table 3.3.6, Graph 3.3.6). The linear model accounted for only marginally more (1%) explanatory power for the variance in leaf tissue Mg concentrations (Equations 3.3.6). These data indicate the rates tested may need to be increased to see optimal leaf tissue accumulation of Mg resources (Table 3.3.6, Equations 3.3.6).

In a study done by Purakayasthaand and Nad [64], increasing Mg concentrations increased protein content within the seeds of B. juncea. Additionally, pervious work in *B. carinata* (Seepaul et al., [40]) indicated a mean seed nutrient content of 0.42% indicating that developing seeds have a higher demand for Mg than the straw (mean Mg value of 0.13%). This would indicate that the developing seeds are a larger sink for Mg resources than the non-reproductive sinks.

3.4. CONCLUSION

Different levels of macronutrients are required at different optimal concentrations at different life stages for *B. carinata*. These data help describe optimal fertility by life stage by identifying the point after which increasing the fertility does not result in a greater biomass or leaf tissue concentration. For each of the macronutrients tested, the optimal fertility concentrations varied and can be summarized in the Tables, Equations, and Graphs (3.3.1, 3.3.2, 3.3.3, 3.3.4, 3.3.5, 3.3.6). These data indicated maximum leaf tissue accumulation was not obtained for S (bolting, flowering, and pod set stages only), Mg (rosette, flowering, and pod set stages only), and Ca (flowering stage only). These results may indicate that the above elements are required at higher

concentrations at the specified life stages. Alternatively, the lack of a plateau could also indicate these resources were being stored and utilized within the plant and concentrated in leaf tissue. More research is needed to elucidate if these results are a concentration and reallocation effect or if higher fertility needs are required. If the above elements are needed in higher concentrations, then fertility levels or additional fertilization may need to be provided at these critical points in *B. carinata* development to optimize mineral resources.

Additionally, each of the above tables for the macronutrients compares tissue values to known *B. carinata* and *B. napus* tissue values from published literature. Within the above tables, cells with two or more similar letters indicate the potential plateau value for leaf tissue accumulation. If the cells contain statistically increasing values, this indicates a linear or quadratic model was exhibited and the upper range is still to be elucidated at higher fertility concentrations than tested. The biomass production often resulted in an unclear optimization model when trying to maximize biomass under differing fertility treatments. This may indicate other factors play into plant biomass production such as genetics, and other abiotic factors.

This work seeks to form a foundation for maximal mineral nutrient levels in leaf tissue based on differing fertility. This forms the foundation for which levels to target in a new and emerging crop. Moving forward, an uptake and partitioning study is needed to elucidate how nutrients are utilized and translocated. These data will form as the reference points for such a study to ensure optimal fertility is provided.

ACKNOWLEDGMENTS

This material is based on work that is supported by the National Institute of Food and Agriculture, USDA, under award number 2016-1123. Any opinions, findings,

conclusions, or recommendations expressed in this publication are those of the author(s) and do not necessarily reflect the view of the U.S. Department of Agriculture.

LITERATURE CITED

1. Govardhan G, Sreedharan KS, Nanjundiah R, Moorthy KK, Surendran SB. Possible climatic implications of high-altitude black carbon emissions. Atmospheric Chemistry and Physics. 2017 Aug 1;17(15):9623.
2. Satheesh SK. High Altitude emissions of black carbon aerosols: potential climate implications. AGUFM. 2017 Dec; 2017 : U21D-01.
3. Craig H. The natural distribution of radiocarbon and the exchange time of carbon dioxide between atmosphere and sea. Tellus. 1957 Jan 1;9(1):1-7.
4. Friend AD, Lucht W, Rademacher TT, Keribin R, Betts R, Cadule P, Ciais P, Clark DB, Dankers R, Falloon PD, Ito A. Carbon residence time dominates uncertainty in terrestrial vegetation responses to future climate and atmospheric CO_2. Proceedings of the National Academy of Sciences. 2014 Mar 4;111(9):3280-5.
5. U.S, Energy Information Administration. Monthly Energy Review. 2016 July. (accessed 8.11.16) http://www.eia.gov/totalenergy/data/monthly/pdf/mer.pdf.
6. Seepaul R, George S, Wright DL. Comparative response of *Brassica carinata* and *B. napus* vegetative growth, development and photosynthesis to nitrogen nutrition. Industrial Crops and Products. 2016 Dec 30;94:872-83.
7. United States, Federal Aviation Administration, and Pratt & Whitney. Evaluation of ARA Catalytic Hydrothermolysis (CH) Fuel. Continuous Lower Energy, Emissions and Noise (CLEEN) Program, 2014. Federal Aviation Administration.
8. Gesch RW, Isbell TA, Oblath EA, Allen BL, Archer DW, Brown J, Hatfield JL, Jabro JD, Kiniry JR, Long DS, Vigil MF. Comparison of several Brassica species in the north central US for potential jet fuel feedstock. Industrial crops and products. 2015 Nov 30;75:2-7.
9. Marschner H. Marschner's mineral nutrition of higher plants. Academic press; 2011 Aug 8.
10. Gibson JL, Nelson PV, Pitchay DS, Whipker BE. Identifying nutrient deficiencies of bedding plants. NC. State university floriculture research. Florex. 2001 ;4:1-4.
11. Grant CA, Bailey LD. Fertility management in canola production. Canadian Journal of Plant Science. 1993 Jul 1;73(3):651-70.
12. Seepaul R, Small IM, Marois J, George S, Wright DL. *Brassica carinata* and *Brassica napus* growth, nitrogen use, seed, and oil productivity constrained by post-bolting nitrogen deficiency. Crop Science. 2019 Nov;59(6):2720-32.
13. Harper FR, Berkenkamp B. Revised growth-stage key for Brassica campestris and *B. napus*. Canadian Journal of Plant Science. 1975 Apr 1;55(2):657-8.
14. Ahmadi M, Bahrani MJ. Yield and yield components of rapeseed as influenced by water stress at different growth stages and nitrogen levels. American-

Eurasian Journal of Agricultural and Environmental Sciences. 2009 Jan 1;5(6):755-61.
15. Angadi SV, Cutforth HW, Miller PR, McConkey BG, Entz MH, Brandt SA, Volkmar KM. Response of three Brassica species to high temperature stress during reproductive growth. Canadian Journal of Plant Science. 2000 Oct 1;80(4):693-701.
16. Polowick PL, Sawhney VK. High temperature induced male and female sterility in canola (*Brassica napus* L.). Annals of Botany. 1988 Jul 1;62(1):83-6.
17. Tayo TO, Morgan DG. Factors influencing flower and pod development in oil-seed rape (*Brassica napus* L.). The Journal of Agricultural Science. 1979 Apr;92(2):363-73.
18. Berry PM, Spink JH. A physiological analysis of oilseed rape yields: past and future. The Journal of Agricultural Science. 2006 Oct 1;144:381.
19. Miller PR, Angadi SV, Androsoff GL, McConkey BG, McDonald CL, Brandt SA, Cutforth HW, Entz MH, Volkmar KM. Comparing Brassica oilseed crop productivity under contrasting N fertility regimes in the semiarid northern Great Plains. Canadian journal of plant science. 2003 Jul 1;83(3):489-97.
20. Govahi M, Saffari M. Effect of potassium and sulphur fertilizers on yield, yield components and seed quality of spring canola (*Brassica napus* L.) seed. Journal of Agronomy. 2006.
21. Gao J, Thelen KD, Min DH, Smith S, Hao X, Gehl R. Effects of manure and fertilizer applications on canola oil content and fatty acid composition. Agronomy Journal. 2010 Mar;102(2):790-7.
22. Durenne B, Druart P, Blondel A, Fauconnier ML. How cadmium affects the fitness and the glucosinolate content of oilseed rape plantlets. Environmental and experimental botany. 2018 Nov 1;155:185-94.
23. Nuttall WF, Ukrainetz H, Stewart JW, Spurr DT. The effect of nitrogen, sulphur and boron on yield and quality of rapeseed (*Brassica napus* L. and B. campestris L.). Canadian Journal of Soil Science. 1987 Aug 1;67(3):545-59.
24. Fismes J, Vong PC, Guckert A, Frossard ET. Influence of sulfur on apparent N-use efficiency, yield and quality of oilseed rape (*Brassica napus* L.) grown on a calcareous soil. European Journal of Agronomy. 2000 Mar 1;12(2):127-41.
25. Ma BL, Biswas DK, Herath AW, Whalen JK, Ruan SQ, Caldwell C, Earl H, Vanasse A, Scott P, Smith DL. Growth, yield, and yield components of canola as affected by nitrogen, sulfur, and boron application. Journal of Plant Nutrition and Soil Science. 2015 Aug;178(4):658-70.
26. Yousaf M, Li X, Ren T, Cong R, Ata-Ul-Karim ST, Shah AN, Khan MJ, Zhang Z, Fahad S, Lu J. Response of nitrogen, phosphorus and potassium fertilization on productivity and quality of winter rapeseed in central China. International Journal of Agriculture & Biology. 2016 Dec 31;18(6).

27. Brennan RF, Mason MG, Walton GH. Effect of nitrogen fertilizer on the concentrations of oil and protein in canola (*Brassica napus*) seed. Journal of Plant Nutrition. 2000 Mar 1;23(3):339-48.
28. Krauze A and Bowszys T. Effect of nitrogen fertilisation on the chemical composition of FIDE cultivars of spring oilseed rape. Rośtliny Oleiste–Oilseed Crops. 2000 22:285-90.
29. Varényiová M, Ducsay L, Ryant P. Sulphur nutrition and its effect on yield and oil content of oilseed rape (*Brassica napus* L.). Acta Universitatis Agriculturae et Silviculturae Mendelianae Brunensis. 2017 Apr 30;65(2):555-62.
30. Ahmad G, Jan A, Arif M, Jan MT, Khattak RA. Influence of nitrogen and sulfur fertilization on quality of canola (*Brassica napus* L.) under rainfed conditions. Journal of Zhejiang University Science B. 2007 Sep 1;8(10):731-7.
31. Ali A, Munir MK, Malik MA, Saleem MF. Effect of different irrigation and nitrogen levels on the seed and oil yield of canola (*Brassica napus* L.). Pakistan Journal of Agricultural Sciences. 2003;40:137-9.
32. Matoh T. Boron in plant nutrition and cell wall development. In Plant Nutrient Acquisition 2001 (pp. 227-250). Springer, Tokyo.
33. Chebli Y, Geitmann A. Cellular growth in plants requires regulation of cell wall biochemistry. Current opinion in cell biology. 2017 Feb 1;44:28-35.
34. Taylor, D.C., Barton, D.L., Rioux, K.P., MacKenzie, S.L., Reed, D.W., Underhill, E.W., Pomeroy, M.K. and Weber, N., Biosynthesis of acyl lipids containing very-long chain fatty acids in macrospore-derived and zygotic embryos of *Brassica napus* L. cv Reston. Plant physiology. 1992. 99(4), pp.1609-1618.
35. Henry JB, Vann M, McCall I, Cockson P, Whipker BE. Nutrient disorders of burley and flue-cured tobacco. Crops & Soils. 2018 Sep;51(5):44-52.
36. Hoagland DR, Arnon DI. The water-culture method for growing plants without soil. Circular. California agricultural experiment station. 1950;347(2nd edit).
37. Barnes J, Whipker B, McCall I, Frantz J. Nutrient disorders of 'Evolution' mealy-cup sage. HortTechnology. 2012 Aug 1;22(4):502-8.
38. Bariya H, Bagtharia S, Patel A. Boron: A promising nutrient for increasing growth and yield of plants. In nutrient use efficiency in plants 2014 (pp. 153-170). Springer, Cham.
39. Henry JB. Beneficial and Adverse Effects of Low Phosphorus Fertilization of Floriculture Species. 2017. NCSU Library Repository.
40. Seepaul R, Marois J, Small IM, George S, Wright DL. Carinata dry matter accumulation and nutrient uptake responses to nitrogen fertilization. Agronomy Journal. 2019 Jul;111(4):2038-46.
41. Bryson, G.M. Mills, H.A. , Sasseville, D.N., Jones Jr., J.B., and Barker, A.V. Plant analysis handbook IV. Athens, GA, USA: Macro-Macro Publ. 2014.

42. Madani H, Malboobi MA, Bakhshkelarestaghi K, Stoklosa A. Biological and chemical phosphorus fertilizers Effect on yield and P accumulation in Rapeseed (*Brassica napus* L.). Notulae Botanicae Horti Agrobotanici Cluj-Napoca. 2012 Nov 5;40(2):210-4.
43. Jullien A, Mathieu A, Allirand JM, Pinet A, De Reffye P, Cournède PH, Ney B. Characterization of the interactions between architecture and source–sink relationships in winter oilseed rape (*Brassica napus*) using the GreenLab model. Annals of botany. 2011 Apr 1;107(5):765-79.
44. Su W, Liu B, Liu X, Li X, Ren T, Cong R, Lu J. Effect of depth of fertilizer banded-placement on growth, nutrient uptake and yield of oilseed rape (*Brassica napus* L.). European Journal of Agronomy. 2015 Jan 1;62:38-45.
45. Suelter CH. Enzymes activated by monovalent cations. Science. 1970 May 15;168(3933):789-95.
46. Ecke W, Uzunova M, Weissleder K. Mapping the genome of rapeseed (*Brassica napus* L.). II. Localization of genes controlling erucic acid synthesis and seed oil content. Theoretical and Applied Genetics. 1995 Nov 1;91(6-7):972-7.
47. Ajisaka H, Kuginuki Y, Yui S, Enomoto S, Hirai M. Identification and mapping of a quantitative trait locus controlling extreme late bolting in Chinese cabbage (*Brassica rapa* L. ssp. pekinensis syn. campestris L.) using bulked segregant analysis. Euphytica. 2001 Mar 1;118(1):75.
48. Khan NA, Singh S, Nazar R, Lone PM. The source–sink relationship in mustard. Asian Aust J Plant Sci Biotechnol. 2007;1:10-8.
49. White PJ, Hammond JP, King GJ, Bowen HC, Hayden RM, Meacham MC, Spracklen WP, Broadley MR. Genetic analysis of potassium use efficiency in Brassica oleracea. Annals of Botany. 2010 Jun 1;105(7):1199-210.
50. Inamullah AA, Din M, Khan AA, Siddiq M. Evaluation of potassium application effect on grain yield, oil and protein content of brassica (*Brassica napus* L.). Sarhad J. Agric. 2013 ;29(3):331-7.
51. Mozaffari SN, Delkhosh B, Rad AS. Effect of nitrogen and potassium levels on yield and some of the agronomical characteristics in mustard (Brassica juncea). Indian J. Sci. Technol. 2012 Feb;5(2):2051-4.
52. Ge LL, Tian HQ, Russell SD. Calcium function and distribution during fertilization in angiosperms. American Journal of Botany. 2007 Jun;94(6):1046-60.
53. Jez J, editor. Sulfur: A missing link between soils, crops, and nutrition. ASA-CSSA-SSSA; 2008.
54. Stansly T, Seepaul R, George S, Small IM, Wright D. Response of Glucosinolate, Oil, and Protein Content to Sulfur Availability in Oilseed *Brassica carinata*. In ASA, CSSA and SSSA International Annual Meetings. 2019 Nov 11. ASA, CSSA, and SSSA.

55. Mobin M, College KP. Photosynthetic and physiological responses of Indian mustard (Brassica juncea L. Czern & Coss) plants as affected by sulfur starvation. Electronic Journal of Environmental, Agricultural and Food Chemistry. 2010 Sep 1;9.
56. McGrath SP, Zhao FJ. Sulphur uptake, yield responses and the interactions between nitrogen and sulphur in winter oilseed rape (*Brassica napus*). The Journal of Agricultural Science. 1996 Feb;126(1):53-62.
57. Varényiová M, Ducsay L, Ryant P. Sulphur nutrition and its effect on yield and oil content of oilseed rape (*Brassica napus* L.). Acta Universitatis Agriculturae et Silviculturae Mendelianae Brunensis. 2017 Apr 30;65(2):555-62.
58. Malhi SS, Gan Y, Raney JP. Yield, seed quality, and sulfur uptake of Brassica oilseed crops in response to sulfur fertilization. Agronomy Journal. 2007 Mar;99(2):570-7.
59. Rehman H, Iqbal Q, Farooq M, Wahid A, Afzal I, Basra SM. Sulphur application improves the growth, seed yield and oil quality of canola. Acta Physiologiae Plantarum. 2013 Oct 1;35(10):2999-3006.
60. Mulvaney MJ, Leon RG, Seepaul R, Wright DL, Hoffman TL. *Brassica carinata* seeding rate and row spacing effects on morphology, yield, and oil. Agronomy Journal. 2019 Mar;111(2):528-35.
61. Kopsell DE, Kopsell DA, Sams CE, Barickman TC. Ratio of calcium to magnesium influences biomass, elemental accumulations, and pigment concentrations in kale. Journal of Plant Nutrition. 2013 Dec 6;36(14):2154-65.
62. Broadley MR, Hammond JP, King GJ, Astley D, Bowen HC, Meacham MC, Mead A, Pink DA, Teakle GR, Hayden RM, Spracklen WP. Shoot calcium and magnesium concentrations differ between subtaxa, are highly heritable, and associate with potentially pleiotropic loci in Brassica oleracea. Plant Physiology. 2008 Apr 1;146(4):1707-20.
63. Rios JJ, Ó Lochlainn S, Devonshire J, Graham NS, Hammond JP, King GJ, White PJ, Kurup S, Broadley MR. Distribution of calcium (Ca) and magnesium (Mg) in the leaves of *Brassica rapa* under varying exogenous Ca and Mg supply. Annals of Botany. 2012 May 1;109(6):1081-9.
64. Purakayasthaand BK, and Nad TP. Effect of sulphur, magnesium, and molybdenum on mustard (Brassica juncea L.) and wheat (Triticum aestivum L.): nitrate nitrogen accumulation and protein yield. Indian J. Plant Physiol. 1997 Apr;2(2):110-3.

TABLES AND FIGURES

Table 3.2.1: Calculations for modified Hoagland's solution utilized to explore the impacts of varying macronutrients on the growth of *Brassica carinata* over its life stages.

Fertility Rate (%)[1]	0.00		25.00		50.00		75.00		87.50		100.00	
	mM • L^{-1}	ppm	mM • L^{-1}	ppm	mM • L^{-1}	ppm	mM • L^{-1}	ppm	mM • L^{-1}	ppm	mM • L^{-1}	ppm
Nitrogen (N) (mM • L^{-1})[2]	0.00	0.0	3.75	50.0	7.5	100.0	11.25	150.0	13.13	175.0	15.0	200.0
Phosphorus (P) (mM • L^{-1})[2]	0.00	0.0	0.25	7.5	0.50	15.0	0.75	22.5	0.875	26.25	1.0	30.0
Potassium (K) (mM • L^{-1})[2]	0.00	0.0	1.5	59.0	3.0	117.0	4.5	175.0	5.25	205.0	6.0	234.0
Calcium (Ca) (mM • L^{-1})[2]	0.00	0.0	1.25	47.0	2.5	93.0	3.75	140.0	4.375	163.0	5.0	186.0
Sulfur (S) (mM • L^{-1})[2]	0.00	0.0	0.5	16.0	1.0	32.0	1.5	48.0	1.75	56.0	2.0	64.0
Magnesium (Mg) (mM • L^{-1})[2]	0.00	0.0	0.5	12.5	1.0	24.0	1.5	36.0	1.75	42.0	2.0	48.0

[1] Values indicate the adjusted fertility concentration provided from a modified Hoagland's Solution with all elements held constant except the adjusted macroelement being studied. These values are expressed as a percentage of the standard Hoagland's Solution. For more detailed information on the system and fertility modifications see Barnes et al. [37].

[2] Values given for each element listed in mM • L^{-1}. To convert mM • L^{-1} to parts per million (ppm) multiply by the molecular weight and divide by 1000.

Table 3.3.1: *Brassica carinata* plant dry weights (g) and leaf tissue concentration (%) based on nitrogen (N) fertility treatments.

Nitrogen Fertility Concentration (mM • L^{-1})[1]	0.0	3.75	7.50	11.25	13.13	15.0
Plant Dry Weight (g)						
Rosette[2]	0.13 A ***	0.48 A ***	1.00 AB ***	1.55 B ***	2.65 C ***	3.40 C ***
Bolting[2]	0.53 D ***	7.45 C ***	15.90 B ***	12.50 BC ***	14.75 B ***	25.60 A ***
Flowering[2]	0.73 C ***	0.80 C ***	27.63 B ***	38.48 AB ***	36.58 AB ***	44.20 A ***
Pod Set[2]	N/A[3]	N/A[3]	43.80 B **	57.28 B **	57.73 B **	109.90 B **
	Nitrogen Leaf Tissue Nutrient Concentrations (%)					
Rosette[2]	0.99 A ***	2.09 B ***	5.82 C ***	6.08 C ***	6.00 C ***	6.19 C ***
Bolting[2]	1.59 A ***	3.03 B ***	5.91 C ***	6.23 C ***	6.43 C ***	6.09 C ***
Flowering[2]	1.31 A ***	1.64 A ***	5.52 B ***	5.75 B ***	6.11 B ***	5.73 B ***
Pod Set[2]	N/A[3]	N/A[3]	3.92 A *	4.84 AB *	4.97 B *	4.72 AB *
	Comparison Nitrogen Leaf Tissue Values (%)[4,5]					
	Brassica carinata[4]			*Brassica napus*[5]		
Rosette[4]	2.35 – 2.48			2.00 – 4.50		
Bolting[4]	2.09 – 2.97					
Flowering[4]	1.29 – 2.33					
Pod Set[4]	0.79 – 1.55					

[1] Values indicate the adjusted fertility concentration provided from a modified Hoagland's solution with all elements held constant except the adjusted macroelement being studied. For more detailed information on the system and fertility modifications see Barnes et al. [40].
[2] *, **, or *** Indicates statistically significant differences between sample means based on F-test at $P \leq 0.05$, $P \leq 0.01$, or $P \leq 0.001$, respectively. NS (not significant) indicates the F-test difference between sample means was $P > 0.05$. Values with the same letter indicate a lack of statistical significance while values with different letters indicate statistically significant results.
[3] N/A indicates results were not available given plants did not progress to the growth stage specified.
[4] Reference values from Seepaul et al., [40]. Values given are based on *Brassica carinata* for above ground tissue concentration tissue from two growing seasons with samples taken based on plant life stages.
[5] Reference values based on 50 mature leaves without petioles taken throughout the season from rosette stage to pod set. Values taken from *Brassica napus* leaf tissue values from Bryson et al. [41].

Equations 3.3.1: Regression models for linear and quadratic for *Brassica carinata* plant dry weights (g) and leaf tissue nutrient concentrations (%) based on nitrogen (N) fertility treatments.

Nitrogen Regression Models	Power and Significance[1]	Regression Equation[3]	R^2 [4]	Adj-R^2 [4]
Plant Dry Weight (g)				
Rosette[2]	L ***	-0.23 + 0.031x	0.82	0.81
	Q ***	0.22 – 0.004x + 0.00003x^2	0.89	0.88
Bolting[2]	L ***	1.75 + 0.200x	0.74	0.73
	Q ***	1.75 + 0.200x + 0.00003x^2	0.74	0.72
Flowering[2]	L ***	-2.27 + 0.481x	0.84	0.83
	Q ***	-3.03 + 0.541x - 0.00006x^2	0.84	0.83
Pod Set[2]	L **	-21.23 + 1.133x	0.44	0.40
	Q **	201.40 – 5.291x + 0.04335x^2	0.59	0.52
Nitrogen Leaf Tissue Nutrient Concentrations (%)				
Rosette[2]	L ***	1.38 + 0.056x	0.84	0.83
	Q ***	0.59 + 0.119x - 0.00006x^2	0.92	0.91
Bolting[2]	L ***	2.12 + 0.05x	0.83	0.82
	Q ***	1.30 + 0.11x - 0.00007x^2	0.94	0.93
Flowering[2]	L ***	1.38 + 0.053x	0.81	0.80
	Q ***	0.76 + 0.102x – 0.00005x^2	0.86	0.84
Pod Set[2]	L *	3.22 + 0.018x	0.32	0.27
	Q **	-1.19 + 0.145x – 0.00004x^2	0.48	0.40

[1] Regression models (L = linear regression model, Q = quadratic regression model) were subjected to linear and higher power polynomial modeling to determine a model of fit. Model fits above the second power resulted in no greater interpretation of data for all models tested, consequently the above models only compare linear and second order polynomials.*, **, or *** Indicates the model's statistical significance at $p \leq 0.05$, $P \leq 0.01$, or $P \leq 0.001$, respectively. NS (not significant) indicates the model resulted in $p > 0.05$.

[2] *Brassica carinata* life stage.

[3] Models were calculated using PROC REG on SAS v 9.4. Determination of best model was accomplished by selecting the model with the best R^2 value and had the lowest p-value.

[4] Best fit statistics: R^2 = coefficient of determination, Adj-R^2 = adjusted coefficient of determination.

Graph 3.3.1: Polynomial regression models for nitrogen (N) fertility impacts on *Brassica carinata* plant dry weights (g) and leaf tissue nutrient concentrations (%).

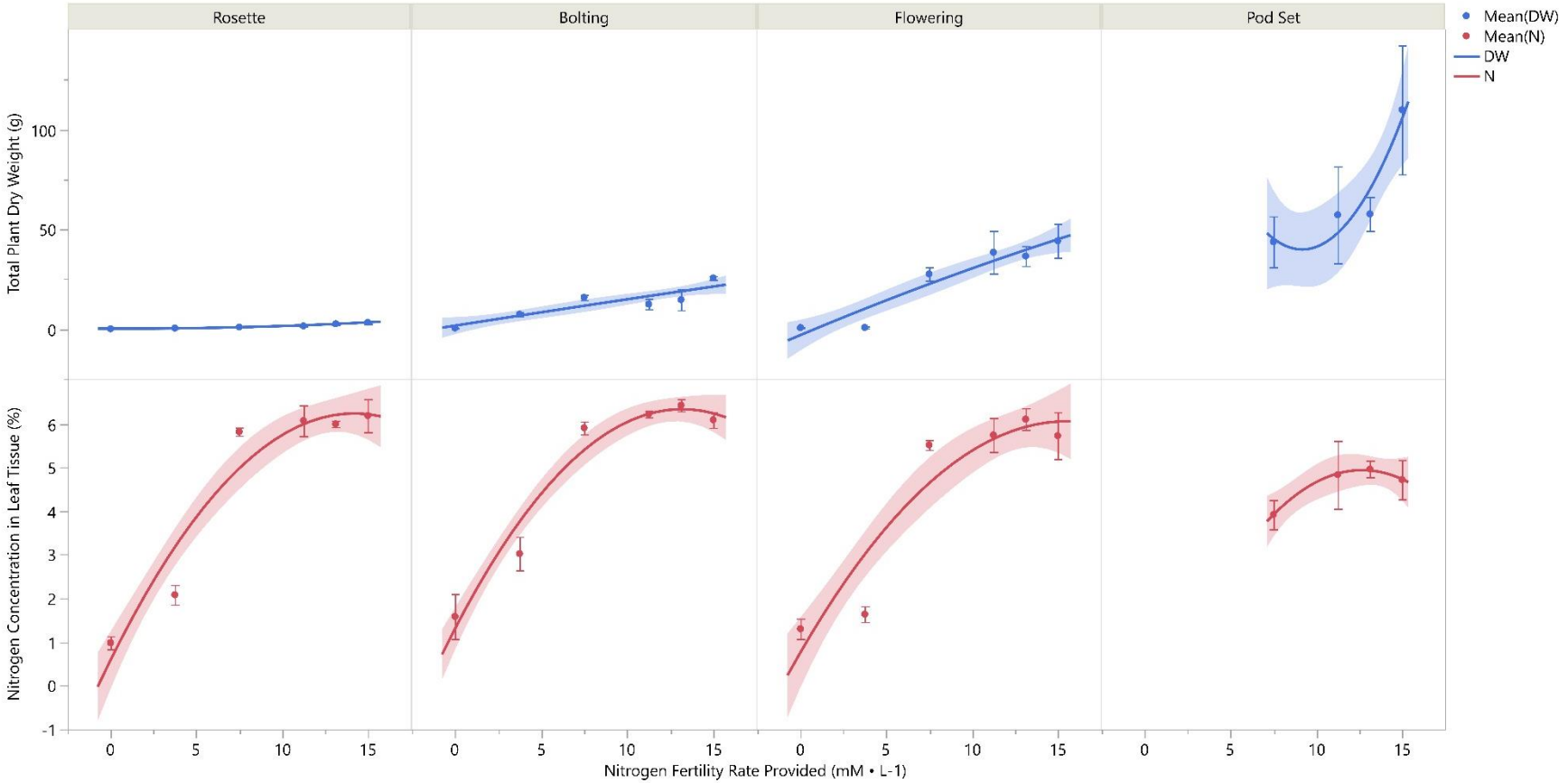

Table 3.3.2: *Brassica carinata* plant dry weights (g) and leaf tissue concentration (%) based on phosphorus (P) fertility treatments.

Phosphorus Fertility Concentration (mM • L^{-1})[1]	0.00	0.25	0.50	0.75	0.875	1.0
Plant Dry Weight (g)						
Rosette[2]	1.13 AB ***	0.73 A ***	1.38 AB ***	1.60 AB ***	1.95 B ***	3.40 C ***
Bolting[2]	6.13 A ***	14.13 BA ***	12.95 BA ***	14.73 B ***	18.03 BC ***	25.60 C ***
Flowering[2]	8.97 A ***	36.45 CD ***	21.77 AB ***	23.45 BC ***	33.98 BCD ***	44.20 D ***
Pod Set[2]	20.50 A ***	39.40 A ***	66.03 AB ***	35.90 A ***	105.68 B ***	109.90 B ***
	Phosphorus Leaf Tissue Nutrient Concentrations (%)					
Rosette[2]	0.25 A ***	0.62 B ***	0.75 BC ***	0.74 BC ***	0.70 BC ***	0.80 C ***
Bolting[2]	0.14 A ***	0.40 B ***	0.75 CD ***	0.73 CD ***	0.80 D ***	0.63 C ***
Flowering[2]	0.06 A ***	0.23 AB ***	0.65 C ***	0.46 BC ***	0.57 BC ***	0.39 BC ***
Pod Set[2]	0.04 A ***	0.17 B ***	0.40 C ***	0.39 C ***	0.22 BC ***	0.18 B ***
	Comparison Phosphorus Leaf Tissue Values (% or g • kg^{-1})[3]					
	Brassica carinata[3]			*Brassica napus*[4]		
Rosette[3]	0.28 – 0.33			0.28 – 0.69		
Bolting[3]	0.30 – 0.33					
Flowering[3]	0.16 – 0.24					
Pod Set[3]	0.12 – 0.20					

[1] Values indicate the adjusted fertility concentration provided from a modified Hoagland's solution with all elements held constant except the adjusted macroelement being studied. For more detailed information on the system and fertility modifications see Barnes et al. [40].
[2] *, **, or *** Indicates statistically significant differences between sample means based on F-test at $P \leq 0.05$, $P \leq 0.01$, or $P \leq 0.001$, respectively. NS (not significant) indicates the F-test difference between sample means was $P > 0.05$. Values with the same letter indicate a lack of statistical significance while values with different letters indicate statistically significant results.
[3] N/A indicates results were not available given plants did not progress to the growth stage specified.
[4] Reference values from Seepaul et al., [40]. Values given are based on *Brassica carinata* for above ground tissue concentration tissue from two growing seasons with samples taken based on plant life stages.
[5] Reference values based on 50 mature leaves without petioles taken throughout the season from rosette stage to pod set. Values taken from *Brassica napus* leaf tissue values from Bryson et al. [41].

Equations 3.3.2: Regression models for linear and quadratic for *Brassica carinata* plant dry weights (g) and leaf tissue nutrient concentrations (%) based on phosphorus (P) fertility treatments.

Phosphorus Regression Models	Power and Significance[1]	Regression Equation[3]	R^2 [4]	Adj-R^2 [4]
Plant Dry Weight (g)				
Rosette[2]	L ***	0.40 + 0.004x	0.64	0.62
	Q ***	0.28 + 0.013x + 0.000002x^2	0.83	0.82
Bolting[2]	L ***	6.67 + 0.148x	0.60	0.58
	Q ***	8.17 + 0.052x + 0.00010x^2	0.62	0.59
Flowering[2]	L **	17.08 + 0.207x	0.34	0.31
	Q *	17.82 + 0.153x + 0.00053x^2	0.34	0.28
Pod Set[2]	L NS	16.51 + 0.817x	0.18	0.00
	Q ***	26.67 - 0.004x + 0.00797x^2	0.56	0.51
Phosphorus Leaf Tissue Nutrient Concentrations (%)				
Rosette[2]	L ***	0.59 + 0.020x	0.55	0.53
	Q ***	1.15 - 0.025x + 0.000445x^2	0.76	0.73
Bolting[2]	L ***	1.26 + 0.006x	0.65	0.64
	Q ***	0.10 + 0.018x - 0.000123x^2	0.89	0.88
Flowering[2]	L **	0.12 + 0.004x	0.40	0.36
	Q ***	0.01 + 0.016x - 0.000003x^2	0.67	0.64
Pod Set[2]	L NS	0.15 + 0.002x	0.13	0.08
	Q ***	0.00 + 0.012x - 0.000105x^2	0.59	0.54

[1] Regression models (L = linear regression model, Q = quadratic regression model) were subjected to linear and higher power polynomial modeling to determine a model of fit. Model fits above the second power resulted in no greater interpretation of data for all models tested, consequently the above models only compare linear and second order polynomials.*, **, or *** Indicates the model's statistical significance at $p \leq 0.05$, $P \leq 0.01$, or $P \leq 0.001$, respectively. NS (not significant) indicates the model resulted in $p > 0.05$.

[2] *Brassica carinata* life stage.

[3] Models were calculated using PROC REG on SAS v 9.4. Determination of best model was accomplished by selecting the model with the best R^2 value and had the lowest p-value.

[4] Best fit statistics: R^2 = coefficient of determination, Adj-R^2 = adjusted coefficient of determination.

Graph 3.3.2: Polynomial regression models for phosphorus (P) fertility impacts on *Brassica carinata* plant dry weights (g) and leaf tissue nutrient concentrations (%).

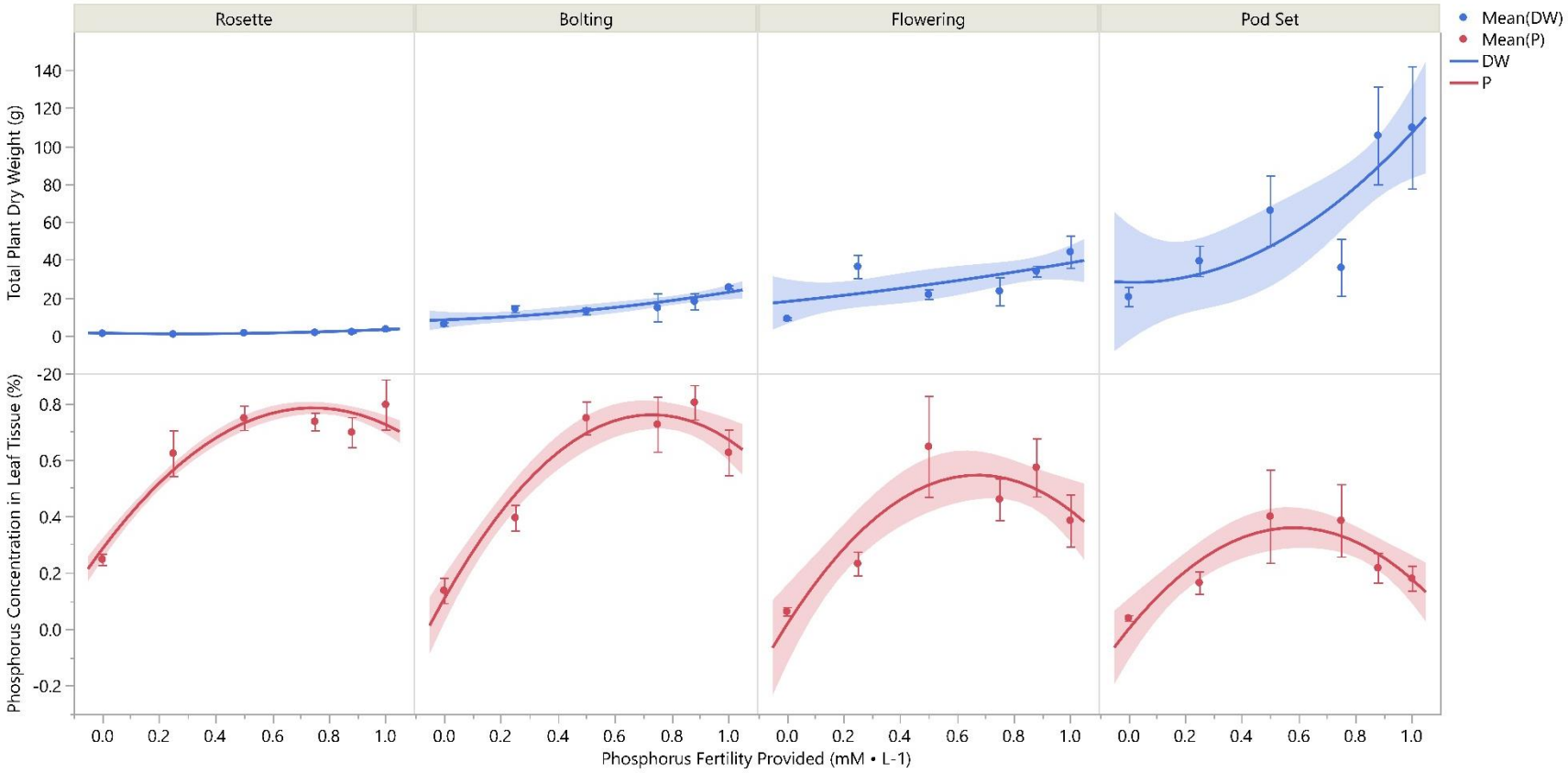

Table 3.3.3: *Brassica carinata* plant dry weights (g) and leaf tissue concentration (%) based on potassium (K) fertility treatments.

Potassium Fertility Concentration (mM • L^{-1})[1]	0.00	1.50	3.0	4.5	5.25	6.0
Plant Dry Weight (g)						
Rosette[2]	1.65 AB ***	1.28 AB ***	1.03 A ***	1.48 AB ***	2.05 B ***	3.40 C ***
Bolting[2]	6.20 A ***	10.53 AB ***	16.60 B ***	12.78 AB ***	12.05 AB ***	25.60 C ***
Flowering[2]	9.83 A ***	22.35 AB ***	42.20 C ***	33.90 BC ***	34.93 BC ***	44.20 C ***
Pod Set[2]	14.37 A ***	66.08 B ***	40.10 AB ***	60.98 B ***	50.50 AB ***	109.90 C ***
	Potassium Leaf Tissue Nutrient Concentrations (%)					
Rosette[2]	0.69 A ***	5.57 B ***	6.37 B ***	5.99 B ***	6.37 B ***	5.88 B ***
Bolting[2]	0.49 A ***	2.47 B ***	3.76 B ***	5.30 C ***	6.30 C ***	5.79 C ***
Flowering[2]	0.40 A ***	2.08 AB ***	3.61 BC ***	5.08 CD ***	5.28 CD ***	7.00 D ***
Pod Set[2]	0.17 A ***	0.86 A ***	4.62 B ***	5.71 BC ***	6.16 C ***	6.34 C ***
	Comparison Potassium Leaf Tissue Values (%)[3]					
	Brassica carinata[3]			*Brassica napus*[4]		
Rosette[3]	2.97 – 4.72			2.90 – 5.10		
Bolting[3]	1.95 – 3.23					
Flowering[3]	1.13 – 2.76					
Pod Set[3]	1.48 – 2.39					

[1] Values indicate the adjusted fertility concentration provided from a modified Hoagland's solution with all elements held constant except the adjusted macroelement being studied. For more detailed information on the system and fertility modifications see Barnes et al. [40].
[2] *, **, or *** Indicates statistically significant differences between sample means based on F-test at $P \leq 0.05$, $P \leq 0.01$, or $P \leq 0.001$, respectively. NS (not significant) indicates the F-test difference between sample means was $P > 0.05$. Values with the same letter indicate a lack of statistical significance while values with different letters indicate statistically significant results.
[3] N/A indicates results were not available given plants did not progress to the growth stage specified.
[4] Reference values from Seepaul et al., [40]. Values given are based on *Brassica carinata* for above ground tissue concentration tissue from two growing seasons with samples taken based on plant life stages.
[5] Reference values based on 50 mature leaves without petioles taken throughout the season from rosette stage to pod set. Values taken from *Brassica napus* leaf tissue values from Bryson et al. [41].

Equations 3.3.3: Regression models for linear and quadratic for *Brassica carinata* plant dry weights (g) and leaf tissue nutrient concentrations (%) based on potassium (K) fertility treatments.

Potassium Regression Models	Power and Significance[1]	Regression Equation[3]	R^2 [4]	Adj-R^2 [4]
Plant Dry Weight (g)				
Rosette[2]	L **	1.04 + 0.014x	0.31	0.28
	Q ***	1.80 - 0.047x + 0.000601x^2	0.75	0.73
Bolting[2]	L **	6.70 + 0.129x	0.43	0.41
	Q **	7.55 + 0.061x + 0.000682x^2	0.44	0.39
Flowering[2]	L ***	15.84 + 0.279x	0.56	0.54
	Q ***	10.21 + 0.673x - 0.00381x^2	0.64	0.60
Pod Set[2]	L **	25.07 + 0.576x	0.38	0.35
	Q **	32.77 + 0.036x + 0.00523x^2	0.41	0.35
Potassium Leaf Tissue Nutrient Concentrations (%)				
Rosette[2]	L ***	2.75 + 0.043x	0.53	0.51
	Q ***	1.15 + 0.171x - 0.00128x^2	0.89	0.87
Bolting[2]	L ***	0.82 + 0.057x	0.89	0.88
	Q ***	0.44 + 0.087x - 0.000310x^2	0.90	0.90
Flowering[2]	L ***	0.45 + 0.062x	0.87	0.85
	Q ***	0.51 + 0.057x + 0.000043x^2	0.87	0.86
Pod Set[2]	L ***	0.08 + 0.069x	0.89	0.88
	Q ***	-044 + 0.106x - 0.000352x^2	0.91	0.90

[1] Regression models (L = linear regression model, Q = quadratic regression model) were subjected to linear and higher power polynomial modeling to determine a model of fit. Model fits above the second power resulted in no greater interpretation of data for all models tested, consequently the above models only compare linear and second order polynomials.*, **, or *** Indicates the model's statistical significance at $p \leq 0.05$, $P \leq 0.01$, or $P \leq 0.001$, respectively. NS (not significant) indicates the model resulted in $p > 0.05$.

[2] *Brassica carinata* life stage.

[3] Models were calculated using PROC REG on SAS v 9.4. Determination of best model was accomplished by selecting the model with the best R^2 value and had the lowest p-value.

[4] Best fit statistics: R^2 = coefficient of determination, Adj-R^2 = adjusted coefficient of determination.

Graph 3.3.3: Polynomial regression models for potassium (K) fertility impacts on *Brassica carinata* plant dry weights (g) and leaf tissue nutrient concentrations (%).

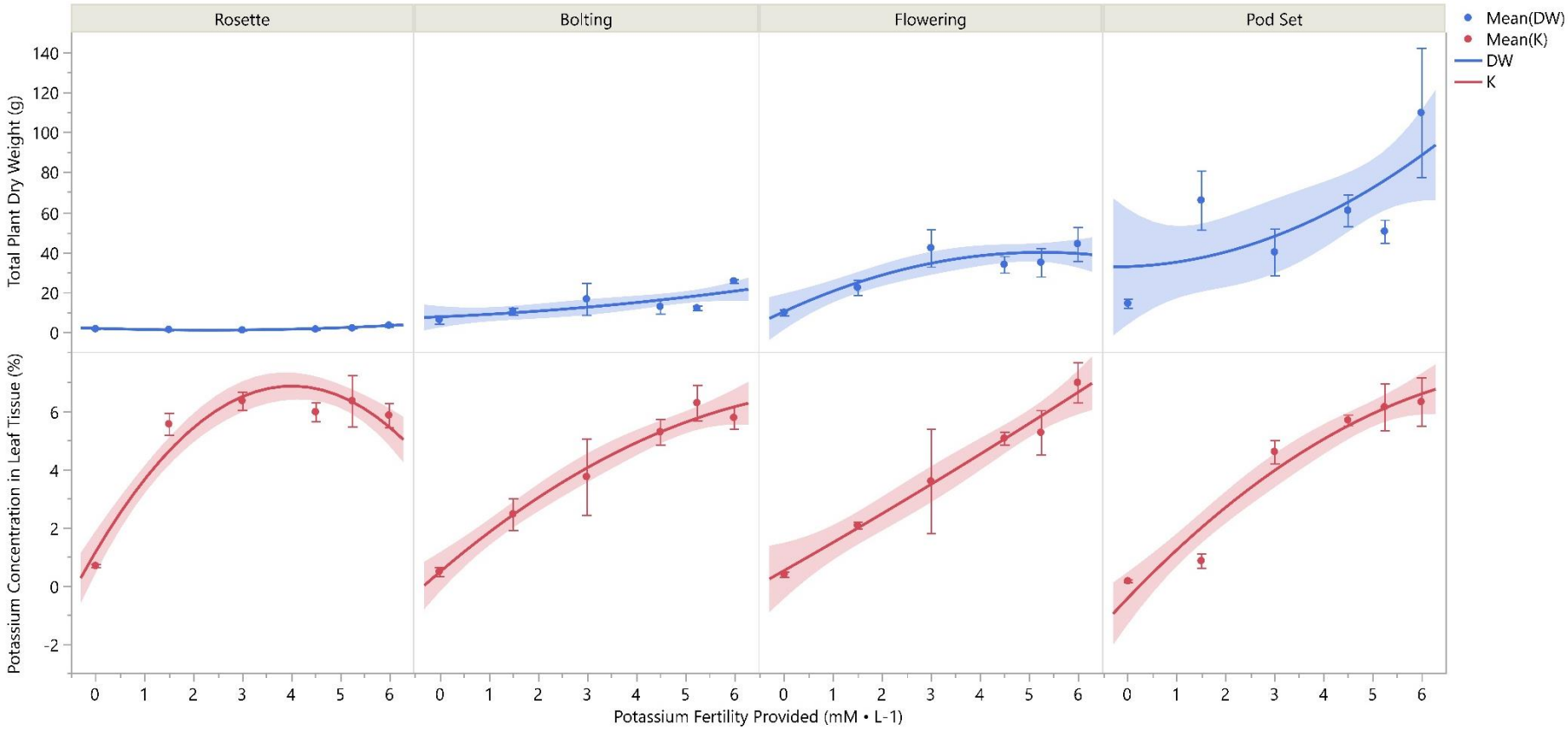

Table 3.3.4: *Brassica carinata* plant dry weights (g) and leaf tissue concentration (%) based on calcium (Ca) fertility treatments.

Calcium Fertility Concentration (mM • L^{-1})[1]	0.00	1.25	2.50	3.75	4.38	5.0
Plant Dry Weight (g)						
Rosette[2]	3.20 AB ***	2.40 ABC ***	1.33 C ***	1.88 C ***	2.23 BC ***	3.40 A ***
Bolting[2]	8.28 A ***	16.35 B ***	18.10 B ***	16.50 B ***	13.80 BC ***	25.60 C ***
Flowering[2]	10.33 A ***	31.97 BC ***	22.93 AB ***	37.33 BC ***	32.38 BC ***	44.20 C ***
Pod Set[2]	N/A[3]	77.53 AB *	72.40 AB *	54.05 B *	59.13 B *	109.90 A *
	Calcium Leaf Tissue Nutrient Concentrations (%)					
Rosette[2]	1.15 A ***	1.67 B ***	2.26 C ***	2.68 CD ***	2.97 D ***	3.07 D ***
Bolting[2]	0.56 A ***	1.65 B ***	1.99 BC ***	2.51 D ***	2.62 D ***	2.22 D ***
Flowering[2]	0.44 A ***	2.30 BC ***	2.30 BC ***	2.05 C ***	2.76 BC ***	3.02 D ***
Pod Set[2]	N/A[3]	2.40 A *	2.59 A *	2.81 AB *	3.14 AB *	3.68 B *
	Comparison Calcium Leaf Tissue Values (%)[4]					
	Brassica carinata[4]			*Brassica napus*[5]		
Rosette[4]	0.35 – 1.47			1.0 – 3.0		
Bolting[4]	0.31 – 1.10					
Flowering[4]	0.28 – 0.89					
Pod Set[4]	0.32 – 0.73					

[1] Values indicate the adjusted fertility concentration provided from a modified Hoagland's solution with all elements held constant except the adjusted macroelement being studied. For more detailed information on the system and fertility modifications see Barnes et al. [40].
[2] *, **, or *** Indicates statistically significant differences between sample means based on F-test at $P \leq 0.05$, $P \leq 0.01$, or $P \leq 0.001$, respectively. NS (not significant) indicates the F-test difference between sample means was $P > 0.05$. Values with the same letter indicate a lack of statistical significance while values with different letters indicate statistically significant results.
[3] N/A indicates results were not available given plants did not progress to the growth stage specified.
[4] Reference values from Seepaul et al., [40]. Values given are based on *Brassica carinata* for above ground tissue concentration tissue from two growing seasons with samples taken based on plant life stages.
[5] Reference values based on 50 mature leaves without petioles taken throughout the season from rosette stage to pod set. Values taken from *Brassica napus* leaf tissue values from Bryson et al. [41].

Equations 3.3.4: Regression models for linear and quadratic for *Brassica carinata* plant dry weights (g) and leaf tissue nutrient concentrations (%) based on calcium (Ca) fertility treatments.

Calcium Regression Models	Power & Significance[1]	Regression Equation[3]	R^{2} [4]	Adj-R^{2} [4]
Plant Dry Weight (g)				
Rosette[2]	L NS	2.48 - 0.001x	0.00	-0.04
	Q ***	3.38 - 0.073x + 0.000713x^2	0.65	0.62
Bolting[2]	L **	10.57 + 0.105x	0.39	0.37
	Q ***	10.22 + 0.132x - 0.000276x^2	0.39	0.34
Flowering[2]	L ***	14.44 + 0.270x	0.58	0.56
	Q ***	13.45 + 0.358x - 0.000885x^2	0.58	0.54
Pod Set[2]	L NS	60.26 + 0.204x	0.03	-0.02
	Q *	148.77 - 3.201x + 0.02698x^2	0.33	0.25
Calcium Leaf Tissue Nutrient Concentrations (%)				
Rosette[2]	L ***	1.18 + 0.020x	0.92	0.92
	Q ***	1.12 + 0.025x - 0.000047x^2	0.93	0.92
Bolting[2]	L ***	0.94 + 0.018x	0.76	0.75
	Q ***	0.57 + 0.047x + 0.000290x^2	0.92	0.91
Flowering[2]	L ***	0.93 + 0.021x	0.69	0.68
	Q ***	0.70 + 0.041x + 0.000210x^2	0.74	0.71
Pod Set[2]	L ***	1.83 + 0.016x	0.48	0.45
	Q ***	2.77 – 0.020x + 0.000286x^2	0.55	0.50

[1] Regression models (L = linear regression model, Q = quadratic regression model) were subjected to linear and higher power polynomial modeling to determine a model of fit. Model fits above the second power resulted in no greater interpretation of data for all models tested, consequently the above models only compare linear and second order polynomials.*, **, or *** Indicates the model's statistical significance at $p \leq 0.05$, $P \leq 0.01$, or $P \leq 0.001$, respectively. NS (not significant) indicates the model resulted in $p > 0.05$.

[2] *Brassica carinata* life stage.

[3] Models were calculated using PROC REG on SAS v 9.4. Determination of best model was accomplished by selecting the model with the best R^2 value and had the lowest p-value.

[4] Best fit statistics: R^2 = coefficient of determination, Adj-R^2 = adjusted coefficient of determination.

Graph 3.3.4: Polynomial regression models for calcium (Ca) fertility impacts on *Brassica carinata* plant dry weights (g) and leaf tissue nutrient concentrations (%).

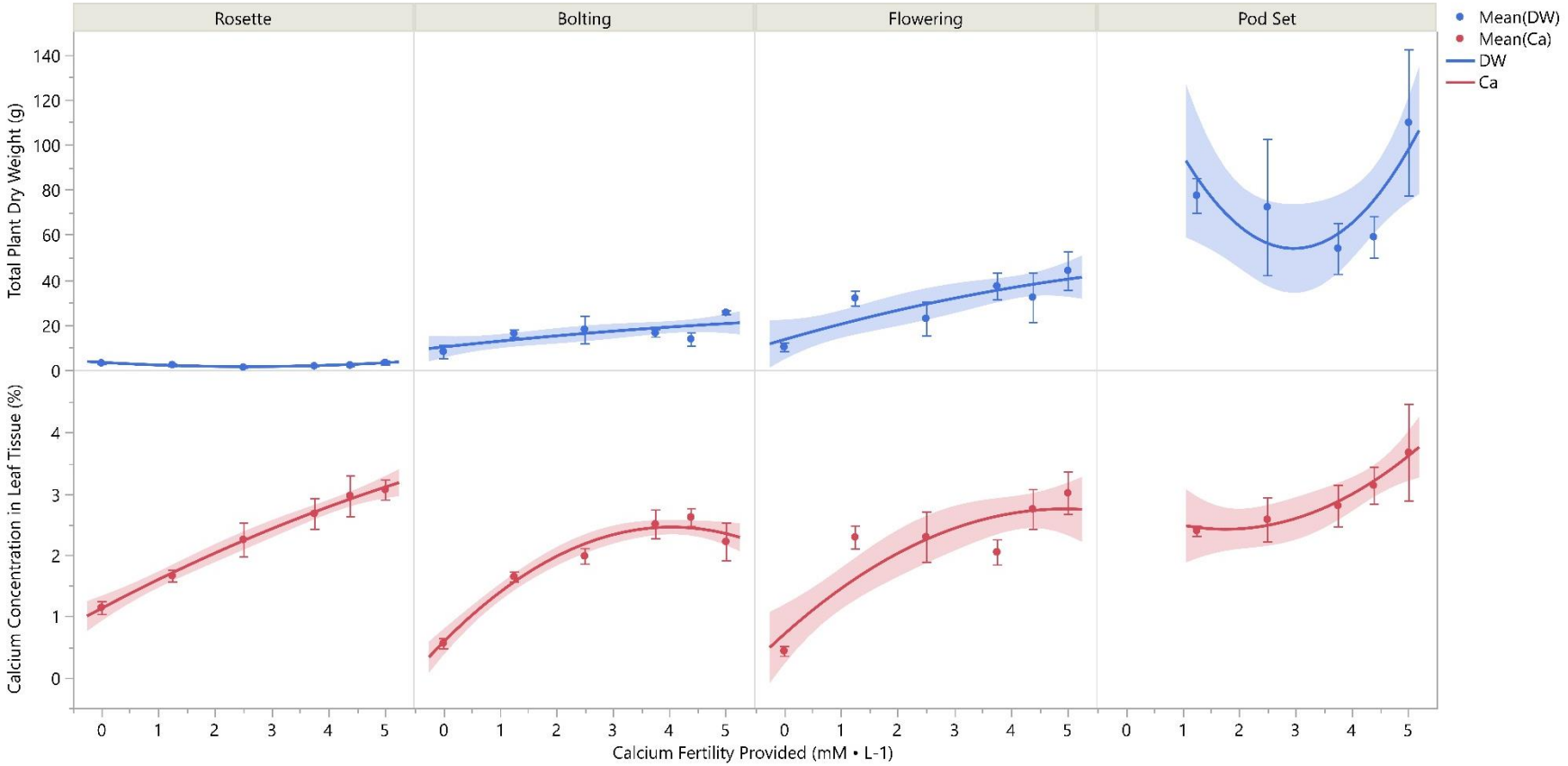

Table 3.3.5: *Brassica carinata* plant dry weights (g) and leaf tissue concentration (%) based on sulfur (S) fertility treatments.

Sulfur Fertility Concentration (mM • L^{-1})[1]	0.00	0.50	1.0	1.5	1.75	2.0
Plant Dry Weight (g)						
Rosette[2]	3.20 A ***	2.40 B ***	1.33 AB ***	1.88 B ***	2.23 C ***	3.40 D ***
Bolting[2]	7.10 A ***	12.95 B ***	11.73 AB ***	13.25 B ***	19.28 C ***	25.60 D ***
Flowering[2]	14.80 A ***	22.40 A ***	24.17 A ***	23.15 A ***	29.55 A ***	44.20 B ***
Pod Set[2]	18.10 A ***	63.23 AB ***	80.53 CB ***	70.93 CB ***	93.88 CB ***	109.90 C ***
	Sulfur Leaf Tissue Nutrient Concentrations (%)					
Rosette[2]	0.96 A ***	0.85 B ***	0.91 C ***	0.98 CD ***	1.04 CD ***	1.10 D ***
Bolting[2]	0.17 A ***	0.82 B ***	1.04 C ***	1.10 CD ***	0.93 BC ***	1.25 D ***
Flowering[2]	0.12 A ***	0.48 B ***	1.15 C ***	1.29 CD ***	1.16 C ***	1.45 D ***
Pod Set[2]	0.08 A ***	0.32 B ***	0.97 B ***	1.11 B ***	1.20 B ***	1.45 C ***
	Comparison Sulfur Leaf Tissue Values (%)[3]					
	Brassica carinata[3]			*Brassica napus*[4]		
Rosette[3]	0.35 – 0.73			0.17 – 1.04		
Bolting[3]	0.28 – 0.61					
Flowering[3]	0.19 – 0.56					
Pod Set[3]	0.21 – 0.54					

[1] Values indicate the adjusted fertility concentration provided from a modified Hoagland's solution with all elements held constant except the adjusted macroelement being studied. For more detailed information on the system and fertility modifications see Barnes et al. [40].
[2] *, **, or *** Indicates statistically significant differences between sample means based on F-test at $P \leq 0.05$, $P \leq 0.01$, or $P \leq 0.001$, respectively. NS (not significant) indicates the F-test difference between sample means was $P > 0.05$. Values with the same letter indicate a lack of statistical significance while values with different letters indicate statistically significant results.
[3] N/A indicates results were not available given plants did not progress to the growth stage specified.
[4] Reference values from Seepaul et al., [40]. Values given are based on *Brassica carinata* for above ground tissue concentration tissue from two growing seasons with samples taken based on plant life stages.
[5] Reference values based on 50 mature leaves without petioles taken throughout the season from rosette stage to pod set. Values taken from *Brassica napus* leaf tissue values from Bryson et al. [41].

Equations 3.3.5: Regression models for linear and quadratic for *Brassica carinata* plant dry weights (g) and leaf tissue nutrient concentrations (%) based on sulfur (S) fertility treatments.

Sulfur Regression Models	Power & Significance[1]	Regression Equation[3]	R^2 [4]	Adj-R^2 [4]
Plant Dry Weight (g)				
Rosette[2]	L NS	$0.54 + 0.008x$	0.16	0.12
	Q ***	$1.21 - 0.046x + 0.000534x^2$	0.75	0.73
Bolting[2]	L ***	$6.69 + 0.148x$	0.67	0.65
	Q ***	$8.94 - 0.032x + 0.00179x^2$	0.74	0.72
Flowering[2]	L ***	$14.12 + 0.218x$	0.52	0.49
	Q ***	$18.38 - 0.095x + 0.00305x^2$	0.59	0.55
Pod Set[2]	L ***	$32.63 + 0.725x$	0.59	0.57
	Q ***	$26.69 + 1.141x - 0.00402x^2$	0.61	0.57
Sulfur Leaf Tissue Nutrient Concentrations (%)				
Rosette[2]	L *	$0.51 - 0.0001x$	0.19	0.15
	Q ***	$8.94 - 0.032x - 0.000739x^2$	0.74	0.72
Bolting[2]	L ***	$0.41 + 0.008x$	0.71	0.69
	Q ***	$0.24 + 0.022x - 0.000138x^2$	0.85	0.83
Flowering[2]	L ***	$0.22 + 0.013x$	0.88	0.87
	Q ***	$0.07 + 0.023x - 0.000104x^2$	0.92	0.91
Pod Set[2]	L ***	$0.09 + 0.014x$	0.92	0.91
	Q ***	$0.03 + 0.018x - 0.000039x^2$	0.92	0.92

[1] Regression models (L = linear regression model, Q = quadratic regression model) were subjected to linear and higher power polynomial modeling to determine a model of fit. Model fits above the second power resulted in no greater interpretation of data for all models tested, consequently the above models only compare linear and second order polynomials.*, **, or *** Indicates the model's statistical significance at $p \leq 0.05$, $P \leq 0.01$, or $P \leq 0.001$, respectively. NS (not significant) indicates the model resulted in $p > 0.05$.

[2] *Brassica carinata* life stage.

[3] Models were calculated using PROC REG on SAS v 9.4. Determination of best model was accomplished by selecting the model with the best R^2 value and had the lowest p-value.

[4] Best fit statistics: R^2 = coefficient of determination, Adj-R^2 = adjusted coefficient of determination.

Graph 3.3.5: Polynomial regression models for sulfur (S) fertility impacts on *Brassica carinata* plant dry weights (g) and leaf tissue nutrient concentrations (%).

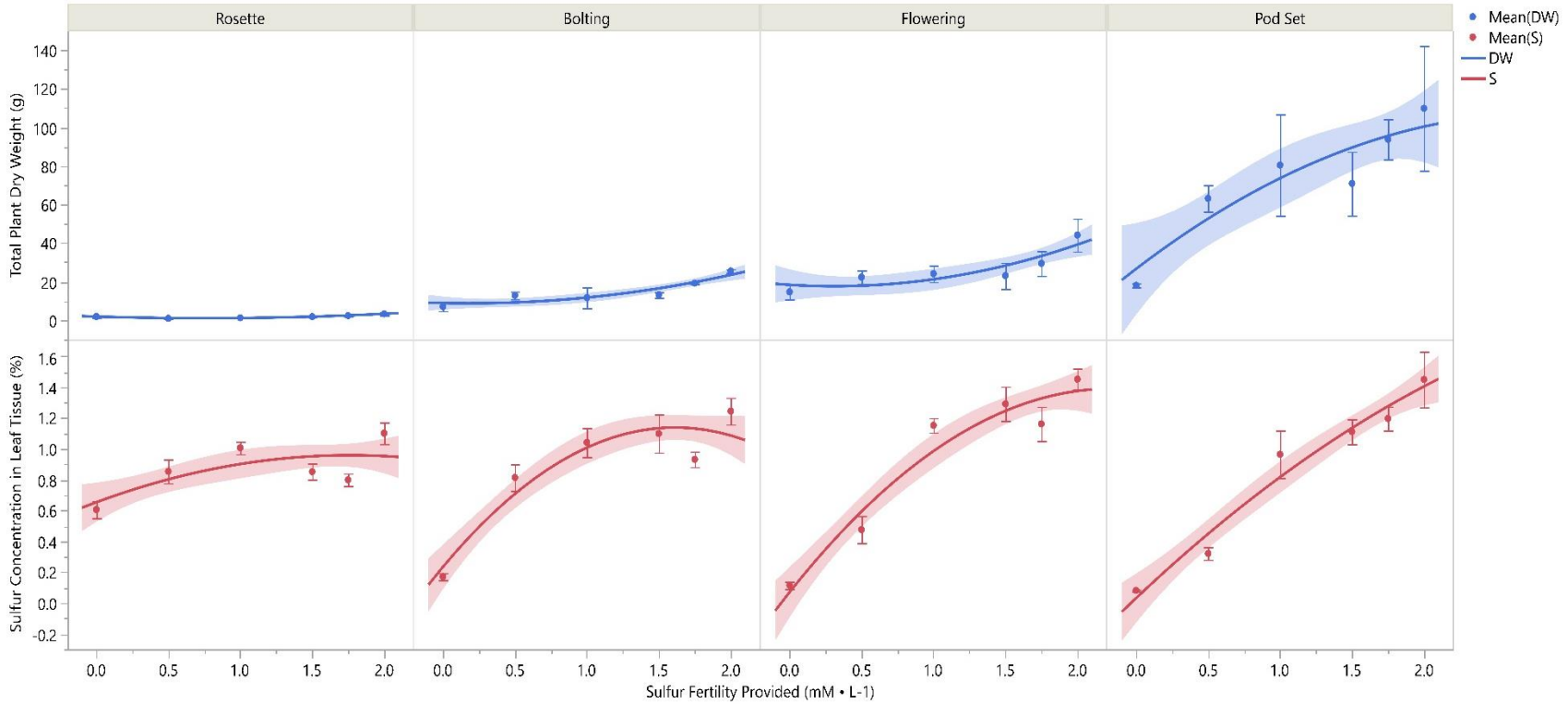

Table 3.3.6: *Brassica carinata* plant dry weights (g) and leaf tissue concentration (%) based on magnesium (Mg) fertility treatments.

Magnesium Fertility Concentration (mM • L^{-1})[1]	0.00	0.50	1.0	1.5	1.75	2.0
Plant Dry Weight (g)						
Rosette[2]	0.93 A ***	1.35 AB ***	1.70 AB ***	2.25 ABC ***	2.43 BC ***	3.40 C ***
Bolting[2]	11.20 A ***	22.18 AB ***	19.48 AB ***	17.48 BC ***	19.50 AB ***	25.60 C ***
Flowering[2]	21.97 C ***	47.83 B ***	32.40 BC ***	40.65 AB ***	39.90 AB ***	44.20 AB ***
Pod Set[2]	40.73 B *	96.30 AB *	71.00 AB *	67.10 AB *	69.83 AB *	109.90 C *
	Magnesium Leaf Tissue Nutrient Concentrations (%)					
Rosette[2]	0.16 A ***	0.22 B ***	0.30 C ***	0.36 CD ***	0.32 D ***	0.52 E ***
Bolting[2]	0.11 A ***	0.22 A ***	0.37 B ***	0.44 BC ***	0.50 C ***	0.51 C ***
Flowering[2]	0.07 A ***	0.20 AB ***	0.30 BC ***	0.41 CD ***	0.51 DE ***	0.61 E ***
Pod Set[2]	0.04 A ***	0.20 AB ***	0.39 BC ***	0.71 CD ***	0.52 DE ***	0.79 E ***
	Comparison Magnesium Leaf Tissue Values (%)[3]					
	Brassica carinata[3]			*Brassica napus*[4]		
Rosette[3]	0.13 – 0.25			0.20 – 0.75		
Bolting[3]	0.13 – 0.22					
Flowering[3]	0.11 – 0.20					
Pod Set[3]	0.11 – 0.17					

[1] Values indicate the adjusted fertility concentration provided from a modified Hoagland's solution with all elements held constant except the adjusted macroelement being studied. For more detailed information on the system and fertility modifications see Barnes et al. [40].
[2] *, **, or *** Indicates statistically significant differences between sample means based on F-test at $P \leq 0.05$, $P \leq 0.01$, or $P \leq 0.001$, respectively. NS (not significant) indicates the F-test difference between sample means was $P > 0.05$. Values with the same letter indicate a lack of statistical significance while values with different letters indicate statistically significant results.
[3] N/A indicates results were not available given plants did not progress to the growth stage specified.
[4] Reference values from Seepaul et al., [40]. Values given are based on *Brassica carinata* for above ground tissue concentration tissue from two growing seasons with samples taken based on plant life stages.
[5] Reference values based on 50 mature leaves without petioles taken throughout the season from rosette stage to pod set. Values taken from *Brassica napus* leaf tissue values from Bryson et al. [41].

Equations 3.3.6: Regression models for linear and quadratic for *Brassica carinata* plant dry weights (g) and leaf tissue nutrient concentrations (%) based on magnesium (Mg) fertility treatments.

Magnesium Regression Models	Power & Significance[1]	Regression Equation[3]	R^2 [4]	Adj-R^2 [4]
Plant Dry Weight (g)				
Rosette[2]	L ***	0.76 + 0.022x	0.63	0.62
	Q ***	1.04 + 0.002x + 0.000191x^2	0.67	0.63
Bolting[2]	L ***	14.58 + 0.083x	0.32	0.29
	Q **	13.80 + 0.145x + 0.000620x^2	0.33	0.27
Flowering[2]	L NS	31.58 + 0.118x	0.17	0.13
	Q NS	28.54 + 0.331x - 0.00206x^2	0.21	0.13
Pod Set[2]	L NS	55.77 + 0.344x	0.16	0.12
	Q NS	57.26 + 0.236x + 0.00105x^2	0.16	0.08
Magnesium Leaf Tissue Nutrient Concentrations (%)				
Rosette[2]	L ***	0.14 + 0.003x	0.79	0.78
	Q ***	0.17 + 0.001x + 0.000012x^2	0.81	0.79
Bolting[2]	L ***	0.12 + 0.004x	0.90	0.90
	Q ***	0.10 + 0.006x + 0.000016x^2	0.91	0.90
Flowering[2]	L ***	0.06 + 0.005x	0.91	0.91
	Q ***	0.09 + 0.003x + 0.000018x^2	0.92	0.91
Pod Set[2]	L ***	0.04 + 0.007x	0.79	0.78
	Q **	0.03 + 0.008x - 0.000009x^2	0.79	0.77

[1] Regression models (L = linear regression model, Q = quadratic regression model) were subjected to linear and higher power polynomial modeling to determine a model of fit. Model fits above the second power resulted in no greater interpretation of data for all models tested, consequently the above models only compare linear and second order polynomials.*, **, or *** Indicates the model's statistical significance at $p \leq 0.05$, $P \leq 0.01$, or $P \leq 0.001$, respectively. NS (not significant) indicates the model resulted in $p > 0.05$.

[2] *Brassica carinata* life stage.

[3] Models were calculated using PROC REG on SAS v 9.4. Determination of best model was accomplished by selecting the model with the best R^2 value and had the lowest p-value.

[4] Best fit statistics: R^2 = coefficient of determination, Adj-R^2 = adjusted coefficient of determination.

Graph 3.3.6: Polynomial regression models for magnesium (Mg) fertility impacts on *Brassica carinata* plant dry weights (g) and leaf tissue nutrient concentrations (%).

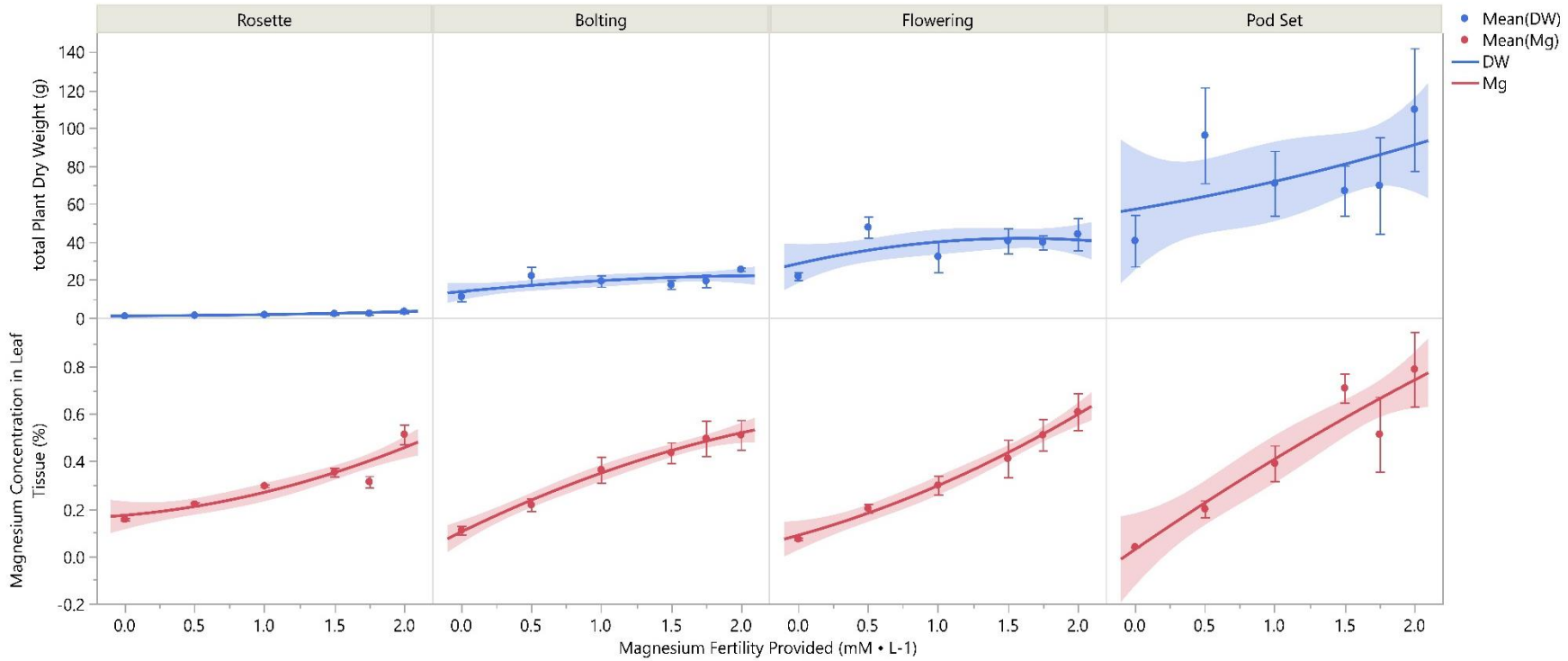

Figure 3.3.1 Nitrogen (N) deficiency (0.0 mM • L^{-1}) first manifested as an overall stunting of the whole plant (right) when compared to the control which received a full N treatment of 15.0 mM • L^{-1}.

Figure 3.3.2 Nitrogen (N) deficiency (0.0 mM • L^{-1}) manifested in the older foliage and as plants paled in coloration, the veins developed a pink or red coloration.

Figure 3.3.3 Nitrogen (N) deficiency at the lowest N treatment (0.0 mM • L^{-1}) notice specifically the pale green coloration of the lower foliage when compared to the developing leaves on the flower spikelet.

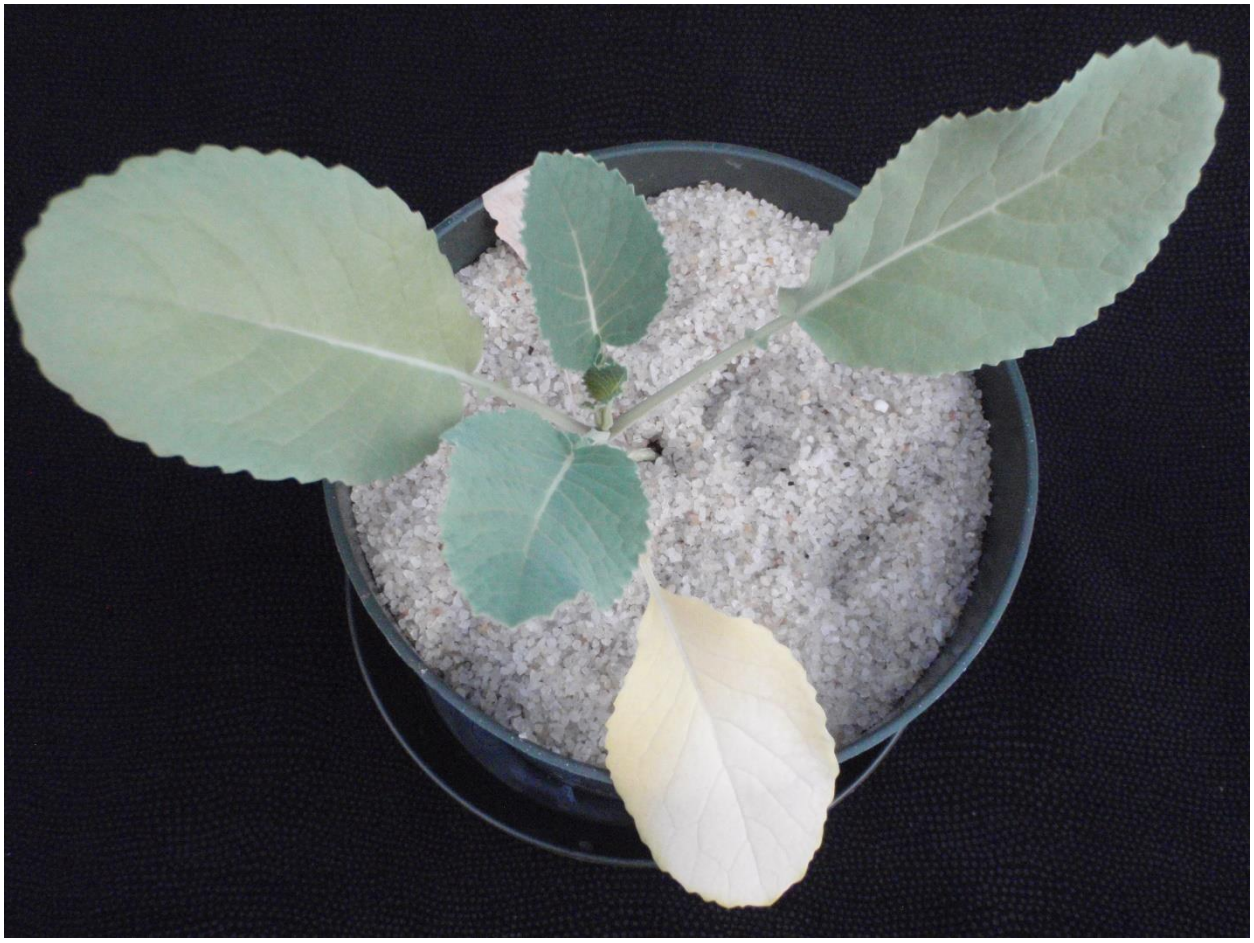

Figure 3.3.4 Nitrogen (N) deficiency (0.0 mM • L^{-1}) will result in the lowest and oldest leaves to bleach and become white in color. The middle leaves will take on a pale green coloration, and the newest leaves will be a lush green coloration.

Figure 3.3.5 Phosphorus (P) deficiency (0.0 mM • L^{-1}) first manifested as an overall stunting of the whole plant (right) when compared to the control which received a full P treatment of 1.0 mM • L^{-1}.

Figure 3.3.6 Phosphorus (P) deficiency (0.0 mM • L^{-1}) symptomology showing a healthy leaf (left) compared to P deficient leaves (symptoms advance in symptomology clockwise from the top leaf to the necrotic leaf at the bottom). Notice specifically the olive green coloration of the leaves which are P deficient.

Figure 3.3.7 Phosphorus (P) deficiency (0.0 mM • L^{-1}) symptomology notice specifically the older leaves appearing yellow and olive green in coloration while the newest leaves are healthy in coloration.

Figure 3.3.8 Phosphorus (P) during the bolting stage. Notice specifically the lack of vigor and branching in the P deficient plant grown at the 0.0 mM • L^{-1} stage (right) compared to the plant grown at the highest P treatment (1.0 mM • L^{-1}).

Figure 3.3.9 Potassium (K) deficiency (0.0 mM • L^{-1}) first manifested as an interveinal yellowing of the leaf margin.

Figure 3.3.10 Potassium (K) deficiency (0.0 mM • L^{-1}) progressed to cause distortions and curling of the leaf margin. Additionally, the leaf margin became necrotic and the interveinal symptomology appeared closer toward the midrib and on the edge of the necrotic regions.

Figure 3.3.11 Potassium (K) deficiency (0.0 mM • L^{-1}) progressed inward toward the midrib and resulted in large necrotic regions and interveinal yellowing while the veins remained a dark green color.

Figure 3.3.12 Potassium (K) deficiency (0.0 mM • L^{-1}) in advanced stages resulted in the distortion of the new and expanding leaves resulting from the necrosis of the leaf margin and produced leaves which had cupping, hooded, or curled distortions.

Figure 3.3.13 Calcium (Ca) deficiency (0.0 mM • L^{-1}) first manifested as a cupping of the leaf margin resulting in a downward orientation of the leaf margin on the new and expanding leaves.

Figure 3.3.14 Calcium (Ca) deficiency (0.0 mM • L^{-1}) progressed to result in the severe distortion of the leaf margin of the new and expanding leaves resulting in morphological changes especially in the newest leaves (center right leaf). Additionally, the leaf surface of the new and expanding leaves developed tan speckling within necrotic regions (left leaf).

.

Figure 3.3.15 Calcium (Ca) deficiency in the bolting stage resulted in plants with shorter stature (right) grown at the 0.0 mM • L^{-1} when compared to plants grown at the highest (left) Ca fertility treatment (5.0 mM • L^{-1}).

Figure 3.3.16 Calcium (Ca) deficiency at the 0.0 mM • L^{-1} resulted in the death of the apical growing point which caused axillary nodes develop. These nodes eventually became necrotic as well.

Figure 3.3.17 Sulfur (S) deficiency (0.0 mM • L^{-1}) in the rosette stage resulted in an overall pale green coloration of the plant.

Figure 3.3.18 Sulfur (S) deficiency in the bolting stage resulted in plants with shorter stature (right) grown at the 0.0 mM • L^{-1} when compared to plants grown at the highest (left) S fertility treatment (2.0 mM • L^{-1}).

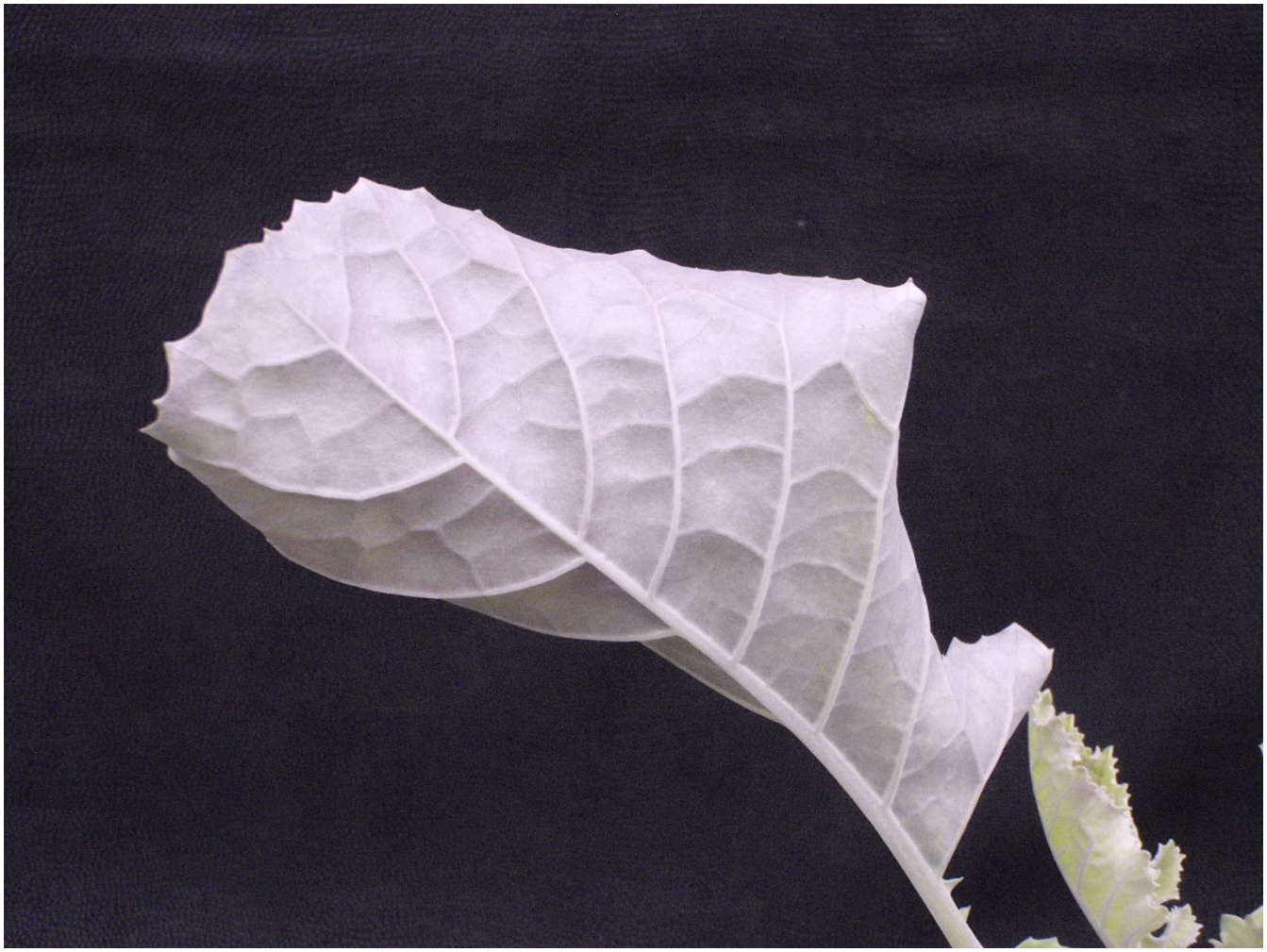

Figure 3.3.19 Sulfur (S) deficiency (0.0 mM • L^{-1}) resulted in leaves which were paler in coloration and whose underside displayed a slight overall purpling.

Figure 3.3.20 Sulfur (S) deficiency (0.0 mM • L^{-1}) resulted in leaves with a more upright orientation (bottom) at the flowering stage compared to the control plant (2.0 mM • L^{-1}).

Figure 3.3.21 Magnesium (Mg) deficiency (0.0 mM • L^{-1}) resulted in leaves with interveinal regions that became yellow and tan in coloration.

Figure 3.3.22 Magnesium (Mg) deficiency (0.0 mM • L^{-1}) symptoms progressed the interveinal regions become sunken and necrotic in the center with the necrotic hallo ringing the necrotic regions.

Figure 3.3.23 Magnesium (Mg) deficiency (0.0 mM • L^{-1}) symptoms progressed the sunken and necrotic regions expanded and merged to form large interveinal regions of necrosis.

Figure 3.3.24 Magnesium (Mg) deficiency (0.0 mM • L^{-1}) symptoms in the most advanced stages resulted in an overall yellowing of the foliage with large tan necrotic regions across the leaf's entire surface.

Figure 3.3.25 Magnesium (Mg) deficiency (0.0 mM • L^{-1}) produced an interesting symptomology on the underside of the leaves with the interveinal regions taking on a magenta or purple coloration with the veins paling.

CHAPTER 4. Characterization of nutrient disorders of ornamental Brassica oleracea ‘Red Bor’.

P. Cockson[1,2] and B. Whipker[1]

[1]Department of Horticultural Sciences, North Carolina State University, Raleigh, N.C. USA

[2]email: pcockson@gmail.com

Abstract

To produce ornamental kale [Brassica oleracea 'Red Bor'], growers must be equipped with cultural information, including the ability to recognize and characterize nutrient disorders. Diagnostic criteria for nutrient disorders of ornamental kale species are absent from the current literature. Therefore, B. oleracea 'Red Bor' plants were grown in silica-sand culture to induce, characterize, and photograph symptoms of nutritional disorders. Plants received a complete modified Hoagland's all-nitrate solution of (macronutrient concentrations in mM) consisting of (macronutrient concentrations in mM) 15 nitrate-nitrogen (NO_3^-), 1.0 phosphate-phosphorus ($H_2PO_4^-$), 6.0 potassium (K^+), 5.0 calcium (Ca^{2+}), 2.0 magnesium (Mg^{2+}), and 2.0 sulfate-sulfur (SO_4^{2-}) plus (micronutrient concentrations in μM) 72 iron (Fe^{2+}), 18 manganese (Mn^{2+}), 3 copper (Cu^{2+}), 3 zinc (Zn^{2+}), 45 boron (BO_3^{3-}), and 0.1 molybdenum (MoO_4^{2-}). Nutrient-deficient treatments were induced with a complete nutrient formula minus a single nutrient. Boron (B) toxicity was induced by increasing the element 10-fold higher than the complete nutrient formula. Plants were monitored daily to document and photograph sequential series of symptoms as they developed. Typical symptomology of nutrient disorders and critical tissue concentrations are presented. Out of 13 treatments, ten exhibited symptomologies; copper (Cu), molybdenum (Mo), and zinc (Zn) remained asymptomatic. Symptoms of nitrogen (N) and phosphorus (P) deficiency, plus boron toxicity (+B), manifested first, followed closely by iron (Fe) and sulfur (S) deficiencies. These disorders may be more likely

problems encountered by growers and therefore plants should be monitored closely for these deficiencies.

Keywords: kale, toxicity, deficiency, macronutrients, micronutrients, fertility

4.1 INTRODUCTION

Ornamental kale and other cultivars within Brassica oleracea are thought to have their origin in Western Europe (Rakow, 2004). There are six main cultivars within Brassica oleracea and each constitute a large economic portion of the global food, fiber, and feed markets (Rakow, 2004; Weiss, 2000). In 2009, total US exports of lettuce were 704,954 (1,000 lb units; USDA, 2011). These export values do not take into account domestic production and only span one of the six key cultivars within Brassica oleracea. One market portion of Brassica oleracea is the ornamental market. Brassicas are grown globally for their ornamental and aesthetic properties. Given the global importance and popularity of brassicas, little quality scientific information exists on ornamental kale production and management. In particular, fertility requirements are lacking from literature. Some work has been reported for boron mobility and nutritional requirements of field produced broccoli (Shelp, 1988). An informational research brief on successful ornamental cabbage and kale production is also present (Whipker et al., 1998), however the information in this publication needs to be expanded upon to include more species. Many species and cultivars, especially within brassicas, will exhibit specific nutrient stress symptomology that can assist growers in rapid identification of nutrition problems (Henry et al., 2017a&b). Thus, due to a lack of ornamental specific production practices, a general deficit of species information, and the nuances in nutritive symptomology that brassicas can exhibit, Brassica oleracea 'Red Bor' plants were subjected to nutrient

deficient conditions and the visual symptomology, symptomological progression, and leaf tissue nutrient concentrations were obtained.

4.2 MATERIALS AND METHODS

Ornamental kale seeds were obtained (Johnny's Select Seeds; Winslow, ME) and sown on 3 Jan. 2012 into 72 trays (6 x 3.5 x 2 cm) and transplanted into 12.7-cm-diameter (0.76 L) plastic pots containing acid washed silica-sand [Millersville #2 (0.8 to 1.2 mm diameter) from Southern Products and Silica Co., Hoffman, NC] on 26 Jan. 2012. The plants were grown in a glass greenhouse with 24°C day and 20°C night temperature in Raleigh, NC (35°N latitude). Treatments started immediately upon transplanting. An automated, recirculating irrigation system was constructed out of 10.2 cm diameter PVC pipe (Charlotte Plastics, Charlotte, NC). Detailed information about formulation of the fertilizer treatments, salts used, and the system can be found in Barnes et al. (2012).

When the initial deficient symptom of each treatment occurred, three plants that exhibited symptoms were selected for sampling, and the remaining five plants were grown to document symptom advancement. Fully expanded leaves were sampled to evaluate the critical tissue concentration for each element. Harvested leaves were washed in a solution of 0.5 N HCl for 1 min and rinsed with deionized water. The remaining shoot tissue was harvested separately. Both sets of tissue were dried at 70°C, and the dry weights were recorded. After drying, tissue was ground in a Foss Tecator Cyclotec™ 1093 sample mill (Analytical Instruments, LLC, Golden Valley, MN) to pass a ≤ 0.5 mm sieve. Tissue analysis was conducted by AgSource Laboratories (Lincoln, NE).

The experiment was terminated on 27 Mar. 2012. The plants did not exhibit symptoms for the Cu, Mo, and Zn deficiency treatments. Asymptomatic plants were

sampled for dry weight and nutrient levels. All the data were subjected to ANOVA using PROC ANOVA SAS program (verion 9.4; SAS Inst., Cary, N.C.). Where the F-test was significant, LSD ($P \leq 0.05$) was used to compare differences among means. Deviations in dry weight were calculated on a percentage basis from the controls.

4.3 RESULTS

Out of 13 treatments, ten exhibited symptomologies. Symptoms of N and P deficiencies, plus B toxicity, manifested early therefore, these nutrients should be monitored more closely by producers. Unique symptom indicators were observed on N, P, S, and Mn deficient plants. The plant dry weights and leaf tissue value results can be found in Table 1.

4.3.1. Nitrogen (N)

Nitrogen, deficiency was the first symptomology to manifest. The N treatment plants had 64.6% less biomass compared to the control. The control tissue N concentration was 3.07% while tissue concentration from plants grown under N-deficient conditions was 0.67% (Table 1). Nitrogen deficiency started as a general stunting of the entire plant when compared to the control, and the plants showed intensity of red coloration especially of the midrib and stems of the lower foliage. In intermediate symptomology, the green coloration decreased in intensity and the red coloration became pinker in coloration on a yellowing background. In the most advanced stages, the lower leaves turned completely yellow in the interveinal regions with the veins and midrib maintaining a red to pink coloration (Figure 1).

Table 4.3.1 Brassica oleracea 'Red Bor' plant dry weights (g) and leaf tissue concentrations (mg·kg^{-1} and % dry weight) based on fertility treatments.

Treatment	-N	-P	-K	-Ca	-Mg	-S	++B[a]	-B	-Fe	-Mn
	Dry mass (g)									
Element	N	P	K	Ca	Mg	S	++B	B	Fe	Mn
Control	2.20	2.87	2.87	5.47	5.47	2.87	2.20	15.00	5.47	16.81
Treatment	0.78	0.78	2.67	3.06	4.92	3.06	0.67	7.80	4.50	17.38
P-value[b]	*	*	NS	**	NS	NS	*	***	*	NS
	Tissue nutrient concentration (% dry weight (g))						Tissue nutrient concentration (mg·kg^{-1})			
Element	N	P	K	Ca	Mg	S	++B	B	Fe	Mn
Control	3.07	0.45	4.14	4.19	0.82	1.63	127.72	168.62	15.87	88.52
Treatment	0.67	0.19	0.30	0.36	0.08	0.20	615.20	10.35	4.71	2.88
P-value[b]	***	**	***	***	***	***	***	***	***	***
	Comparison tissue values[c]									
Element	N	P	K	Ca	Mg	S		B	Fe	Mn
Optimal Range	3.5-4.5	0.20-0.60	3.00-4.00	0.50-1.00	0.20-0.40	0.20-1.00		20-40	50-300	59.7-77.5

[a]Toxicity treatments indicated by ++B; Boron deficiency indicated by -B.

[b]*, **, or *** Indicates statistically significant differences between sample means based on F-test at $P \leq 0.05$, $P \leq 0.01$, or $P \leq 0.001$, respectively. NS (not significant) indicates the F-test difference between sample means was $P > 0.05$.

[c]Values from Gibson et al. (2007) for ornamental cabbage Brassica oleracea var. acephala 'Osaka White'

This N deficiency progression of yellowing of the background color of the leaf but the maintenance of the red colorations was also seen in red and lettuce varieties (Henry et al., 2017a; Henry et al., 2017b).

4.3.2. Phosphorus (P)

Phosphorous deficiency symptomology was quick to manifest in kale. Plants subject to P deficient conditions produced 72.8% less biomass than the control plants. The control tissue P concentration was 0.45% while tissue concentration from plants grown under P-deficient conditions was 0.19% (Table 1). Phosphorus deficiency started as a general stunting of the entire plant when compared to the control. Additionally, an increase in red coloration was observed in the lower foliage. Unlike nitrogen deficiency, the background leaf color became a darker olive-green color and the red coloration was more maroon than red or pink. In intermediary symptomology, the maroon coloration of the interveinal region enhanced in brilliance and the leaf veins and midrib were the same color as the interveinal regions. In the most advanced stages, the lower leaves became completely necrotic and abscised (Figure 1).

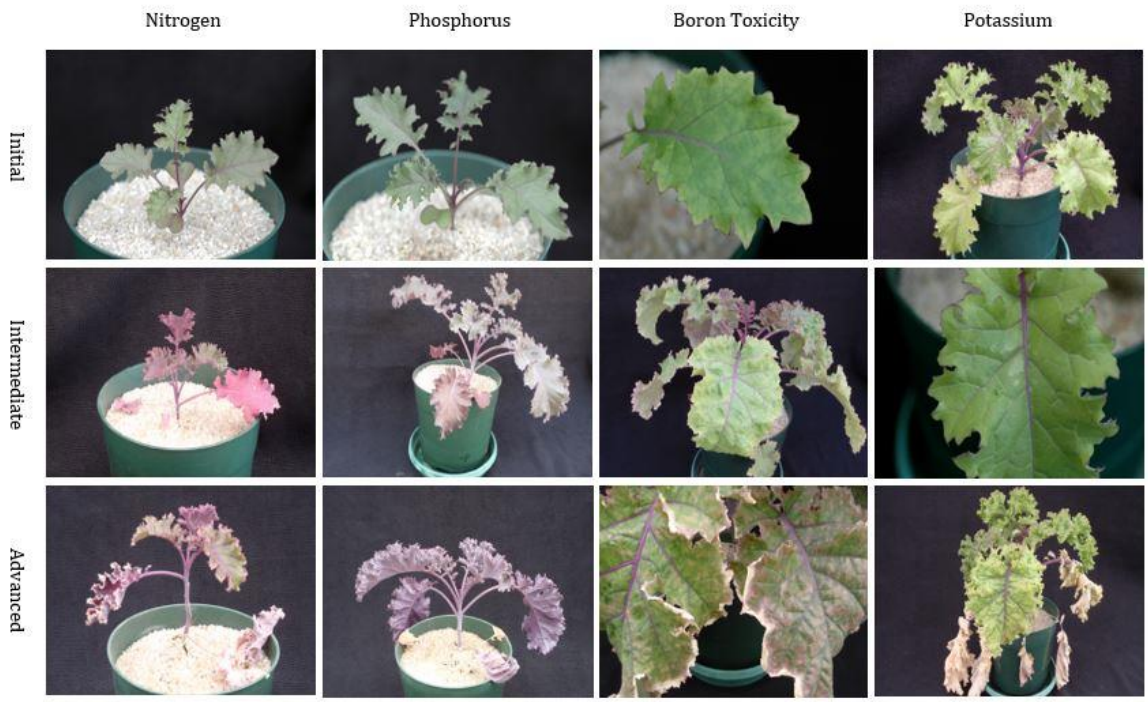

Figure 4.3.1 Composite image of nitrogen (N), phosphorus (P), boron toxicity (B+), and potassium (K) deficiency symptomology as it progresses (initial, intermediate, and advanced) of Brassica oleracea 'Red Bor'.

4.3.3. Boron Toxicity (+B)

Boron Toxicity treatment resulted in plants with 69.4% less biomass when compared with the control. Boron levels in the control plants were at 127.72 $mg \cdot kg^{-1}$ while the toxicity treatment had levels at 615.20 $mg \cdot kg^{-1}$ (Table 1). Boron toxicity conditions resulted in a marginal chlorosis of the lower leaves. As boron toxicity conditions continued, the marginal chlorosis became more severe and eventually resulted in marginal necrosis. As symptomology progressed, the interveinal regions of the lower leaves also become chlorotic and eventually necrotic. Final stages resulted in the severe burning of the leaf margin and the interveinal regions of the leaves (Figure 1).

4.3.4. Potassium (K)

Potassium deficient plants manifested sixteen days after N, P, and B+ symptomology. There was no difference between the control plants and the treatment dry weights. Potassium leaf tissue concentrations were significant with 4.14% K in the control and 0.30% in the deficient treatment plants (Table 1). The symptomology of K

starvation first manifested on the lower foliage as an overall yellowing of the leaf especially around the leaf midrib and petiole. As symptoms progressed, the lower leaves developed sunken pale regions in the interveinal areas. In the intermediate stages of K deficiency resulted in the sunken pale regions becoming necrotic and the lower leaves becoming extremely pale yellow in color. The final stages of deficiency resulted in completely yellow leaves, necrosis and eventually abscission from the plant (Figure 1).

4.3.5. Sulfur (S)

Sulfur deficiency manifested early, and plants did not have a difference in dry weight. Despite the lack of biomass differences, the control plants had 1.63% S and the deficient plants had 0.20% resulting in a very pronounced statistically significant decrease in leaf tissue S concentration (Table 1). Sulfur deficiency first manifested as an overall increase in red coloration of the middle and top portion of the plant. As symptoms progressed, the purpling become more uniform in the middle and upper portion of the plant while the lower portions remained asymptomatic. In the advanced stages, marginal and interveinal necrotic tan spotting of the mid-level leaves occurred. (Figure 2).

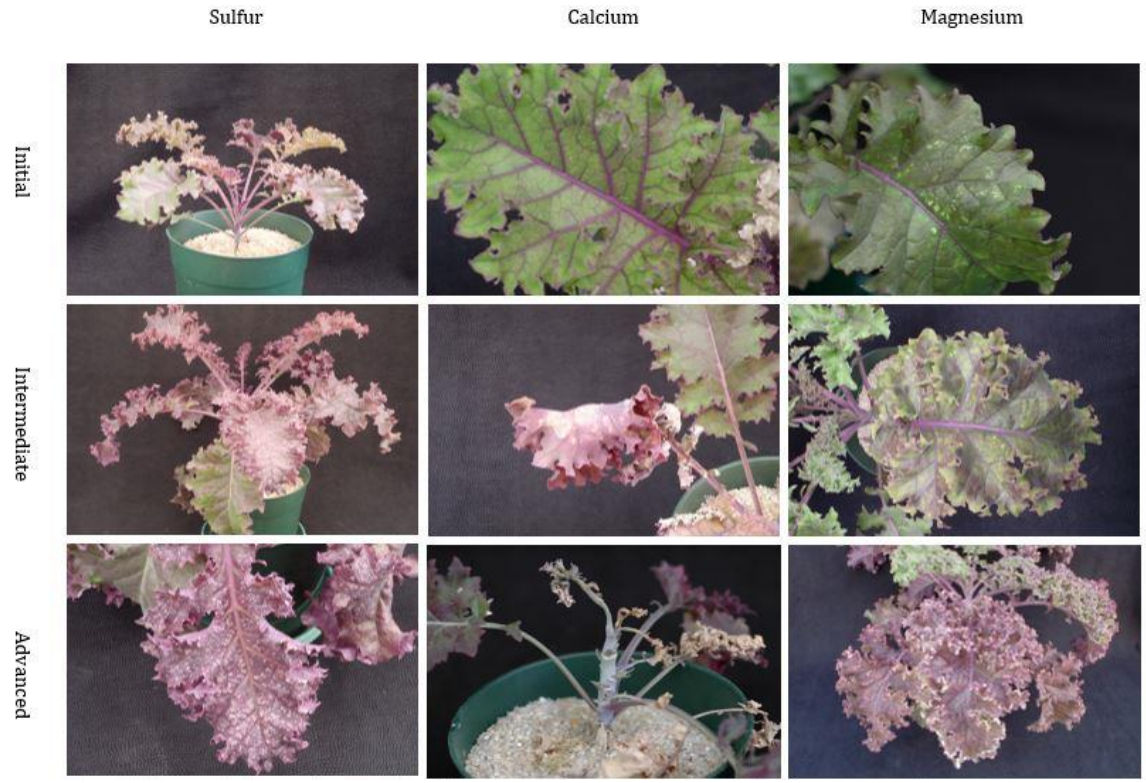

Figure 4.3.2 Composite image of sulfur (S), calcium (Ca), and magnesium (Mg) deficiency symptomology as it progresses (initial, intermediate, and advanced) of Brassica oleracea 'Red Bor'.

4.3.6. Calcium (Ca)

Calcium deficient plants had 44.0% less dry weight compared to the control (Table 1). At termination, control plants had 4.19% calcium and the treatment plants had 0.36%. Calcium deficiency first manifested in the upper leaves of the rosette as small pale evenly distributed tan stippling of the leaf surface. As symptoms progressed, the new and expanding leaves began to show marginal distortions. These distortions became extreme with the leaf margin curling and wrinkling severely into bizarre leaf shapes. In advanced stages, the new leaves become severely stunted and necrotic with the growing tip eventually becoming necrotic and the proliferation of axillary shoots due to a loss of apical dominance (Figure 2).

4.3.7. Magnesium (Mg)

Magnesium deficient plants had no significant difference in dry weight. However, statistically significant changes in tissue concentration of Mg were observed, with 0.08%

in the deficient treatment compared to the control with 0.82% (Table 1). Mg symptomology began as sunken tan irregular shaped spots of the lower foliage. These spots then expanded within the interveinal regions of the leaves and along the leaf margin in the intermediate stages of deficiency. Advanced Mg symptoms manifested as larger necrotic spots on the lower foliage and along the leaf margin and an increase in the red coloration of the lower leaves with the upper leaves maintaining a healthy green coloration (Figure 2).

4.3.8. Iron (Fe)

Iron deficient plants had 17.6% less biomass compared to the control (Table 1). Iron deficient treatments resulted in leaf tissue with 4.71 $mg \cdot kg^{-1}$ Fe compared to the control with 15.87 $mg \cdot kg^{-1}$ Fe. Iron deficiency first manifested as a slight yellowing in the interveinal regions of the upper foliage of the rosette. As symptoms progressed, the yellowing became more severe while the lower leaves still maintained their healthy green coloration. In intermediate stages, the new leaves became stunted in their development and their interveinal regions became extremely pale and almost cream colored while the veins took on a bright purple coloration (Figure 3).

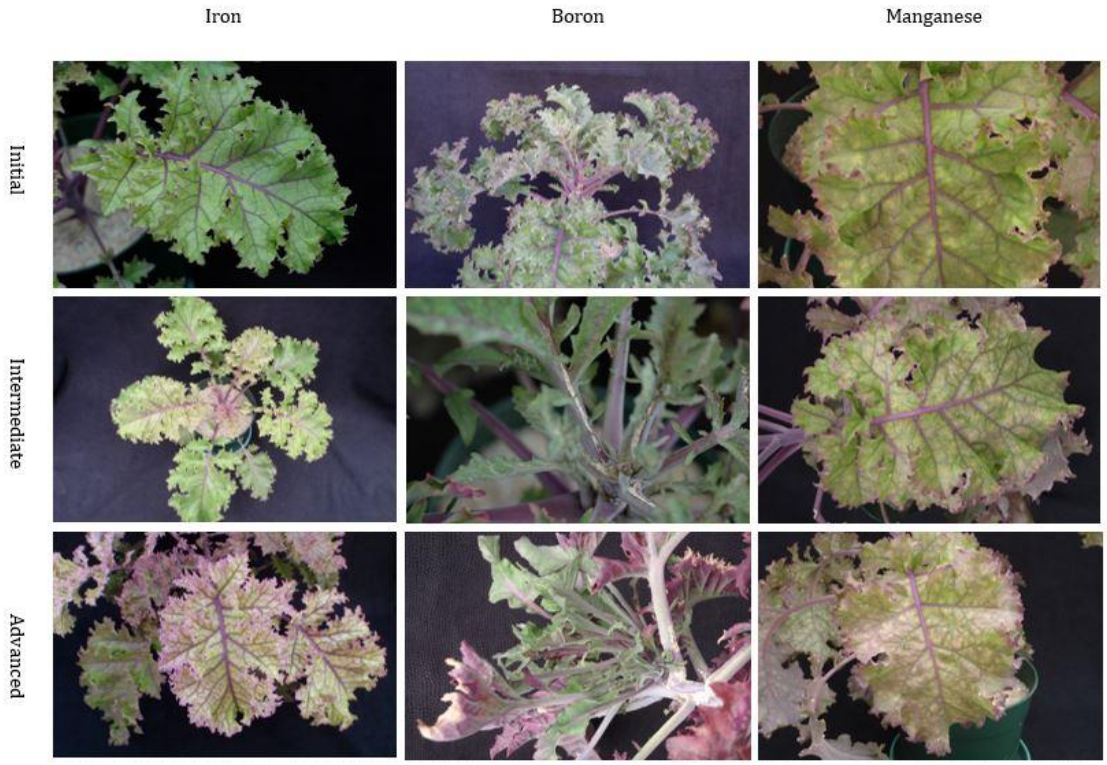

Figure 4.3.3 Composite image of iron (Fe), boron (B), and manganese (Mn) deficiency symptomology as it progresses (initial, intermediate, and advanced) of Brassica oleracea 'Red Bor'.

4.3.9. Boron Deficiency (B)

Boron Deficiency in kale resulted in plants with 48% less total plant biomass when compared to the control (Table 1). Boron deficient plants also contained 10.35 $mg \cdot kg^{-1}$ B in the leaf tissue. Boron deficiency first manifested as a general slowing of the growth and expansion of the new and emerging leaves when compared to the control plant. This stunting of the new and expanding leaves became more prominent and the leaf margin failed to expand resulting in marginal distortions. Intermediate stages of boron deficiency resulted in the new leaves being very distorted and necrotic and brittle. The petiole and leaf midrib showed cracking in the leaf waxy cuticular surface. The growing tip eventually become necrotic and died and the axillary shoots began to proliferate and experienced the same distortions and necrosis as the terminal growing tip (Figure 3).

4.3.10. Manganese (Mn)

Manganese deficient plants had no significant difference in dry weight when compared with the control. The control plants had 88.52 $mg \cdot kg^{-1}$ Mn in the leaf tissue, while the treatment plants contained 2.88 $mg \cdot kg^{-1}$ (Table 1). Manganese deficiency first manifested in the new leaves as an olive-green mottling of the interveinal region especially around the midrib. As the symptomology progressed, the new leaves became paler in green coloration and the mottling olive-green spots became tan in coloration and became necrotic. In advanced stages, the necrotic regions became prevalent in the interveinal regions, and the overall leaf color became yellow-green (Figure 3).

4.3.11. Zinc, Copper, and Molybdenum (Zn, Cu, and Mo)

Zinc, Copper, and Molybdenum deficient plants had no symptomology at termination. Plant dry weights were taken, and leaf tissue was run however neither the dry weights nor the leaf tissue values were statistically significant and thus are not reported here (Table 1).

4.4 DISCUSSION

Kale plants are grown especially for their ornate appearances and their unique leaf coloration. Consequently, any production practice that would alter or blemish that appearance creates a decrease in customer satisfaction and could result in an economic loss to the grower. The above results illustrate not only that different nutrients can affect plant appearance, but also that such nutrient stresses will occur at different times. By understanding which nutrient deficiencies are likely to occur first, and the associated symptomology, growers will be better equipped to take corrective measures early before plant appearance is compromised.

In the timeline of symptomological progression, N and P deficiencies, and B+ were first to manifest. These nutrients would most likely be the first nutritive issues a grower

would face. The next deficiencies to manifest were K and S. These elements are the next most likely to cause issues for growers.

Unique symptomological indicators were observed on N, P, S and Mn. By looking specifically for nuances in coloration and location of the coloration, growers can help to distinguish among the above nutrient deficiencies. To distinguish among N, P, S and Mn one must look at the coloration and progression of coloration as well as the location of the symptomology. Sulfur will manifest on the upper to mid-level foliage with the lower foliage remaining relatively healthy and normal in coloration. Nitrogen and P symptomology will manifest on the lower foliage and Mn will manifest on the upper portions of the plant.

To distinguish N from P understanding the symptomological progression is helpful. At the beginning stages, N and P are almost indistinguishable, however as symptoms progressed, the background leaf color in N deficient plants becomes more-pale and the veins become more purple to pink. In P deficient plants, as symptoms progress, the lower leaves will take on a deeper red coloration and this coloration will be relatively even between the interveinal regions, the leaf background color, and the veins.

To then distinguish Mn looking at the location of the symptomatic leaves will be helpful. Manganese is an immobile element whereas N and P are mobile, and S is partially mobile. This means that N and P will appear in the lower leaves and plant portions given the plant will reallocate these resources into the new and developing leaves. Given S is partially mobile, the plant cannot easily reallocate this resource from the older and developed plant portions to the new and growing parts. Thus, S deficiency will manifest in the middle and upper portions of the plant. Manganese is immobile in the plant. This means that the plant cannot allocate these resources into the new and developing plant tissues. Thus, the symptomology will manifest in the upper or new portions of the plant and in the developing tissue. Therefore, to distinguish among N, P, S and Mn purpling looking at the location is vital in determining which element is

deficient. While there are exceptions to every rule, these guidelines will help growers identify nutrient disorders. A tissue sample should always be taken in conjunction with visual symptoms and symptomological progression to confirm the specific nutrient disorder. The above unique symptomologies further highlight how vital species-specific nutrient deficiency work remains to the producer and scientist alike.

4.5 CONCLUSION

By paying attention to the nutrient deficiency timeline for a specific species and the unique symptoms that manifest, growers and scientists can more accurately diagnose and prevent nutritive damage and losses. This study highlights the importance of species-specific diagnostic criteria. By preventing nutritive damage to plants, a more efficient use of nutrients is perpetuated, decreases in quality to consumers and producers are avoided, and the highest quality of plant appearance and vigor is obtained.

LITERATURE CITED

Barnes, J., Whipker, B., McCall, I., and Frantz, J. (2012). Nutrient Disorders of 'Evolution' Mealy-cup Sage. HortTechnology 22:502–508. http://horttech.ashspublications.org/content/22/4/502.full

Cresswell, G.C. and Weir, R.G. (1997). Plant Nutrient Disorders 5: Ornamental Plants and Shrubs. Inkata Press, Melbourne, Australia.

Gibson, L., Dharmalingam, P., Williams-Rhodes, A., Whipker, B., Nelson, P., Dole, M. (2007). Nutrient Deficiencies in Bedding Plants. (West Chicago, IL, US: Ball Publishing), pp. 125.

Henry, J. (2017a). Beneficial and Adverse Effects of Low Phosphorus Fertilization of Floriculture Species. (Raleigh, NC, US: North Carolina State University Library Repository Publishing), pp. 22-190.

Henry, J., I. McCall, and B. Whipker. (2017b). Nutrient disorders of Lactuca sativa 'Salanova Red'. 10.13140/RG.2.2.17583.43681.

Rakow, G. (2004). Species Origin and Economic Importance of Brassica. In Brassica (pp. 3-11). Springer, Berlin, Heidelberg.

Shelp, B. J. (1988). Boron mobility and nutrition in broccoli (Brassica oleracea var. italica). Annals of botany, 61(1), 83-91.

USDA. (2011). Lettuce: U.S. Monthly and Annual Exports, 1990 - 2010. USDA ERS - By Commodity. www.ers.usda.gov/data-products/vegetables-and-pulses-data/by-commodity.aspx.

Weiss, E. A. 2000. Oilseed Crops. (No. Ed. 2). Blackwell Science Ltd.

Whipker, B. E., J. Gibson, R. Cloyd, C. Campbell and R. Jones. (1998). Success with ornamental cabbage and kale. Horticulture Information Leaflet, 507, 1-9.

APPENDIX

CARINATA GROWTH STAGES

Growth Stage 0: Germination
0.0 Dry seed
0.1 Beginning of seed imbibition
0.3 Seed imbibition complete
0.5 Radicle emerged from seed
0.7 Hypocotyl with cotyledons breaking through seed coat
0.9 Emergence: cotyledons break through soil surface

Growth Stage 1: Leaf development (Main shoot)
1. 0 cotyledons completely unfold
1.1 first true leaf unfolds
1.2 two leaves unfold
1.3 three leaves unfold
1.4 four leaves unfold
1.5 five leaves unfold
1.6 six leaves unfold
1.7 seven leaves unfold
1.8 eight leaves unfold
1.9 nine or more leaves unfold

Growth Stage 2
This growth stage (2.0-2.9) refers to the development of side shoots (tillering) and occurs in many plant species but it is not applicable to carinata.

Growth Stage 3: Stem Elongation
3.0 stem elongation (bolting) begins
3.1 stem 10% of final length
3.2 stem 20% of final length
3.3 stem 30% of final length
3.4 stem 40% of final length
3.5 stem 50% of final length
3.6 stem 60% of final length
3.7 stem 70% of final length
3.8 stem 80% of final length
3.9 maximum stem length

Growth Stage 4
This growth stage (4.0-4.9) is not important for carinata but applies in the development of harvestable vegetative plant parts such as broccoli or cauliflower.

Growth Stage 5: Inflorescence emergence
5.0 flower buds present, but still enclosed by leaves
5.1 flower buds visible from above (green bud)
5.2 flower buds free, level with the youngest leaves
5.3 flower buds raised above the youngest leaves
5.5 individual flower buds (main inflorescence) visible but still closed
5.8 individual flower buds (secondary inflorescence) visible but closed
5.9 first petals visible, but flower buds still closed (yellow bud)

Growth Stage 6: Flowering
6.0 First flowers open (sporadically)
6.1 Beginning of flowering: 10% of flowers open
6.2 20% of flowers open
6.3 30% of flowers open
6.4 40% of flowers open
6.5 Full flowering: 50% of flowers open
6.7 Flowering finishing: majority of petals fallen or dry
6.9 End of flowering

Growth Stage 7: Fruit/Pod development
7.1 First fruits formed
7.2 20% of fruits have reached typical size and hard
8.5 50% of the fruits ripe, or 50% of seeds of typical color, dry and hard
8.9 Fully ripe: seeds on the whole plant of typical color and hard

Growth Stage 9: Senescence
9.2 Leaves and shoots beginning to discolor
9.5 50% of leaves yellow or dead
9.7 Plants or above ground parts dead
9.9 Harvested product (seeds)

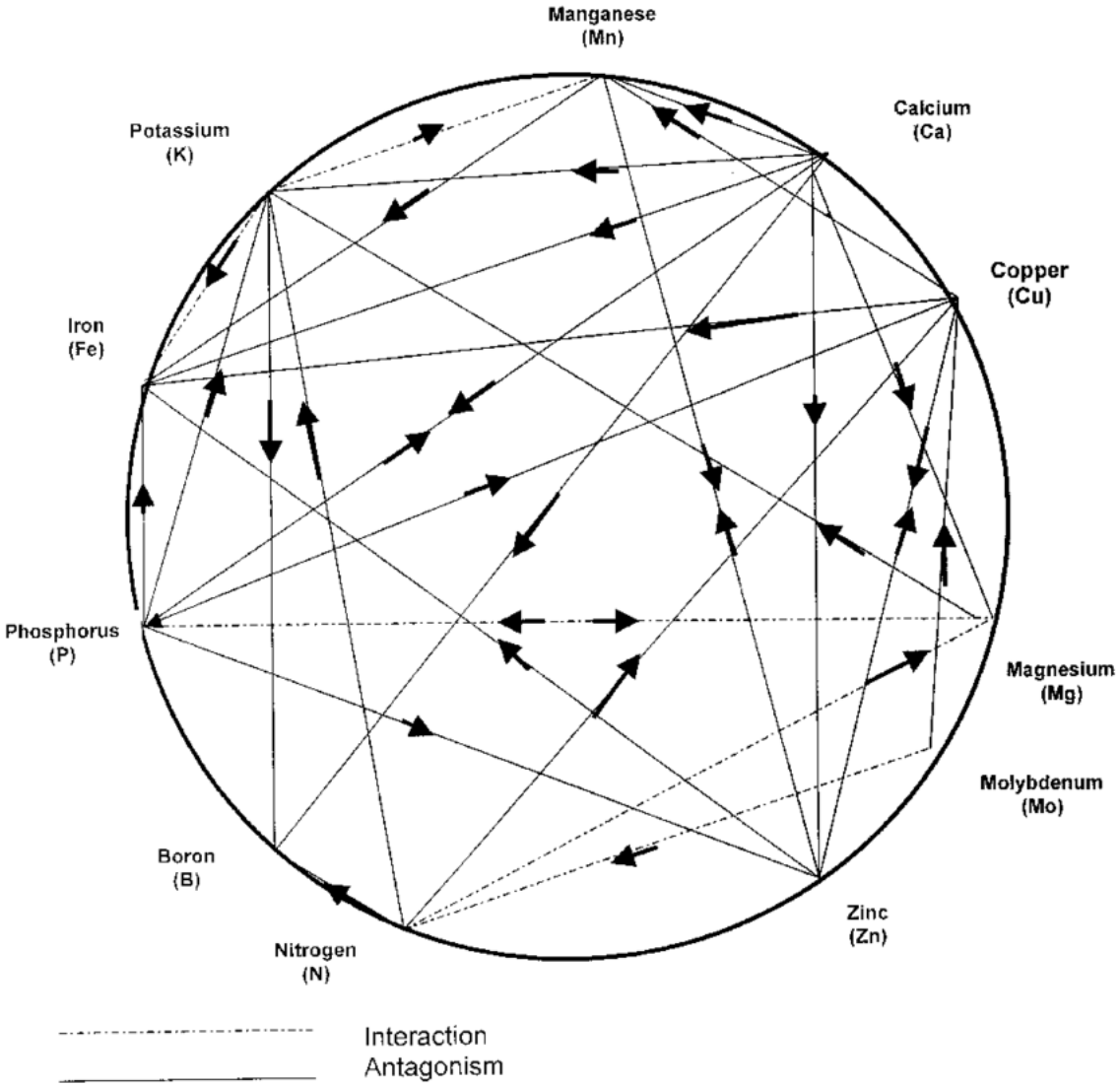
Manganese
(Mn)
Potassium
(K)
Calcium
(Ca)
Copper
(Cu)
Iron
(Fe)
Phosphorus
(P)
Magnesium
(Mg)
Molybdenum
(Mo)
Boron
(B)
Zinc
(Zn)
Nitrogen
(N)
Interaction
Antagonism

EQUATIONS

All data was subjected to first and second order polynomials through PROC REG treating the fertility concentration as the predictor and the plant dry weight and plant leaf tissue nutrient concentration as the response variables. If the data set seemed to have a plateau at which point no increase or decrease was seen in the resultant values mentioned above, the data was subjected to PROC NLIN to obtain the X0 value at which the parameter in question reached its maximum value. The equation below was used to determine the best fit for data deemed to be non-linear to obtain the quadratic plateau model.

$$Y_i = \begin{cases} \beta_0 + \beta_1 X_i + \beta_1 X_i^2 + \varepsilon_i & if\ X < X_0 \\ Y_0 + \varepsilon_i & if\ X \geq X_0 \end{cases}$$

The above equation was subjected to the following parameters and constraints:

$$X_0 = -\frac{\hat{\beta}_1}{2\hat{\beta}_2}, \text{and}$$

$$Y_0 = \hat{\beta}_0 - \frac{\hat{\beta}_1^{\,2}}{4\hat{\beta}_2}$$

To determine which model, quadratic or non-linear, provided the best fit for the data regression models were compared, and the polynomial model or non-linear model which resulted in the greatest statistical significance (α = 0.05, 0.01, 0.001) and the greatest r^2 values were selected.

This method of data analysis has been successful in determining optimal fertility concentrations for over six different species. More information on this method can be found at:

Henry, J.B., 2017. Beneficial and Adverse Effects of Low Phosphorus Fertilization of Floriculture Species.